STRATIGRAPHY AND SOILS OF FLUVIAL TERRACES ON THE CATAWBA RIVER, NC AND SC: LANDSCAPE EVOLUTION OF THE SOUTHEASTERN US

by

Jordan Vincent Arey

A thesis submitted to the faculty of
The University of North Carolina at Charlotte
in partial fulfillment of the requirements
for the degree of Master of Science in
Earth Sciences

Charlotte

2018

Approved by:

_____
Dr. Martha Cary Eppes

_____
Dr. John A. Diemer

_____
Dr. Andy R. Bobyarchick

Abstract

JORDAN VINCENT AREY. Stratigraphy and soils of fluvial terraces on the Catawba River, NC and SC: Landscape evolution of the southeastern US. (Under the direction of DR. MARTHA C. EPPES)

Few studies provide data that can document the long-term landscape evolution of the Piedmont of the southeastern United States. Here we present the results of field mapping and a soil chronosequence for fluvial terraces along a ~46 km reach of the Catawba River, NC and SC. Five terrace units (Qt1 – 5) have been mapped along the reach, and in certain regions a sixth surface (Qt0) was mapped. Observations of bedrock surfaces on Qt3 – Qt0 confirmed that these units are strath terraces. Longitudinal profiles of terrace units constructed from mapping data revealed static channel convexities in Qt5 – Qt1 in the lower reach of the study area at Landsford Canal State Park, and a lack of an obvious influence on terraces profiles within the Gold and Silver Hill shear zones in the middle reach. Age dating of terraces in this study included deriving ages based on surface height above the channel (Mills, 2000) and IRSL samples obtained from Qt3 exposures. Ages, reported in ka, are as follows: Qt0 - 4591 ± 404 ka, Qt1 - 1852 ± 365 ka, Qt2 - 1181 ± 194 ka, Qt3 (average of two IRSL ages) – 142 ± 32 ka, Qt4 – 50 ± 8 ka, and Qt5 – 5 ± 2 ka. Up to 3 soil pits were dug on each terrace unit Qt5 – Qt2, and soils described as per Birkeland (1999). Chronofunction trends of soil morphological properties include soil colors in the most developed B horizons reddening and clay films increasing in amount and prominence with surface age. Soil samples were analyzed for particle size, pedogenic iron (AAS), bulk density and major elements (XRF). Some of these analyses show expected trends with respect increasing surface age for terraces of the Catawba River,

such as increases in clay content (%) and decreases in iron activity ratios in most weathered B horizons with increasing surface age. Overall the history Catawba River is one of five distinct periods of lateral planation of the valley, possibly driven by transitions to interglacial periods, punctuated by periods of incision, whose cause is currently unknown. The soil chronosequence, ages, and data derived from mapping, however, provide a strong foundation that can be used in further studies of the long-term landscape evolution of the SE Piedmont of the SE United States.

Acknowledgements

The author would like to extend grateful appreciation to Dr. Missy Eppes, for guidance and cooperation with this research. Special thanks to Jon Watkins and Dr. Céline Martin for providing training and assistance with Atomic Absorption Spectrometer, Laser Diffraction Particle Counter and X-Ray Fluorescence machinery. Thank you to Pamela Mefferd, Erik Milde, Sean Taylor and Tariq Ghaffar of the SC Department of Natural Resources, and Michelle Nelson of the Utah State University Luminescence Laboratory for assistance with mapping, soil sampling, and luminescence sampling field methods. Thank you to North Rock Hill Church, The Graham Family of the Ivy Place, and Al James, Park Manager of Landsford Canal State Park, who allowed permission to perform sampling on their respective properties. Finally, thank you to my parents and partner for their unending love, care and support of my education and well-being.

Table of Contents

List of Tables: viii

List of Figures ix

CHAPTER 1: Introduction 1

CHAPTER 2: Literature Review 2

2.1: Stream Processes 2

2.2: Fluvial Terraces 3

2.3: Fluvial Terrace Studies 5

2.4: Tectonics of the Southeastern US 9

2.5: Paleoclimates of the Southeastern US 12

2.6: Previous work on the Catawba River 14

CHAPTER 3: Study Area and Geology 21

CHAPTER 4: Methods 23

4.1: Field Methods 23

4.2: Age Dating Methods 25

4.3: Topographic Analysis and Laboratory Methods 26

CHAPTER 5: Results 51

5.1: Mapping, Stratigraphy and General Morphological Data 51

Qt0 – Average 69 m elevation above the modern channel 52

Qt1 – Average 46 m elevation above the modern channel 52

Qt2 – Average 38 m elevation above the modern channel 53

Qt3 – Average 24 m elevation above the modern channel 54
Qt4 – Average 9.5 m elevation above the channel 56
Qt5 – Average 3 m elevation above the channel 57
5.2: Age Control..... 58
5.3.1: Chronofunctions of Soil Properties..... 62
5.3.2: Grain Size analysis..... 63
5.3.3: Pedogenic Fe Analysis..... 64
5.3.4: Elemental Analysis (XRF)..... 65
5.4 Channel Morphology and Longitudinal Profiles 66
CHAPTER 6: Discussion..... 86
6.1: Soil Chronosequence: 86
6.2: Channel Morphology: 89
6.3: Causes of Catawba River incision and terrace formation..... 90
CHAPTER 7: Conclusions 98
REFERENCES: 99
APPENDIX A: Detailed Surficial Geology Maps of the Catawba River..... 104
APPENDIX B: Annotated Soil Pit Photographs 120
APPENDIX C: Supplementary Figures and Tables 135

List of Tables:

Table 4.1: Summary Table of Catawba River terrace units. 36

Table 4.2: Birkland (1999) descriptions of soil pits and exposures. 37

Table 4.3: Summary of Lab Analysis data 47

Table 5.1: Summary table of clast data collected on Catawba River terraces. 71

Table 5.2: Summary table of age control. 76

Table 5.3A: Statistical T-Test for d10 particle size distribution (p-value < 0.05). 83

Table 5.3B: Statistical T-Test for d50 particle size distribution (p-value < 0.05). 83

Table 5.3C: Statistical T-Test for d90 particle size distribution (p-value < 0.05). 83

List of Figures

Figure 2.1: Schematic drawing of terrace anatomy 16

Figure 2.2: Illustration of A) Cut and Fill terraces; and B) Strath terraces 17

Figure 2.3: Catawba River Watershed 18

Figure 2.4: Paleo-temperatures of the White Pond pollen section 19

Figure 2.5: Log-log plot of surface age vs. elevation above stream level modified from Mills (2000) 20

Figure 4.1: Surficial geologic map of study area 30

Figure 4.1A: Inset surficial geology map of the upper reach 31

Figure 4.1B: Inset surficial geology map of the upper reach 32

Figure 4.1C: Inset surficial geology map of the middle reach 33

Figure 4.1D: Inset surficial geology map of the lower reach 34

Figure 4.1E: Inset surficial geology map at the end of the study area 35

Figure 4.2: Photograph of cobbles and pebbles on Qt4 tread 41

Figure 4.3: Qt3 exposure (JAC 11) 42

Figure 4.4: Qt3 exposure (JAC 15) 42

Figure 4.5: Log-log plot surface age vs. elevation curve developed in Mills (2000) 43

Figure 4.6: A) RCN – 1; B) RCN – 2; and C) RCN – 3 sample locations 44

Figure 4.7: A) OSL – 1 depth below surface; B) OSL – 1 height above gravels, and C) OSL – 2 depth below surface 45

Figure 4.8: Longitudinal Profile of terrace units (Qt0-5) and the modern channel 46

Figure 5.1: Photograph of relatively unweathered bedrock surface (Qt0) 68

Figure 5.2: Photograph of Qt0 pebbles 69

Figure 5.3: Exposure of Qt1 profile weathered into bedrock 70

Figure 5.4: Photograph of the largest rounded boulder found in the study area 72

Figure 5.5: A) Photograph of gravels found at JAC 15 (Qt3); and B) Photograph of gravels found at JAC 11(Qt3) 73

Figure 5.6: Photograph of the basal contact of the Qt4 terrace unit 74

Figure 5.7: Log-log plot of terrace heights above stream level for Qt5 – Qt0 terraces of this study using Mills (2000) equation..... 75

Figure 5.8: A lin-log plot highlighting the decrease in Hurst color index for most weathered B horizons with surface age (Mills, 2000) 77

Figure 5.9: A lin-log plot of clay fims and surface age (ka)..... 78

Figure 5.10: Lin-log plot of soil texture index values and surface age (ka). 79

Figure 5.11: Lin-log plot of wet consistence index values and surface age (ka)..... 80

Figure 5.12: A lin-log plot of clay content (%) and surface age (ka) 81

Figure 5.13: Ternary plot diagram of particle size analysis (Qt5 - Qt2)..... 82

Figure 5.14: Lin-log plot of iron activity ratios and surface age (ka)..... 84

Figure 5.15: Depletion/Enrichment vs. depth plots for Qt5 - Qt2 surfaces 85

Figure 6.1: Soil depth profile of clay content (%) by location in the study area 94

Figure 6.2: Lin-log plot of iron activity ratios and surface age by location in the study area..... 95

Figure 6.3: Lin-log plot of clast length (cm) and surface age (ka). 96

Figure 6.4: A) Chronostratigraphic chart of the Neogene to present; and B) Inset Marine Isotopic Stages curve from 1.8 Ma – present, with Qt5 – Qt1 ages from Mills (2000) chronology and IRSL dates (Qt3 only)..... 97

CHAPTER 1: Introduction

Rivers and their terraces can give useful insight into Quaternary landscape evolution (e.g. Leigh et al., 2004). Terraces can provide insight on how environmental controls influence the behavior of river systems, can be used to deduce timing and external causes of channel abandonment, and can give insight into topographic generation via isostatic or tectonic processes (Merritts et al., 1994; Pazzaglia and Brandon, 2001). Many studies have been conducted on river systems around the world identifying main driving factors for fluvial processes. In the Piedmont of the eastern US, however, little if any river terrace data exist south of Virginia. Streams in this region differ from their northern US counterparts in that they have not had obvious capture in their Blue Ridge escarpment headwaters, have not faced the effects of glacial loading/unloading, and they head in higher-relief terrain that has possibly endured tectonic rejuvenation (Gallen et al., 2013). Given ongoing debates regarding influences of Cenozoic tectonics and climate variability on landscape evolution (Gallen et al., 2011, Gallen et al., 2013; McKeon, 2014; Pazzaglia and Gardner, 1993), a detailed study of fluvial processes and soil development on fluvial landforms in the Piedmont could yield valuable information into these questions. Objectives of this study are to: 1) produce a detailed geologic map of fluvial terraces of a 45.71 km reach of the Catawba River, and 2) investigate the soils and sedimentology of the terraces. The objectives will provide new insight into the chronology of terrace formation and associated incision of the Catawba in the Piedmont of North and South Carolina, and may therefore serve to generate a new understanding of the river's potential behavior as it pertains to ongoing global change.

CHAPTER 2: Literature Review

2.1: Stream Processes

Streams are unidirectional flowing bodies of water that head in areas of higher elevation. The flow of water in streams will continue to lower elevations until the stream reaches its base level. Base level features are generally a larger channel or an ocean/sea. Streams are a major contributor to landscape evolution, working via incision, lateral planation, and aggradation. The process of incision refers to vertical erosion of the stream channel, resulting in deepening of the channel. Lateral planation is used to refer to migration or widening of the channel. Lastly, aggradation is the vertical accretion of sediments on a stream's floodplain.

All stream processes can be influenced by both tectonic and climatic variations. Variations in these external factors can create changes in base level, the main driving force behind the fluvial processes of vertical/lateral incision and aggradation (Merritts et al., 1994). Tectonics can influence erosion rates and stream morphology through uplift and propagation of stream features, such as knickpoints. Rivers adjust to changes in vertical deformation or base level change through channel modification, specifically by incising, aggrading or altering sinuosity (Merritts et al., 1994). Global and regional scale climate changes can also alter stream behavior, altering discharges of sediment and water. In particular, transitions between glacial and interglacial periods strongly influence streams via changes in eustasy, sediment supply and/or discharge. For example, during transition to glacial periods Pazzaglia and Brandon (2001) found that streams in the Cascadia Forearc, WA carved strath surfaces during sea level lows and glaciation, and

aggraded sediments on the floodplain/fill abandoned channels during transitions to interglacial periods. In this setting, transition to glacial periods and sustained uplift of the forearc caused streams to have sustained periods of incision.

2.2: Fluvial Terraces

Fluvial terraces are planar landforms standing above the modern floodplain or channel that were once a part of the active stream channel and its adjacent floodplain, but are now abandoned due to stream incision. Terraces are composed of three to four main parts (Fig. 2.1): 1) a terrace remnant – refers to isolated portions of a once continuous floodplain, a single terrace unit (same vertical elevation) may be comprised of many individual remnants; 2) the tread – the top, relatively flat, horizontal surface of a remnant; 3) the riser – the sloped separation between adjacent treads; and 4) the strath – the surface laterally carved by the river upon which sediment is deposited. There are three main types of terraces: fill, cut and strath terraces (Fig. 2.2). These terrace types are distinguished by their sediment composition or morphology as it relates to incision of the channel.

In an alluvial river, the channel boundaries and floor are composed of sediment transported by the river. Aggradation on valley floodplains followed by incision into that valley 'fill' will result in the abandonment of the aggradation surface from further deposition, and thus the formation of fill terraces. If incision into the fill is followed by lateral planation, fill-cut terraces will be formed as tread surfaces carved into fill whose total thickness rises higher than the fill-cut terrace's tread.

In a bedrock channel, the channel lies directly on (or within a meter or so) of rock (Merritts et al., 1994). The channel forms the flat, bedrock surface by laterally cutting the

channel. Once this laterally extensive bedrock surface is abandoned from further occupation by the stream, following incision of the channel, a strath surface is left behind. A strath terrace will also contain alluvial sediment, but its thickness is much less than that of a fill terrace. Within these three main terrace classifications, terraces can present themselves as being paired or unpaired. These designations describe whether terraces of the same height above the channel form on both sides of the river (paired) or if only one terrace remnant is formed on one side of the river (unpaired). Over time, fluvial terraces record a stream's response to tectonics and changes in climate. The study of fluvial terraces is important because of the valuable information they provide about the history of a stream and the landscapes they produce.

Fluvial terraces reflect the competition between processes of rock uplift and erosion, i.e. incision and lateral planation. However, it can be difficult to pinpoint the direct mechanism, tectonism or climate change, that produced the landform. Generally, it is thought that during high eustatic stands, channel elevation is static due to higher base level, and erosive powers instead work laterally to carve the valley, forming the floodplains that will become terraces. When base level is lowered via tectonism in the headwaters, sea level drop or incision due to climate change, a surface is abandoned. While studies in the past have looked toward a single mechanism motivating landscape evolution (Leigh, 2008; Castelltort et al., 2015, Picotti et al., 2009, Prince and Spotila, 2013), it is likely that tectonics and climate change both play an important role in the development of fluvial landforms. Below are several studies that support this idea.

2.3: Fluvial Terrace Studies

It is well documented that dramatic changes to global and regional climate can be reflected in river systems (Castelltort et al., 2015; Gallen et al., 2011, Gallen et al., 2015; Leigh et al., 2004, Leigh, 2008, Marple and Talwani, 2000; Merritts et al., 1994; Prince and Spotila, 2013; Reusser et al., 2004, Eaton et al., 2003; Wegmann and Pazzaglia, 2009). Studies around the world have used terraces to evaluate rates of stream erosion, incision, and climatic and tectonic histories along a stream profile. In the Cascadia Forearc, Washington, Pazzaglia and Brandon (2001) used strath terraces along the Clearwater River to evaluate steady-state uplift and erosion. Their findings pointed to increased bedrock incision rates going upstream, <0.1 m/yr. – 0.9 m/yr., respectively, indicating that the cause of incision was uplift of the mountain range, not base level fall of the sea. These calculated rates were similar to published long-term erosion, demonstrating that steady-state landscape evolution has been sustained >10 k.y., meaning that the Clearwater River profile has maintained the same slope through time (Pazzaglia and Brandon, 2001). Dating of terrace units consisted of radiocarbon dates in younger surfaces and relative dating via correlation to well-studied glacial stratigraphy in the region. These dates showed a pattern of strath cutting occurred during glacial advancement cycles at Olympic glacial periods ~ 29, ~71 and ~191 thousand years ago, or at Marine Isotopic Stages (MIS) 2, 4, and 6, respectively. Transitions from these stages into interglacial periods led to increased sediment discharge and aggradation on the strath surfaces due to local deglaciation and eustatic high stand (Pazzaglia and Brandon, 2001).

In another study, Wegmann and Pazzaglia (2009), used fluvial stratigraphy and dating methods to constrain an incisional history of the Bidente and Musone Rivers of the

Po River drainage, in the tectonically active foothills of the Northern Appenines, Italy. Their results from dating of terrace deposits indicated that periods of valley widening and strath formation preceded the coldest and driest climatic conditions during glacial cycles, beginning at MIS 22, or ~1 Ma. Straths were preserved following channel incision during transition into interglacial periods (Wegmann and Pazzaglia, 2009). Incisional events predating MIS 22 are more tectonically driven via base-level change, evident in incised bedrock channels downstream and localized evidence of streams incising through fault-related deposits, and deformation of terraces at the mountain front. Their results contrasted with another study by Antoine, et al. (2007), where incision was found to occur during transition into glacial periods in rivers of tectonically stable Northwestern Europe. This contrast highlights regional differences in channel cutting between stable and active tectonic settings (Wegmann and Pazzaglia, 2009).

Though little research has been conducted on fluvial landscape evolution in the Piedmont of the southeastern US, river systems north of the NC/VA border, such as the Roanoke, James and Susquehanna Rivers have had significant study. The Roanoke River heads north of the border of NC near Lafayette, VA. Prince et al. (2011), documented the river's capture from the New River drainage basin via observation of unique fluvial gravel deposits in the lower relief area along the New River – Roanoke River divide. These sediments contain clasts, such as quartz mylonite, metaquartzite and blue and clear veined quartz, that can be traced back to Blue Ridge lithologies. Evidence of the gravels at several locations along both sides of the divide confirm that incision on the Roanoke River has been caused by its relatively young capture from the New River drainage (Prince et al., 2011). Prince et al. (2011) also noted that the timing of incisional response

caused by rapid base-level lowering is evident in preservation of gravels on upland surfaces and limited weathering of fluvial deposit clasts compared to similar deposits on the New River (1 – 2 Ma). Evidence of a lack of control by structures or lithologic contacts on migratory knickpoints and the observed amount of knickpoint retreat (17 km) supported the idea that stream capture events can create landscape disequilibrium in tectonically quiescent settings.

Further north into Central VA, the James River exhibits similar geomorphic features as the Roanoke River, in migratory knickpoints. Hancock et al. (2003) constructed a paleo-river longitudinal profile, using disconnected terraces along ~200 km of the James River to observe prominent channel convexities and migratory knickzones. ^{10}Be dates of highest terraces at three locations give an age of ~1 Ma. This suggests that incision has been occurring at a rate of ~55 m/m.y. since the late Quaternary. The initiation of such rapid incision was attributed to the headward migration of knickpoints, with migration rate increasing from the Piedmont headward, from ~1 m/m.y. to ~250 m/m.y., respectively (Hancock et al., 2003). Hancock et al. (2003) hypothesized that incisional events were caused by either response to flexural-isostatic uplift induced stream capture followed by denudation, or a shift in climatology from a stable glacial period to rapid interglacial/glacial fluctuations.

Lastly, the Susquehanna River heads at Otsego Lake in southeastern New York and runs through the Valley and Ridge and Piedmont physiographic provinces of Pennsylvania. Pazzaglia and Gardner (1993) used petrography, elevation and correlation of downstream fluvial deposits to derive relative ages of strath terraces of the Susquehanna River in the Piedmont. Upland terraces were found to be middle to late

Miocene in age, while lower terraces ranged from Pliocene to Pleistocene. It was interpreted that straths were cut over the last ~10 m.y. during stable base-level conditions in Miocene and into the Pliocene, with frequency of cutting increasing during interglacial stands in the Pleistocene. These stable conditions were achieved by simultaneous slow, isostatic uplift and eustatic rise. Straths were abandoned via incision during periods of base-level fall caused by eustatic fall during glaciation, with steady isostatic uplift. (Pazzaglia and Gardner, 1993). Three years later, Engel et al. (1996) would expand terrace age constraints on the Susquehanna by studying soil chronosequences in the Valley and Ridge and lower Piedmont. Terrace deposit ages were developed using soil development, observation of glacial derived sediments and correlation to glacial stratigraphy and various glacial and fluvio-glacial deposits in the region. Ages were consistent with Pazzaglia and Gardner (1993), with dates ranging from early Pliocene (~2400 ka) to late Pleistocene (<150 ybp) (Engel et al., 1996). Terrace deposits correlated with the history of the Laurentide glaciation in the region suggested that terraces were the result of heavy sediment load and discharge near the glacial front during glacial intervals. Oldest terraces were of the pre-Illinoian (2500 – 200 ka) glacial period, while subsequent strath terraces were a result of advancement and retreat of the Wisconsin glacial period (75 – 11 ka) (Engel et al., 1996).

Insights developed in these studies can be used as comparison to results found along the Catawba River. Headwaters of the largest rivers in this southeast region, where the Catawba is located, originate on the south-facing escarpment of the Southern Blue Ridge Mountains. In contrast, the Roanoke River and other large rivers northward, originate further west in the Valley and Ridge province (Prince et al., 2011; Leigh, 2008).

Streams north of this project's study area are characterized by increases in incision over the last 10 m.y. that is thought to reflect the influence of visible stream capture occurring across the Blue Ridge Escarpment (Pavich et al., 1985; Hancock et al., 2003; Pazzaglia and Gardner, 1993). Stream capture in the headwaters of the Catawba into the Blue Ridge, however, is not significant (Fig. 2.3). A large turn along the front edge of the Blue Ridge Escarpment appears to be a small capture event, in comparison to neighboring systems in the Yadkin and Roanoke/New River which have large, curved captures. In addition, rivers of the northern Appalachians have been strongly influenced by base level changes associated with glacial loading and unloading (Pazzaglia and Gardner, 1993). It is not likely that effects of glacial rebound influence terrace formation along the Catawba River because the nearest ice was ~600 km to the north. Thus, the Catawba River likely provides the potential to more clearly evaluate the influence of glacial versus interglacial climates on stream aggradation and incision.

2.4: Tectonics of the Southeastern US

The Appalachians and southeastern United States are thought to have been, relatively, tectonically dormant for approximately ~180 to ~270 Ma (Dallmeyer et al., 1986, Goldstein and Brown, 1988; Miller et al., 2013; Gallen et al.,2013; Bank, 2001). Evidence for deformation in the Appalachians occur in the form of ancient fold and thrust belts, most of which also accommodate normal and shear components (Bank, 2001; Berger and Johnson, 1980; Cook et al., 1979; Goldstein and Brown, 1988; Roper and Justus, 1973). Furthermore, active tectonics of the Piedmont and Coastal Plain has been observed in the form of rare, shallow seismic response to deep crustal and buried faulting. This seismicity is typified by the historic 1860 Charleston earthquake, and more recently

the 2011 Mineral, VA earthquake (Marple and Talwani, 2000; Horton and Williams, 2012). What is not clearly documented, are intervening times of deformation that may have occurred during the Cenozoic. The deep weathering of deposits of this age precludes identifying contacts of offset materials. Nevertheless, the steep morphology of the Piedmont and adjacent Blue Ridge are suggestive of possible active tectonics (e.g. Gallen et al., 2013).

At the base of the eastern margin of the Blue Ridge province along NC, SC and northern GA lies the Blue Ridge Escarpment. The origin of this sharp boundary has been poorly understood for a better part of the last century (Bank, 2001). In his thesis, Bank describes Wright's (1927) investigation into the escarpment genesis by crustal extension. This hypothesis was predicated on the presence of a straight slope break at the base of the escarpment, unequal slopes on either side of the proposed fault zone, the presence of short parallel streams draining the upthrown block, and the existence of bedrock displacement. Wright found no evidence of more recent faulting along the escarpment (Bank, 2001). On the northwestern side of the escarpment, within 10 km (Bank, 2001), lies the Brevard Fault Zone. This zone is a distinctive easterly dipping zone stretching over 600 km, from Horseshoe Bend, AL to the NC/VA border (Roper and Justus, 1973). It has been interpreted as a stratigraphically coincident thrust fault (Cook et al., 1979) with localized brittle faulting (Goldstein and Brown, 1988).

Moving into the Piedmont physiographic province of NC, SC and VA, there are relatively few named and unnamed bedrock faults, that are buried and thus interpreted to be dormant. Two such faults occur within proximity to the Catawba River. They are the Eufola fault and the Boogertown shear zone, and it's neighboring en echelon shear zones,

i.e. Kings Mountain shear zone and Gold/Silver Hill shear zone. Many of these structures, particularly the latter, have been shown to be associated with the accretion of the Charlotte and Carolina Terrane to Laurentia. However, evidence of this is limited and poorly understood due to overshadowing by Alleghanian shortening after these sutures formed. The Gold Hill and Silver Hill shear zones have been established as sinistral reverse faults and strike-slip structure. This structure introduces phyllonite and phyllonitic schist into the center of the study area, but this does vary as you move along the fault, likely due to reactivation throughout the late Paleozoic (Hibbard et al., 2012). Studies regarding recent activity of these faults is nonexistent, and therefore analysis of fluvial response to such activity is also nonexistent (Price, 2011). These structures, however, are important to the general overview of this study in their potential to reactivate causing minor to moderate earthquakes. Evidence of such events are being recorded on a daily basis, the last known event to have occurred approximately four months ago near Cumberland, VA; at a depth of 7 km and a magnitude of 2.6 (Earthquake tracker, 2015). The most notable of the past five years occurred on August 23, 2011 near Mineral, VA. This quake was recorded at a magnitude of 5.8, and was among the largest on the eastern seaboard during a 400-year historic record. The epicenter of the event is located within the Central Virginia seismic zone (CVSZ), a zone of persistent low-level seismicity (Horton and Williams, 2012).

A last tectonic zone of interest is that of the largest eastern U.S. earthquake (M_w7.3, Johnston, 1996; as cited in Marple and Talwani, 2000) in historical times. This system, known as the East Coast fault system is a ~600 km long north-northeast trending buried fault system spanning the Coastal Plain of the Carolinas and Virginia. Marple and

Talwani (2000) observed geomorphic evidence of localized long-term uplift (~0.16 mm/yr.) in the presence of preserved marine terraces and landforms, and longitudinal profiles of several streams as a possible influence of stream flow deflection in a north-northeast direction in rivers in the Coastal Plain by causing the valley to tilt in the north-northeast direction. Such features, as those mentioned above, present along the Catawba River upstream from the Coastal Plain and fall line could possibly indicate fluvial response to displacement along the East Coast fault system.

2.5: Paleoclimates of the Southeastern US

Knowledge concerning how paleoclimatology has influenced rivers and streams of the southeastern Piedmont of the United States is poorly understood (Leigh, 2008). In Leigh (2008), pollen section data collected from the North American Pollen Database was used to construct paleoclimates in the lower Piedmont and Coastal Plain of the Carolinas and Georgia. Pollen was derived from White Pond, SC, located near the western bank of the Catawba River, and Clear Pond near Myrtle Beach, SC. In the study, it was inferred that the region experienced the same global cooling events of the MIS 5e/5d boundary (~115 ka) and MIS 5/4 boundary (~80 – 70 ka) based on deep sea and ice core records. Streams during this period are interpreted to be braided systems dominated by eolian sedimentation based on OSL dates of parabolic dune deposits from ~85 – 30 ka (Ivester et al.,2001; as cited in Leigh, 2008) and a >36,000 ^{14}C ypb date (Thom, 1967; as cited in Leigh, 2008). After 30 ka, pollen data suggested that the climate continued to remain relatively cool and sedimentation continued to be controlled via eolian processes until ~16 ka. The paleo-biome during 30 – 16 ka is reconstructed with the presence of widely spaced pine forests and fields of herbaceous vegetation, much like a savanna

biome. Given the cooler climate, it is inferred that snowfall and snowpack were common throughout the colder months during 30 – 16 ka, suggesting that periglacial processes might have operated in the highlands such as those in the headwaters of the Catawba (Leigh, 2008). This inference is further based on the observance of block fields and solifluction deposits in the Southern Appalachians and adjacent foothills (Hadley and Goldsmith, 1963; Kerr 1881, as cited in Leigh, 2008). At ~16 ka, Leigh (2008) suggests that a transition to a warmer climate occurred at the end of the Pleistocene. Based on pollen sections, this period (16 – 11 ka) exhibits the highest dissimilarity in pollen types, advocating a rapidly changing climate regime (Leigh, 2008). Warmer temperature induced more precipitation in the region, allowing for more vegetation to grow and retain the heat through the area's moisture rich biome. It has been suggested that the Piedmont and Coastal Plain was dominated by temperate deciduous forests during this warming event (16 – 11 ka) (Leigh, 2008). Leigh (2008) cites Watts (1980) who argues that though temperatures warmed, they were still cooler than today. He also argued that it was moister between 16 – 11 ka than present day conditions, based on the abundance of beech (*Fagus*) pollen, which requires moist soils through the warmer growing seasons (Leigh, 2008). Leigh (2008) also suggested that this transition in climate signaled a transition in streams from braided channels to channels with large scrolled meanders (Fig. 2.4). This switch was dated at ~16-15 ka, and characterized by reduction in hillslope sediment yield via stabilization of banks through increased vegetation and abundant runoff induced channel incision and terrace formation. Features of the transition to meandering channels are well preserved on the southeast Coastal Plain in the form of meander scars, oxbow lakes and sandy scrolled point bars on all major river systems of the southeast Coastal

Plain (Leigh 2008). Small scale fluctuations in climate from ~16 – 11 ka were followed by the early Holocene warming (~11 – 5.5 ka). This period was characterized by progressive overall warming of the planet, reflected in deep sea and ice core data, and a reduction of meander size. Finally, in the last ~5.5 k.y. temperature, precipitation and vegetation established the assemblage that is identical to conditions today (Leigh, 2008). These conditions are characterized as humid subtropical with hot and moist summers and mild to cool winters, where precipitation peaks in the summer months.

2.6: Previous work on the Catawba River

There have been two studies of fluvial terraces along the Catawba River, both in the large meander bend found south of Lake Norman (Layzell et al., 2012; Aquino, 2014). Layzell et al. (2012) mapped terraces at Duck's Cove at the Cowan's Ford Wildlife Refuge within the USGS Mountain Island Lake and Lake Norman South 7.5' Quadrangles. Terraces units were identified by terrace tread elevation, soil development, stratigraphy, and sedimentology. Terrace ages were assigned based on a comparison of tread elevation above the channel to regional surface age/elevation curves published by Mills (2000) (Layzell et al., 2012). Layzell et al. (2012) mapped five distinct unpaired terrace treads ranging from 3 – 42 m in elevation above the modern channel. The highest tread (Qt1) at 42m, was dated using the Mills (2000) empirical relationships at 1,470± 180 ka. Subsequent terraces were dated at: Qt2 610± 75 ka, Qt3 128± 16 ka, Qt4 50± 6 ka, and Qt5 4± 0.5 ka (Fig. 2.5).

Layzell et al. (2012) observed progressive increments in color hue and pedogenic iron and clay content from young to old terraces. Soil clay content (21.9% to 62.6%,

R^2=0.951) and pedogenic iron (3.6% to 6.4%, R^2 = 0.827) showed statistically strong correlations with increasing age and tread elevation. Soil hue in all treads ranged from 10YR in the lowest terrace (Qt5) to 2.5YR in the highest terrace (Qt1) (Layzell et al.,2012). All terrace units contained prominent Bt horizons. Overall, soil development plateaued after an estimated terrace age of 128 ka (Layzell et al., 2012), as is typical in older soils (Birkeland, 1999). Qt5 exhibited the weakest soil development because of its horizonation (A/B/Bt) and its loamy texture and lack of clay content. Qt4 comprised of sandy and silty parent material, and exhibited slightly more development with A/Bt horizonation. Qt3 was distinguished by a well sorted, compacted sandy layer at 2.4 m depth and clay grading upward into clay loam and loam, and similar horizonation as Qt4. Qt2 contained pebbly quartzite clasts, a clay grading upward to silty loam and an Ap horizon. Qt1 was characterized by alluvial sediments and clayey structure grading upward to clay loam, with similar disturbances in the A horizon as Qt2 (Layzell et al., 2012).

Aquino's (2014) study mapped nine additional terrace remnants found within Layzell's et al. (2012) field area at Duck's Cove. Sediment size distribution changed markedly from youngest to oldest terraces with clay content ranging from 15 to 70%. These changes were interpreted as evidence for significant instances of change in river competence and capacity, possibly coinciding with large-scale events, such as climate change or increased construction and industrialization. Here, I seek to expand these studies – which were limited in geographic scope – to determine if they are characteristic of the entire Catawba River in the Piedmont.

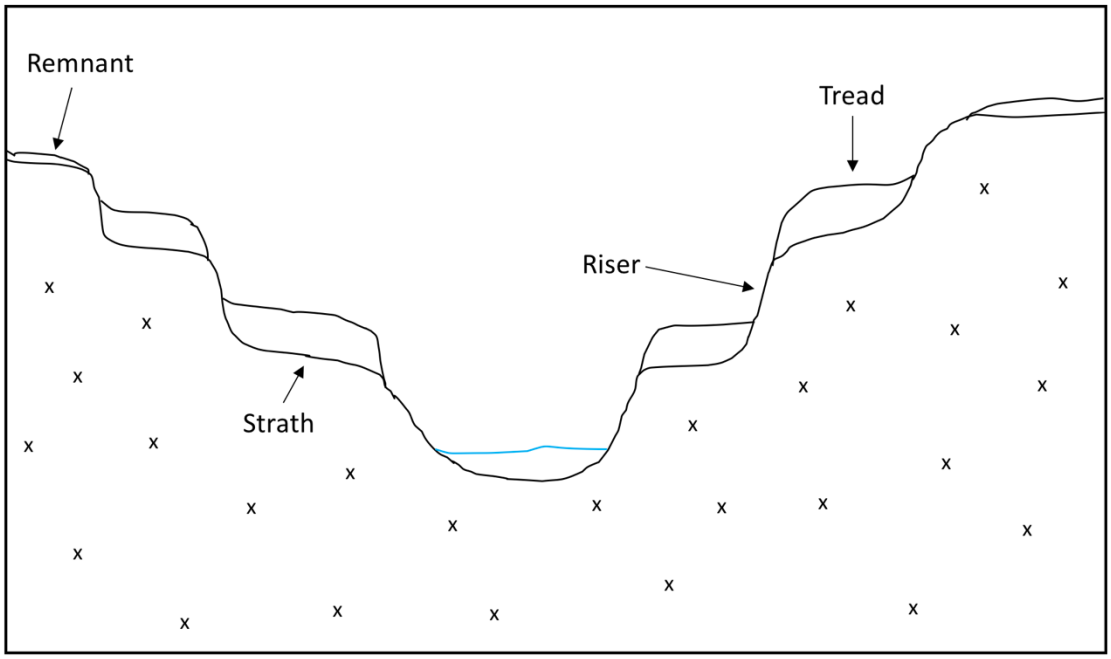

Figure 2.1: Schematic drawing of terrace anatomy, where the vertical wall represents the riser, the flat top of the step is the tread, and the top of the ‘x’ surface beneath each blank lobe represents the strath.

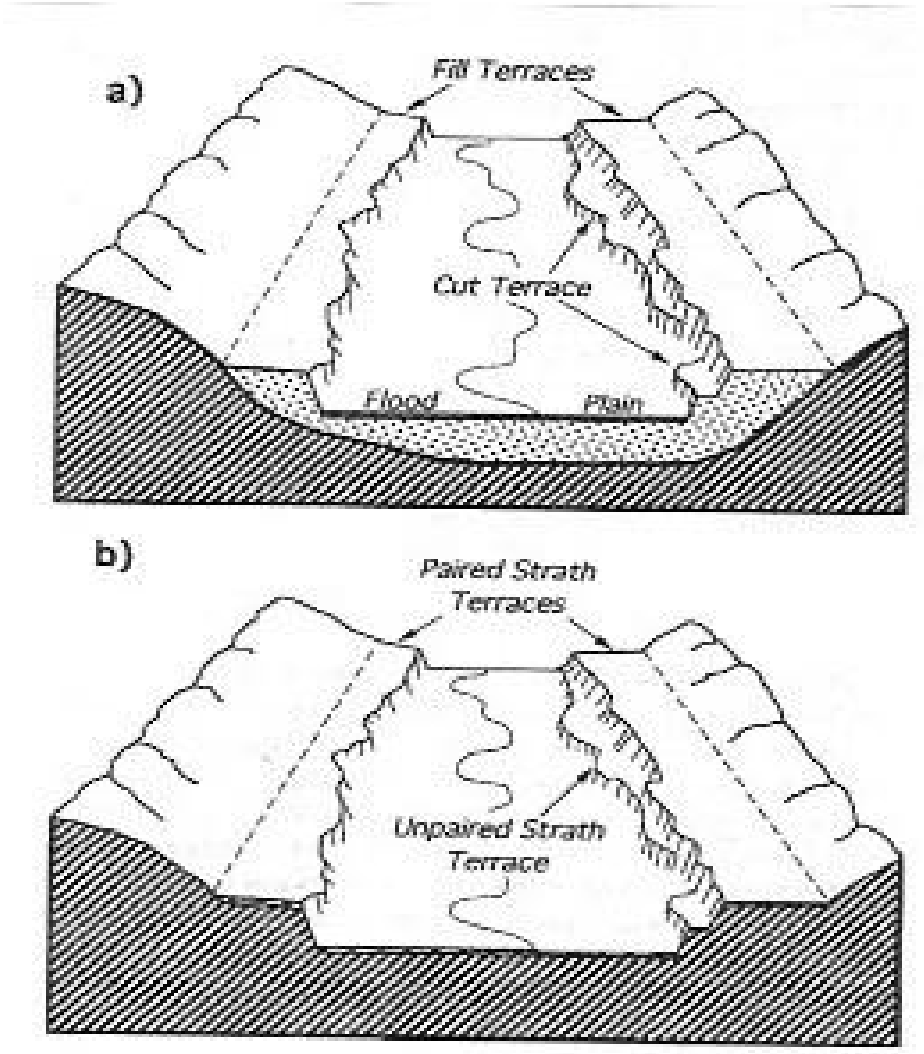

Figure 2.2: Illustration of the three different types of terraces. A) Cut and Fill terraces above the floodplain in an alluvial valley fill (stipple), and B) Strath terraces, both paired and unpaired, on underlying bedrock (diagonal lines). Image retrieved from Merritts et al., (1994).

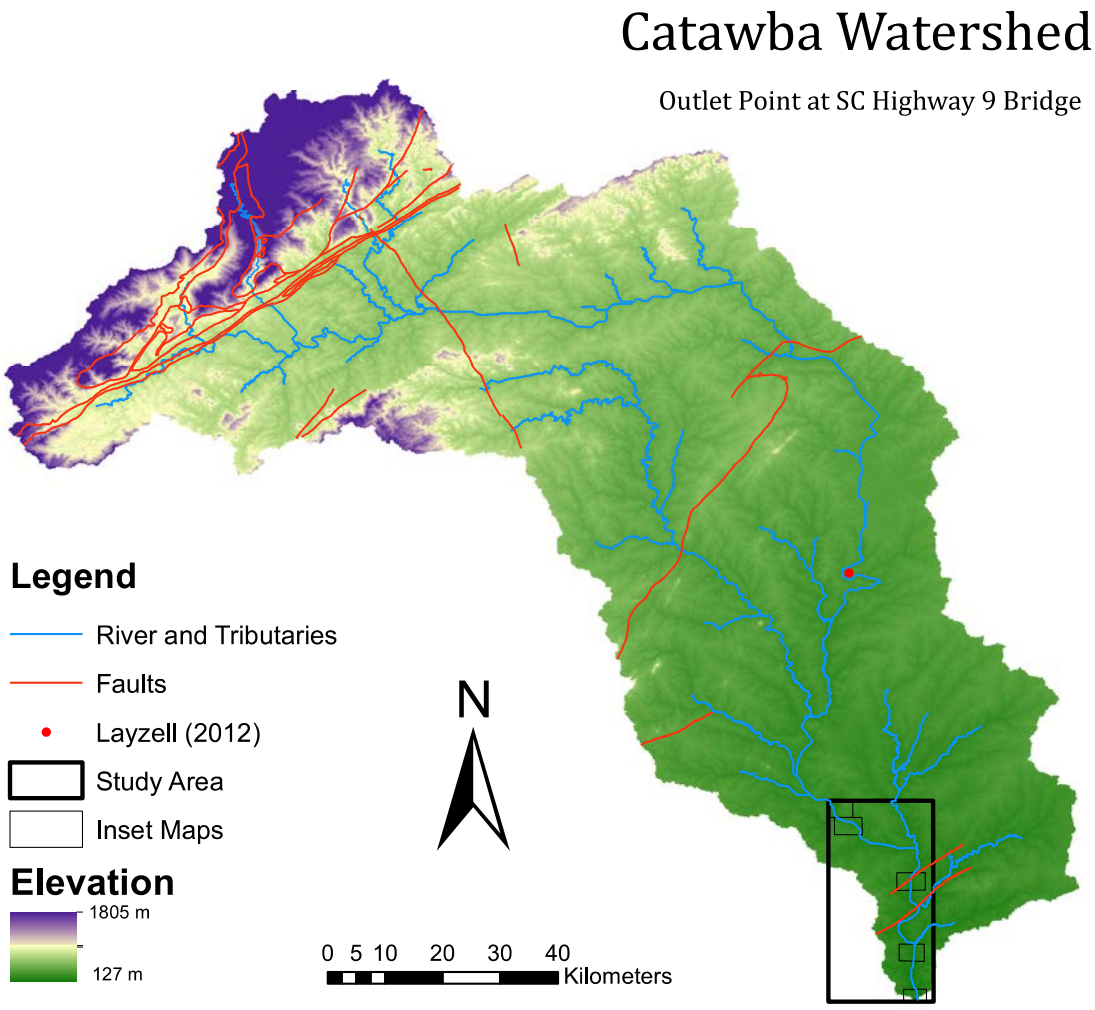

Figure 2.3: Catawba River Watershed, from headwaters to the end of the Study Area. Base Map is shaded relief DEM with stream network of main channel and tributaries. Layzell (2012) and study area represent in lower reach of stream network. Study Area is represented in Figure 4.1. Inset Maps are represented in Figures 4.1A, B, C, D and E.

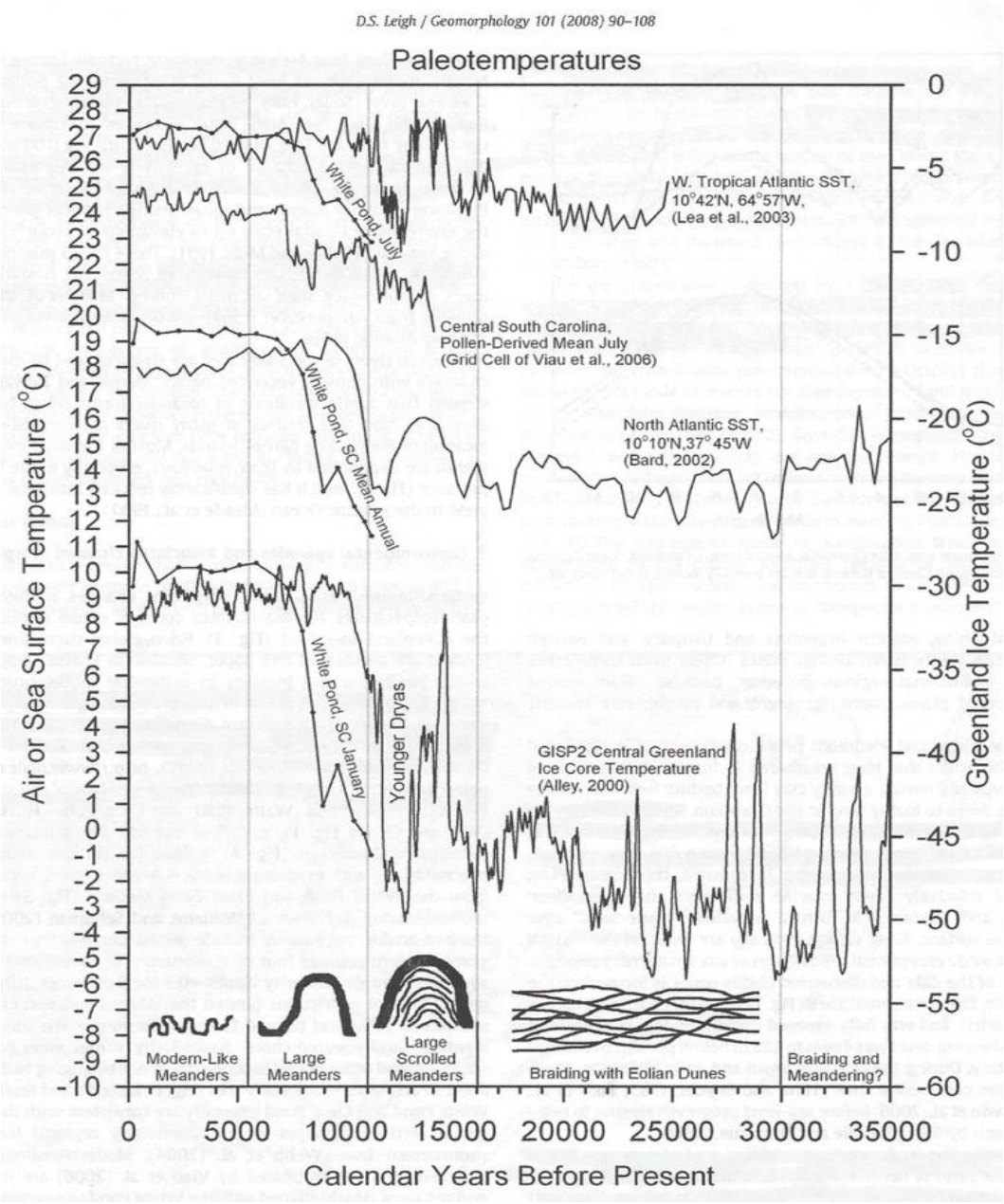

Figure 2.4: Paleo-temperatures of the White Pond pollen section, highlighting January, July and the mean annual temperature over the last ~11,000 years. These are compared to Greenland Ice temperatures based on several cored samples. At the top of the x-axis are assumed periods of river behaviors of the Piedmont and Coastal Plain rivers, highlighting Leigh (2008) overall conclusion of a transition from braided to meandering systems ~16ka. Figure retrieved from Leigh (2008).

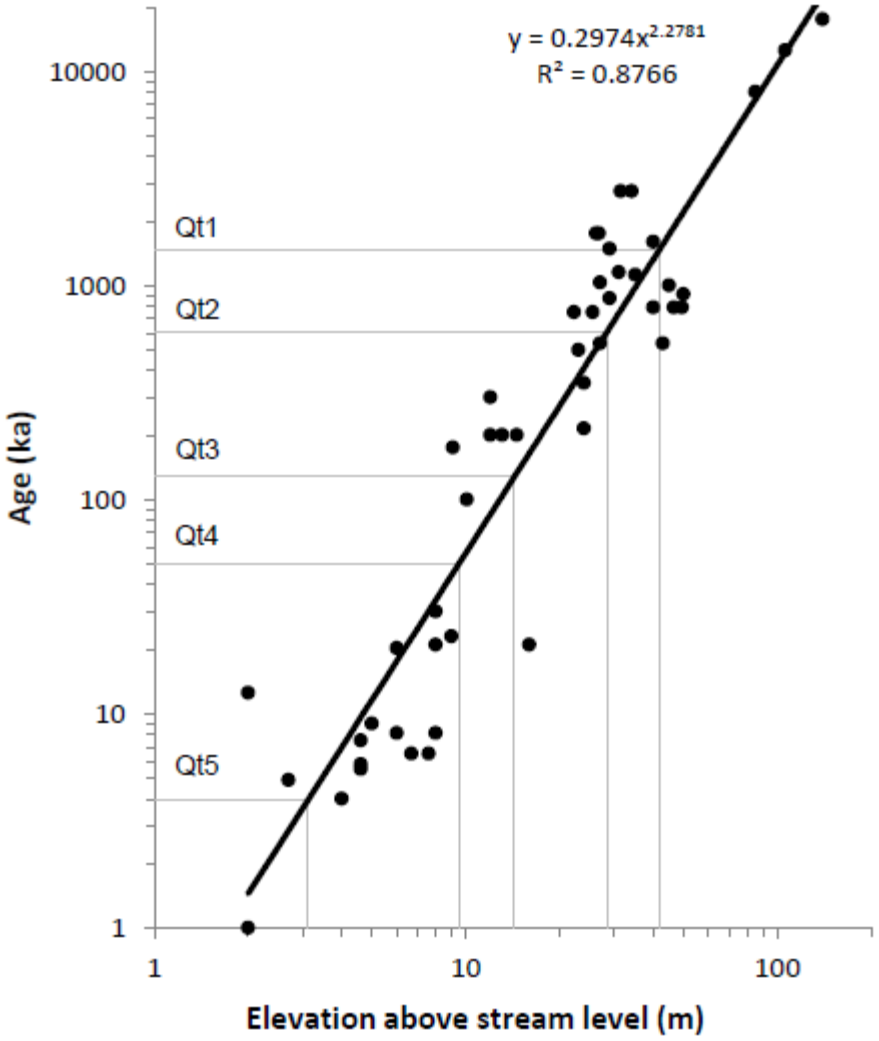

Figure 2.5: Log-log plot of surface age vs. elevation above stream level modified from Mills (2000) by Layzell et al., (2012).

CHAPTER 3: Study Area and Geology

The Catawba River is approximately 350 km long and heads on the eastern slopes of the Blue Ridge Mountains at elevations of ~1805 m in western North Carolina (Fig. 2.3). The Catawba River ends in the Piedmont of South Carolina where it flows into Lake Wateree, and becomes the Wateree River. Further downstream within the Coastal Plain this body of water becomes the Santee River at its junction with the Congaree River. The entire fluvial system deposits its waters and sediment load into the Atlantic Ocean, northeast of Charleston. SC. On the piedmont, the Catawba is a relatively straight – with only minor meandering – bedrock stream channel. The watershed of the Catawba-Wateree at its outlet into the Congaree drains approximately 9,000 km^2 of North and South Carolina. The river is supplied by its major tributaries the Johns, South Fork Catawba, Henry Fork, and Jacob Fork Rivers. It also contains eleven man-made lakes, which serve as a source of hydroelectric power for several communities in the Foothills and Piedmont of North and South Carolina. The study area is located within the longest free flowing stretch of water that stretches from the Lake Wylie Dam to SC Highway 9, north of the next impoundment at Fishing Creek Reservoir.

The USDA NRCS soil surveys indicate that higher terrace tread soils of this study area (generally Qt3 – 0, see below) are Typic, Aquic, or Oxyaquic Hapludults, of the Cecil, Pacolet, Masada, Georgeville, Hard Labor and Helena Series. Lower terrace tread soils (Qt5 – 4) are characterized by soils that include Fluventic Dystrudepts and Typic Udifluvents, of the Starr, Chewacla, Riverview, and Toccoa Series.

The bedrock of the field area reach within the Catawba Basin comprises a group of meta-intrusive and meta-volcanic rocks, known as the Charlotte Belt Group. Rock

types range from gabbro to granite, and include some metamorphosed diorites and biotite gneisses. Upstream of the field area, rock types include: biotite, mica and amphibolite gneisses and schists.

The climate of the field area reach of the Catawba Basin is characterized as a humid subtropical climate with dry and cool winters, and hot and moist summers. Modern average annual precipitation is approximately 111 cm. Average temperatures range from -1.2°C in January to 32.6°C in July. Mean annual temperature for the region is 15.9°C (NOAA, 1981 – 2010). The highest elevations of the basin are currently characterized by relatively warm and wet summers and cold, dry winters. Average annual precipitation is ~133 cm. Average temperatures range from -4.5°C in January to 32.2°C in July, with an annual mean of 14.2°C (NOAA, 1981 – 2010).

CHAPTER 4: Methods

4.1: Field Methods

Terraces were mapped using USGS topographic US 2D overlay maps in Google Earth, with a map scale of 1:18,180 and a 3 m contour interval (Fig. 4.1, Fig 4.1 A – E). During mapping, a GPS unit was used to aid in determining location. The elevation feature was not employed due to errors of +/- 10 m. Terrace units (Qt0 – Qt5, where Qt5 is the youngest terrace, by convention) were assigned based on relative height above the channel, and stratigraphic context. Terraces were thus identified by walking perpendicularly up from the modern Catawba River to the highest point in the drainage. Treads remnants were identified based on flatness of the surface (1 3-meter contour per tread area) and, more importantly, if the surface contained at least several rounded cobbles or pebbles gravels of obvious fluvial origin (Fig. 4.2). For each mapped terrace, we collected measurements of the length of the long axis (from 2 – 3 of these found pebbles), as well as making note of their roundness/sphericity using a comparison chart (Krumbein and Sloss, 1963). Surface clasts were chosen based on availability on older surfaces, size, smoothness and roundness. Generally, the size of the largest surface clast found on any given mapped terrace was recorded, while making note of smaller surface clasts.

For each terrace, in any location where large (> ~60 m^2) patches of river gravels were found, clast counts were recorded in the following manner: a 10 m tape was laid out along the collection of gravels. At every 50 cm the clast that intersected the transect was selected. The long and short axes of each clast were then measured in inches using

calipers. These measurements were later converted to centimeters. This method was repeated for five transects, spaced at least 0.3 m apart, until 100 cobbles/pebbles had been measured. At least two clast counts were completed for each terrace unit, apart from the highest terrace units (Qt1 and 0), which lacked sufficient gravels in any given location.

In addition to mapping terrace treads, strath surfaces as well as exposed bedrock were mapped wherever they were encountered, typically in small channels incised into terraces. Their location, elevation, extent of weathering (ex: saprolite vs. oxidation), and any geologic structures present were noted. After mapping in the field, the elevations of these mapped treads and straths were taken from the topographic maps based on their GPS locations.

A total of thirteen soil pits were dug and described on the mapped terraces (Figures 4.1A, B, C, D, and E; Table 4.1), generally with 2 – 3 pits per terrace unit. No pits were dug on the Qt1 or Qt0 terrace units due to complete erosion of any fluvially deposited sediments. In addition to the thirteen soil pits, two construction site exposures of Qt3 sediments were also described.

All soil pits were dug in the center and on the highest points of terrace treads, away from slopes and terrace scarps in order to minimize both erosion and deposition via colluvium from higher treads. Pits were dug until relatively unweathered material was identified or, in case of younger units, until ~150 – 200 cm depth was reached. Overall, the locations of the pits were grouped in three major locations along the study area (Fig. 4.1A, B, C, and D), whose locations were identified based on access and permission from landowners. The three locations were located along the entire study reach near Rock Hill, Van Wyck, Landsford and Fort Lawn, SC, from north to south respectively – hereafter

referred to as: the upper, middle, and lower reach. The two excavated exposures of the Qt3 were in Riverview, SC in the upper reach and in Fort Lawn near SC Highway 9 in the lower reach (Fig. 4.1B, E, Fig. 4.3, and Fig. 4.4).

Soils were described in detail using Birkeland Appendix A (1999), including color, gravel percentage, texture, structure, consistence (moist and wet), clay films, horizon boundaries roots and pores (Table 4.2). Parent Material was also described based on type (saprolite vs. sediments), grain size, minerals present and structures. Soil horizons were identified by changes with depth of various soil properties. Samples were collected from each horizon in each soil pit for laboratory analyses (see below). Where horizons were >15 cm thick, multiple samples were taken by subdividing horizons.

4.2: Age Dating Methods

After mapping, in order to determine the age of terraces mapped in the study area, I combined terrace tread height, soil and stratigraphic data with two numeric age dating techniques. First, Mills (2000) demonstrated that surface age can be estimated using height above the channel for river terraces in the eastern United States. A regression was developed for terraces that had been independently dated (Mills, 2000). Using this regression, combined with measured tread heights from this study, an age can be calculated for the terraces mapped herein. I estimated heights above the modern channel of the Catawba River by noting the highest elevation of each mapped terrace remnant using the 1:18,180 scale of the topographic maps. For long remnants that experience elevation changes on their surfaces downstream, the highest upstream elevation recorded was used. Distances downstream for terrace remnants were based on the starting distance of the remnant in the study area. Every five kilometers downstream from the beginning of

the study area, an average elevation was calculated for each terrace unit that was exposed in the 5 km reach. This average was then subtracted by the elevation of the channel in the 5 km reach. These differences were then averaged to reveal the height values, and plugged into the surface age/elevation curve (Fig. 4.5).

In pits on younger surfaces, where charcoal was encountered, three samples were collected and sent for analysis at DirectAMS. Specifically, the following samples were collected and sent: 1) RCN – 1, collected at ~1 m depth below surface and ~1 m height above base in soil pit JAC 10 (Qt5) in the lower reach, this sample did not survive analysis; 2) RCN – 2, collected ~ 1 m depth below surface and ~9 m height above base in soil pit JAC 1 (Qt4) in upper reach; and 3) RCN – 3, collected at ~1 m depth below surface and ~1.5 m height above base in soil pit JAC 3 (Qt5) in Riverview, SC (Fig. 4.6 A, B and C).

In addition to radiocarbon sampling, tube samples were obtained for Infrared Stimulated Luminescence in the two excavated exposures and in two soil pits. Two samples were collected and sent to the Utah State Luminescence Laboratory in North Logan, UT for analysis and evaluation. Specifically, the following samples were collected and sent for analysis: 1) IRSL – 1, collected ~2.5 m depth below surface and ~1 m height above base in soil exposure JAC 11 (Qt3) in Fort Lawn, SC; and 2) IRSL – 4, collected ~ 4 m depth below surface and ~ 0.01 m height above basal gravels, in JAC 15 (Qt3) exposure in Riverview, SC (Fig.4.7 A, B and C).

4.3: Topographic Analysis and Laboratory Methods

Mapped terrace remnants were plotted on a longitudinal profile in order to evaluate channel morphology. This was completed by first, carefully drawing out the

thalweg of the Catawba River from the beginning of the field area at Lake Wylie Dam, down to the end of the field area at SC Highway 9. The length of each segment of the thalweg was measured on the map in mm, and recorded to estimate distance downstream in the study area. Thalweg segments were converted to km by using the map scale (1:18,180), then added up to get a cumulative distance of 45.71 km. Then, two lines from each mapped terrace remnant were drawn perpendicular to the thalweg to determine the remnant's position downstream in the study area. The position and length of each remnant was calculated using the map scale (1:18,180). Distances (km) for the beginning and end of each mapped terrace remnant were recorded and then plotted in MS Excel from 0 – 45.71 km, i.e. the reach distance of the study area (Fig. 4.8).

Soil samples obtained from exposures and pits were taken back to the Soils laboratory at UNC Charlotte and analyzed for major elements (XRF), pedogenic iron, particle size analysis, and bulk density (Table 4.3). From each sample, two to three peds were removed from bulk samples to be analyzed for bulk density using the paraffin clod method (Blake 1965; Singer 1986). Samples were then split using a large splitter to ensure random sampling. After splitting, one split was sieved to the 2 mm fraction and set aside to air dry for at least 24 hours. Weighed portions of some of the air-dried samples were then crushed on the SampleTek vial rotator Model 200, until samples could pass through a 100-mesh sieve. For each analysis run, there were 25 duplicate samples set aside in order to derive analytical error for each analysis.

Crushed samples were also used for elemental analysis on an X-Ray Fluorescence analyzer. XRF samples were run against a blank (ambient air) and standards comprised of dunite, andesite and rhyolite, with known concentrations of several elements. Standards

and blanks were measured at the beginning and ending of sample runs to ensure accurate readings of samples. Standard concentrations were then subtracted by blank background measurements to build standard curves for each set of sample runs. Standard curves were then used to derive semi-quantitative concentrations of chosen elements in each sample. Crushed samples were used for extractive chemical analysis of pedogenic iron via citrate-dithionite (Mehra and Jackson 1960). and hydroxylamine methods (McDonald et al., 2015). Extracted samples were then analyzed on an Atomic Absorption Spectrometer.

Bulk density results were utilized to assess total iron (g/cm^2) for each sampled horizon. To derive total iron, the following equation was used:

$$\text{Amount of Fe per Horizon (g)} = (\text{Hth} * \text{BD}) * (\text{Fe}_D/100)$$

Where: Hth is Horizon thickness (cm), BD is Bulk Density (g/cm^3), and Fe_D is weight percent of Fe from Dithionite extraction. For each pit, total iron (g/cm^2) was summed then normalized by dividing by total pit depth.

Particle size was measured on < 2 mm portion using a Laser Diffraction Particle Counter to assess particle size of each horizon (Day, 1965; Jackson 1969). For the latter, organic digestions were completed on all A horizons to avoid interference or organic particles.

In addition to laboratory analysis, field data were consolidated into indices for each soil pit. Specifically, Hurst Index values were calculated to evaluate color as a morphological property. This index converts Munsell Hue to a single number (i.e. 10YR = 20) and then multiplies this number by the quotient of Munsell Value/Munsell Chroma (see below). For example, a Munsell color of 10YR 5/6 would result in a Hurst Index Value of 16.67.

Hurst Index Value = Assigned Hue value * (Munsell Value/ Munsell Chroma)

Indices for evaluating clay films were developed by assigning numbers 0.5 – 3 based on amount of clay films, and 1 – 3 based on prominence of clay films.

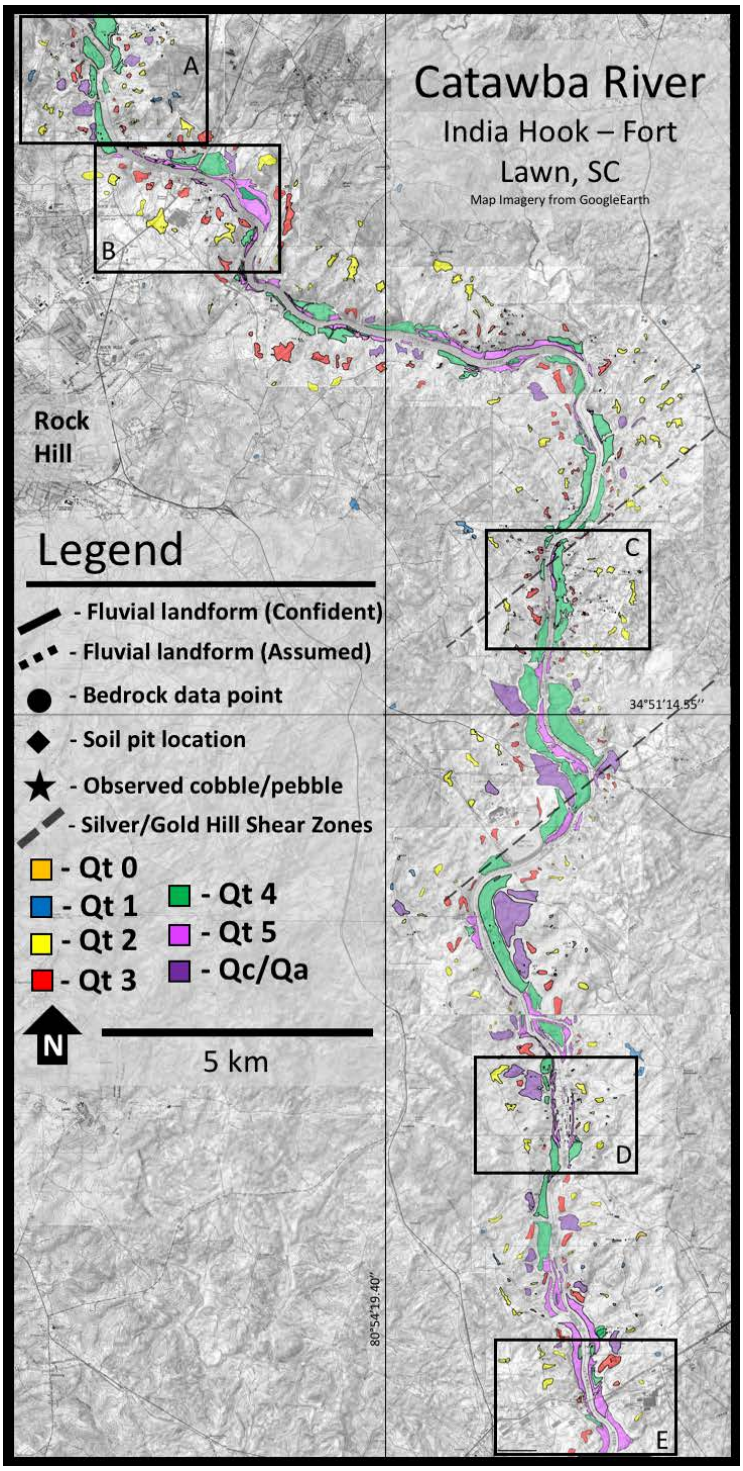

Figure 4.1: Surficial geologic map of study area (Inset from Fig. 2.3), from India Hook, SC to SC Hwy. 9 in Fort Lawn, SC. Maps shows Quaternary terraces unit tread remnants and treads (Qt0– Qt5), where Qt5 represents the modern floodplain. Base maps were derived from USGS topographic overlay in GoogleEarth.

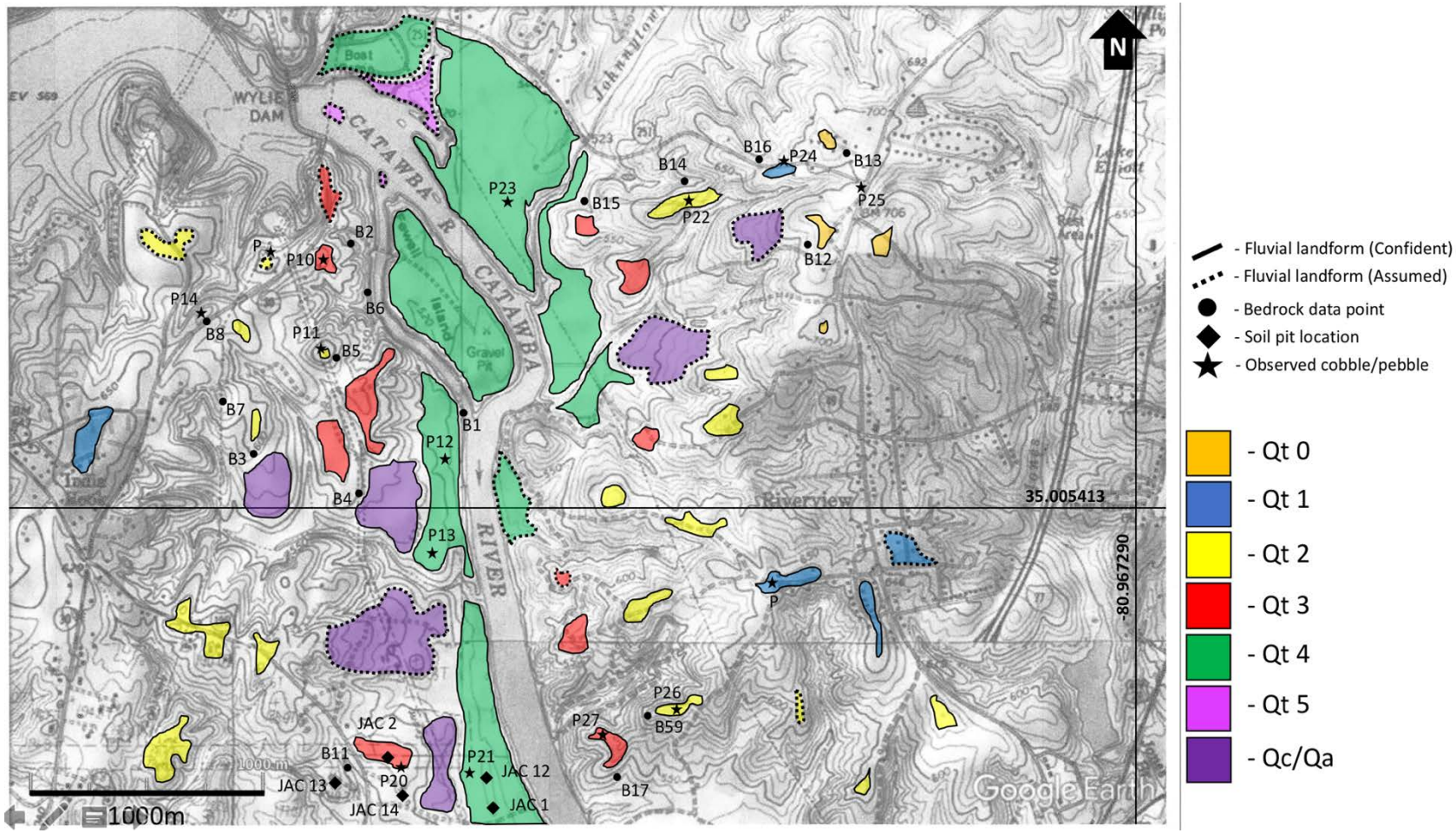

Figure 4.1A: Inset surficial geology map of the upper reach of the study area, Riverview, SC.

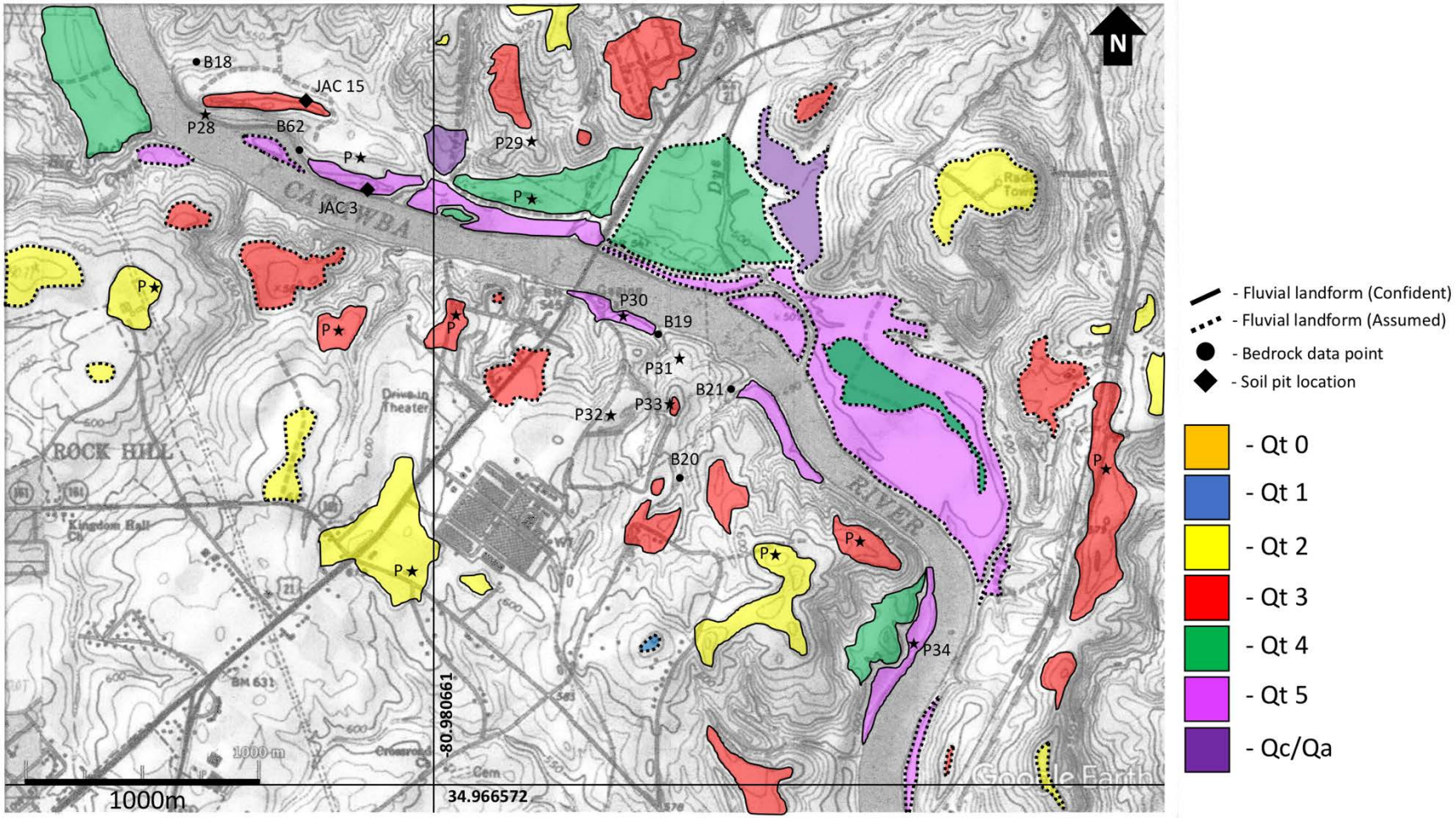

Figure 4.1B: Inset surficial geology map of the upper reach of the study area, Riverview, SC.

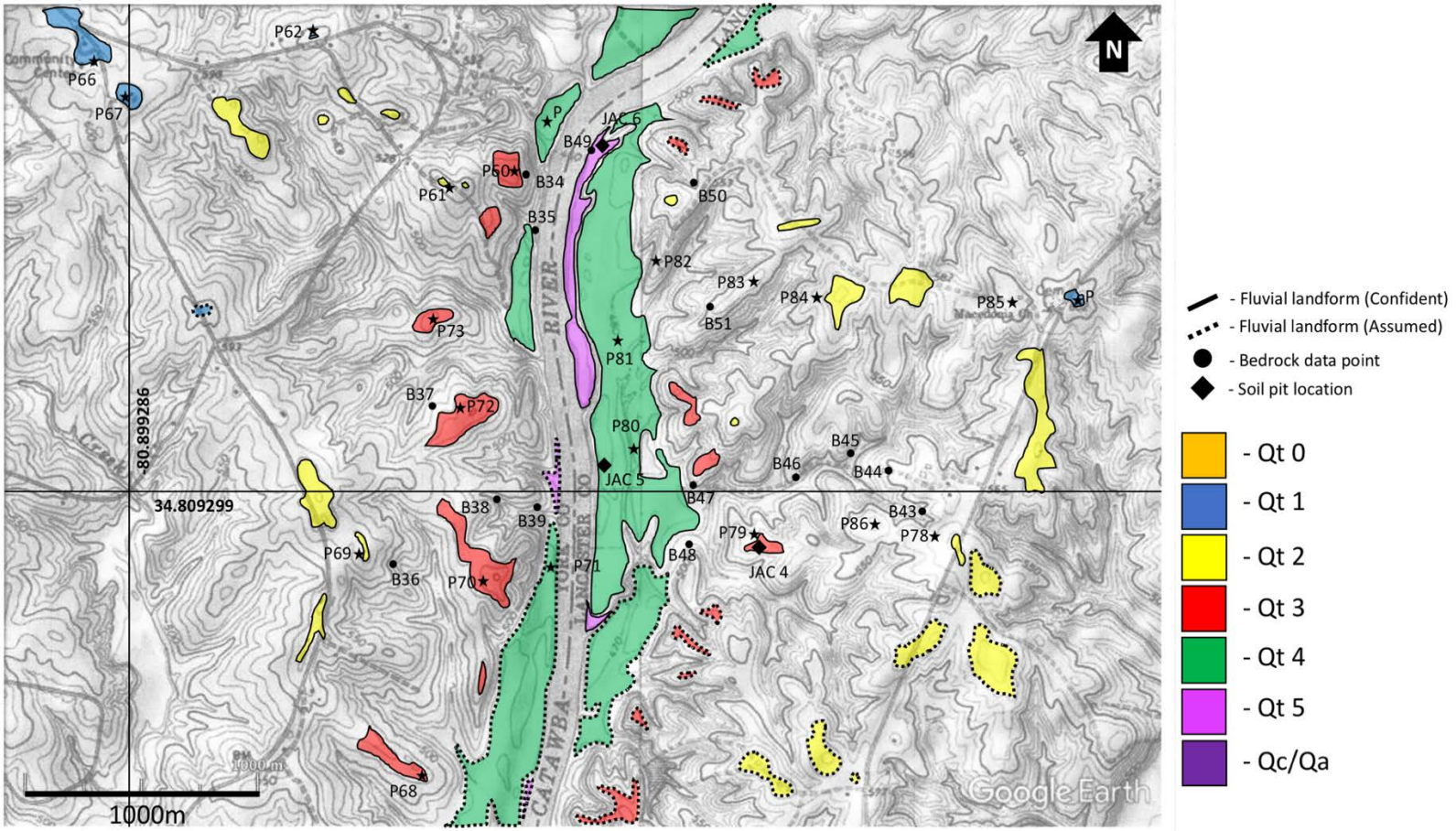

Figure 4.1C: Inset surficial geology map of the middle reach of the study area, Van Wyck, SC.

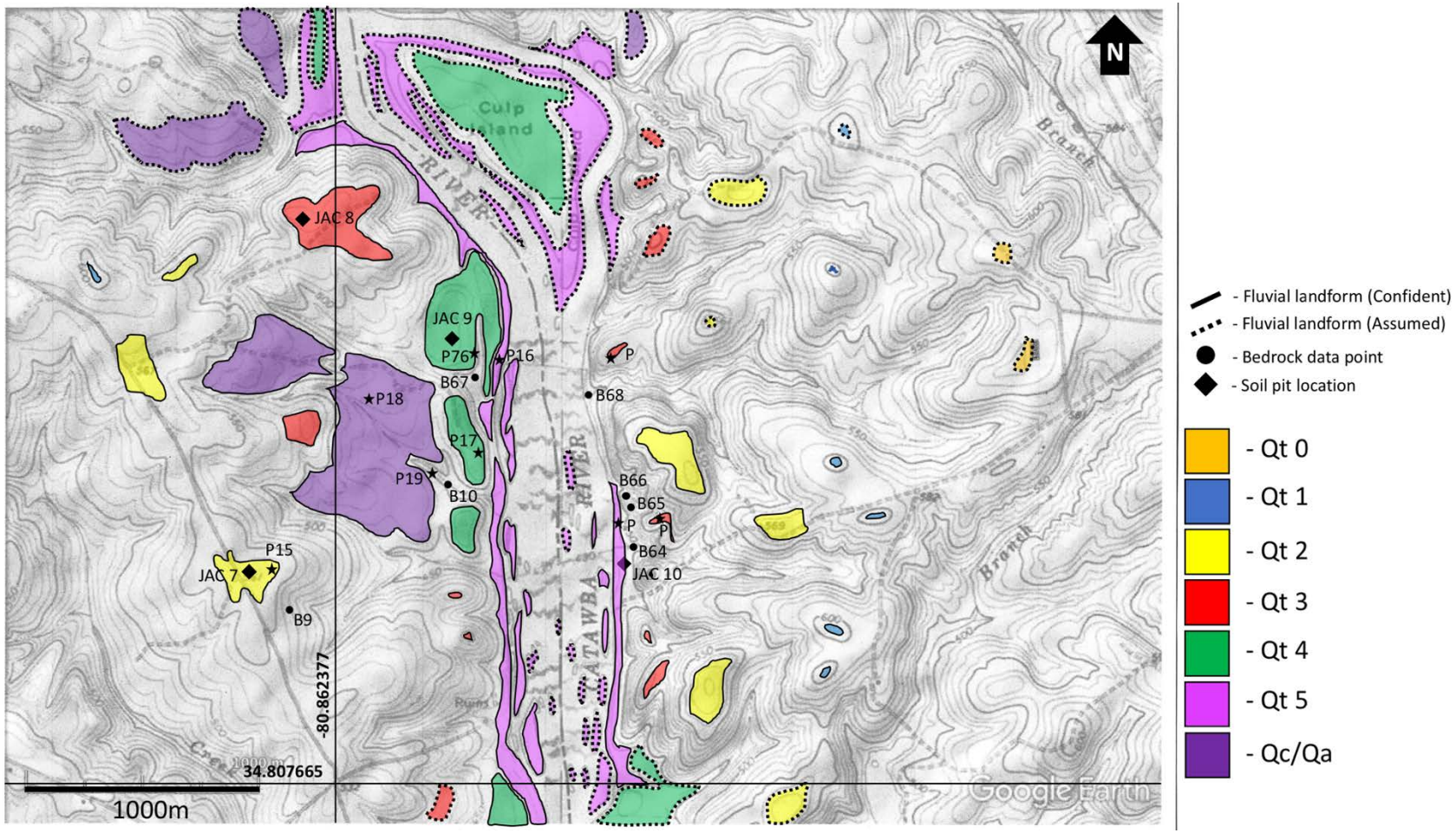

Figure 4.1D: Inset surficial geology map of the lower reach of the study area, Landsford, SC.

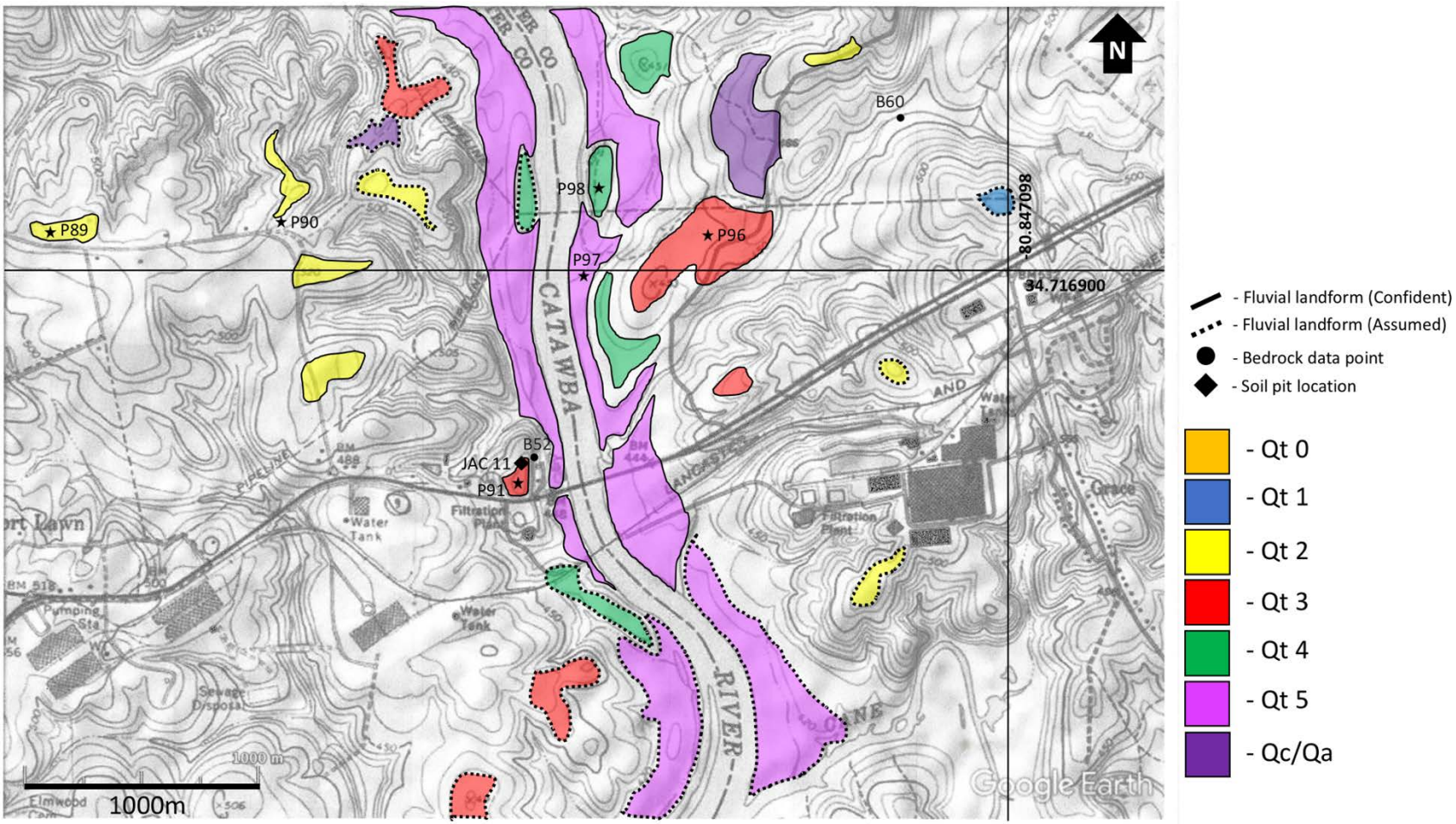

Figure 4.1E: Inset surficial geology map at the end of the study area, Fort Lawn, SC.

Table 4.1: Summary Table of Catawba River terrace units, where HATC = height above the channel.

Unit	HATC (m)	# of pits	# of Fe samples	# Particle Size samples	# clast counts
Qt0	69	-	-	-	-
Qt1	46	-	-	-	-
Qt2	38	1	5	5	2
Qt3	24	7	48	48	3
Qt4	9	4	26	26	3
Qt5	3	3	24	24	3

Table 4.2: Birkland (1999) descriptions of soil pits and exposures on terrace unit (Qt5 – Qt2).

Unit	Pit	Depth (cm)	Horizon	Color Wet	Structure	Gravel %	Consistence Wet - Moist	Pores	Roots	Texture	Clay Films	Boundaries
Qt2	JAC 7	0-1	A	7.5 YR 3/4	1 vf gr	<10	ss/ps - vfr	3f 3vf	3f 3vf	SL	-	a s
		1-12	2Bwt	5 YR 4/6	2 fm abk	<10	s/p - fi	2f 3vf	2f 3vf	SCL	1 f po	a s
		12-56	2Bt	2.5 YR 4/8	2 fm abk	<10	sp - vfi	2f 3vf	1m 1f 3vf	SICL	2 d pf/po	a s
		56-	2Bt2	2.5 YR 4/8	2 fm abk	<10	s/p - fr/fi	1f 3vf	1vf	SCL	3 p pf/po	-
Qt3	JAC 2	0-11	Ap	10 YR 4/2	1 f abk	20	so/po - fr	1f 2vf	1f 2vf	SL	v1 f pf	c s
		11-35	Apw	10 YR 4/5	2 f abk	20	so/po - fr	1f 3vf	1f 3vf	SL	v1 f po	a w
		35-40	E	7.5 YR 6/4	m m abk	10	s/p - fi	1f 2vf	1f 1vf	L	v1 f po	c s
		40-60	Bt	5 YR 6/6	m m abk	<10	s/p - fi	1f 2vf	1f 1vf	SC	2 d pf/po	c s
		60-100	2Bt2	5 YR 5/8	1 mc abk	0	s/ps - fr	1f 2vf	1	SC	2 p/d pf/po	a s
		100-	2Bt3	7.5 YR 6/8	m m abk	<10	ss/ps - lo	1f 2vf	-	SL	3 p pf/po	-
	JAC 4	0-1	A	10 YR 3/3	sg vf gr	0	so/po - fr	3f 3vf	2f 3vf	L	-	a s
		1-12	A/B	10 YR 6/3	m f abk	<10	s/p - fi	2f 3vf	2f 2vf	L	1 f po	a l
		12-21	Bw	10 YR 6/8	m f abk	<10	ss/ps - fi	2f 2vf	1c 2f 2vf	SIL	v1 f po	a l
		21-32	Bt	7.5 YR 6/8	1 fm abk	0	vs/ps - fi	2f 2vf	2f 2vf	SIC	1 d pf/po	c s
		32-51	Btr	7.5 YR 5/8	1 f abk	0	s/p - vfi	2f 2vf	1m 3f 1vf	SICL	1 d pf	a s
		51-	Cr	10 YR 6/4	1 mc abk	<10	s/p - efi	1vf	-	SC	-	-
	JAC 8	0-5	A	10 YR 3/6	1 f abk	<10	ss/ps - fr	1c 2m 3f 3vf	1m 3f 3vf	SL	-	a s
		5-15	Bwt	5 YR 4/6	1 f abk	<10	s/p - fi	1c 2m 3f 3vf	1m 3f 3vf	SCL	2 d pf/po	a s
		15-45	2Bt	2.5 YR 4/8	1 m abk	<10	s/p - fi	3f 3vf	2m 2f 3vf	SCL	2 d pf/po	c s
		45-95	2Bt2	2.5 YR 5/6	1 m abk	<10	s/p - fi/vfi	1f 3vf	1f 2vf	SCL	1 d pf/po	c s
		95-	2Bt3	7.5 YR 5/8	1 f abk	<10	ss/ps - fr	1f 2vf	2m 1f 1vf	L	1 f po	-
	JAC 11	0-25	A/Bw	2.5 YR 4/6	1 fm abk	<10	s/p - vfr	2f 3vf	1m 3f 3vf	SC	vf f po	c s
		25-70	Bt	2.5 YR 4/8	1 f abk	<10	s/p - fr	1f 2vf	3f 3vf	SC	2 p pf/po	g s
		70-150	Bt2	2.5 YR 4/8	1 f abk	<10	s/p - fi/vfi	1f 2vf	2f 3vf	SCL	2 p pf/po	g s
		150-200	Bt3	2.5 YR 4/8	1 f sbk	<10	s/p - fi/vfi	1f 2vf	3f 3vf	SCL	2 d pf/po	g s
		200-250	Bt4	2.5 YR 4/8	1 f sbk	10	s/p - fr	1f 2vf	1f 2vf	SCL	2 f pf	g s
		250-300	Bt5	2.5 YR 4/8	1 f sbk	25	s/p - fr	2vf	1m 3f 3vf	SCL	1 f pf/po	d s

		300-	Bt6	2.5 YR 4/8	1 f sbk	25	s/p - fr	2f 2vf	1vf	SCL	2 d pf	-
	JAC 13	0-5	A	7.5 YR 4/3	1 mc sbk	<10	so/ps - fr	1c 2m 2f 3vf	1f 3vf	SL	-	a s
		5-13	Bw	7.5 YR 6/6	1 c abk	<10	ss/ps - fi	1m 1f 3vf	1f 1vf	SL	1 f pf/po	a s
		13-40	2Bt	5 YR 5/6	2 cvc abk	<10	s/ps - vfi	1c 2m 3f 3vf	1c 1f 1vf	SCL	3 d pf/po	c s
		40-85	2Bt2	7.5 YR 5/8	1 cvc abk	<10	ss/ps - fi	1m 3f 3vf	1c 1f 1vf	L	2/3 d pf/po	c w
		85-108	2Bt3	7.5 YR 6/6	2 vc sbk	<10	ss/ps - vfr	3f 3vf	1f	L	3 p pf/po	a w
		108-	2Cr	10 YR 5/8	1 fm sbk	<10	so/po - lo	2f 3vf	1vf	SL	2 f pf/po	-
	JAC 14	0-11	A	7.5 YR 5/3	1 m sbk	10	so/ps - vfr	1c 1m 3f 3vf	1c 2m 2f 2vf	SCL	vf/2 f pf/po	a w
		11-36	Bwt	7.5 YR 5/3	m c abk	<10	ss/ps - fi	1c 1m 3f 3vf	1m 1f	SCL	2 d pf/po	a s
		36-52	2Bt2	7.5 YR 6/6	m c abk	<10	ss/vp - fi	3f 3vf	1f 1vf	SC	2/3 d pf/po	c w
		52-76	2Bt3	5 YR 6/8	m cvc abk	<10	ss/p - vfi	2f 2vf	1f	SC	2/3 p pf/po	c w
		76-96	2Bt4/C	5 YR 7/6	m cvc abk	<10	ss/ps - fi	1f 2vf	1f 1vf	SCL	2/3 d pf/po	a i
		96-	2Cr	7.5 YR 7/6	m c abk	<10	ss/ps - vfi	1f 2vf	1f	SCL	2/3 d/p pf/po	-
	JAC 15	0-10	A	7.5 YR 4/4	1 f sbk	<10	so/ps - fr	1c 1m 3f 3vf	1c 3m 3f 3vf	SL	-	a s
		10-30	Bw	5 YR 4/6	2 m abk	<10	s/p - fi	1c 3f 3vf	1c 2m 3f 3vf	SCL	1 f po	a s
		30-130	Bt	2.5 YR 4/6	2 fm sbk	<10	s/p - fi	2f 3vf	1m 2f 3vf	CL	2/3 d/p pf	g s
		130-220	Bt2	2.5 YR 4/8	3 mc abk	<10	s/p - fi	3f 3vf	2f 2vf	CL	1 f/d pf/po	a s
		220-315	Cox	7.5 YR 6/8	2 m abk	<10	s/p - fi	2f 3vf	1f 2vf	SL	1 f po	g s
		315-480	Cox2	7.5 YR 5/8	2 mc sbk	<10	ss/ps - vfi	2f 2vf	1vf	SL	vf d pf/po	a s
		480-	2Cox	5 YR 6/6	1 fm sbk	<10	s/p - fr	2f 2vf	1vf	SICL	vf f po	-
Qt4	JAC 1	0-9	A	10 YR 4/4	1 mc sbk	0	ss/ps - fi	3f 3vf	2f 3vf	SL	-	a w
		9-24.5	Ap/Bw	10 YR 4/6	1 mc sbk	0	ss/ps - fr	3f 3vf	2f 3vf	SL	1 f pf/po	a s
		24.5-35	Ab/Bt1	10 YR 5/4	1 mc sbk	<10	ss/ps - fr	2f 3vf	2f 2vf	SICL	-	a s
		35-108	Bt2	10 YR 5/8	1 vc sbk	0	s/vp - fi	3f 3vf	1f 2vf	SIC	-	a w
		108-	Bt3	10 YR 5/8	1 vc abk	0	s/ps - vfi	1f 2vf	1f	SIC	-	-
	JAC 5	0-12	Ap	10 YR 4/4	m fm abk	0	so/ps - fr	3f 3vf	3f 3vf	SL	v1 f po	a s
		12-30	Bw	10 YR 2/6	m fm abk	0	ss/ps - fr	2f 3vf	3f 3vf	SL	1 f po	a s
		30-51	Ab/Bwt	10 YR 4/6	m f abk	<10	ss/ps - fr	2f 3vf	2f 2vf	SL	v1 f po	a s
		51-85	Bt	10 YR 5/6	2 fm abk	0	ss/ps - fr	2f 3vf	2f 2vf	SL	v1 f po	a s

		85-110	Bt2	10 YR 5/6	1 fm abk	0	s/p - fi	3f 3vf	2f 3vf	SCL	1 d po	a/c s
		110-	Bt3	10 YR 5/8	m fm abk	0	s/p - fi	2f 2vf	1f 2vf	SCL	v1 f po	-
	JAC 9	0-9	A	10 YR 3/2	1 f sbk	<10	ss/ps - fr	1m 3f 3vf	3f 3vf	SL	v1 f pf	a s
		9-19	Ap/Bw	10 YR 4/4	2 f abk	<10	ss/ps - vfr/fr	3f 3vf	1f 3vf	SL	v1 f pf/po	a s
		19-52	Ab/B	7.5 YR 4/6	2 fm abk	<10	s/p - fr	1m 1f 3vf	1f 3vf	SCL	1 f po	g s
		52-85	Bt	7.5 YR 4/6	2 f abk	<10	s/p - fr	3f 3vf	1f 3vf	SCL	v1 f po	c s
		85-95	Bt2	10 YR 5/8	1 f sbkabk	<10	s/ps - fr	1f 1vf	1m 1f 3vf	SCL	1 f po	a s
		95-	Bt3	10 YR 5/8	1 fm abk	<10	s/p - fr	2f 2vf	1m 1f 1vf	SCL	1 f pf	-
	JAC 12	0-3	A	10 YR 4/4	1 m sbk	0	so/po - fi	1m 3f 3vf	1m 3f 3vf	LS	-	a s
		3-22	Ap/Bw	10 YR 5/4	1 m abk	0	ss/ps - fr	1m 2f 3vf	1m 1f 2vf	LS	-	a w
		22-50	Ab/Bt1	10 YR 6/6	1 mc abk	0	ss/ps - fr	1m 2f 3vf	2f 2vf	SIC	2 f po	g s
		50-88	Bt2	10 YR 7/6-8	m m abk	0	s/p - fr	1f 2vf	1f 2vf	SIC	vf/2 f/d po/pf	g s
		88-	Bt3	10 YR 7/6-8	m m abk	0	s/p - fr	2f 3vf	1vf	SIC	2 d po	-
Qt5	JAC 3	0-9	Aw	10 YR 4/2	1 f abk	0	so/ps - fr	2f 3vf	1m 2f 3vf	SL	v1 f po	a w
		9-32	Bw	10 YR 4/6	1 mc abk	0	so/po - fr	1f 3vf	2m 3f 3vf	SL	v1 f po	c s
		32-48	Bb	10 YR 4/6	1 fm abk	0	so/po - fr	1f 1vf	1f 1vf	S	v1 f po	c s
		48-62	B	10 YR 4/6	m m abk	0	s/p - fr	1f 2vf	1f 1vf	SL	v1 f pf/po	c s
		62-82	Bb2	10 YR 4/6	m m abk	0	so/po - fr	1f 2vf	1f 1vf	SL	v1 f pf/po	a s
		82-108	B3	10 YR 4/6	m f abk	0	s/p - fr	1f 2vf	1m	SL	1 f pf/po	c s
		108-125	B4	10 YR 4/6	1 fm abk	0	ss/ps - fr	1f 2vf	1c 1f	SIL	v1 f po	c s
		125-	B5	10 YR 4/6	m f abk	0	ss/ps - fr	1f 1vf	1c 1m 2f 1vf	SL	v1 f po	-
	JAC 6	0-10	A	10 YR 3/4	m f abk	0	s/p - fi	1m 2f 3vf	1m 3f 3vf	CL	1 f po	a w
		10-49	Bw	7.5 YR 4/6	1 fm abk	<10	s/p - fr	2f 3vf	1m 2f 3vf	CL	1 d po	a s
		49-60	Bt	7.5 YR 5/6	m fm abk	0	ss/ps - fr/fi	2f 3vf	1m 3f 3vf	SL	1 d pf/po	a i
		60-80	Bt2	7.5 YR 5/8	1 fm abk	0	s/p - fi	3f 3vf	2f 3vf	LS	2 d pf/po	a s
		80-130	Bt3	7.5 YR 5/8	1 fm abk	0	s/p - fr/fi	3f 3vf	2m 3f 3vf	LS	2 d pf	a s
		130-	Bt4	7.5 YR 5/6	1 m abk	0	s/p - fi	2f 3vf	1f 3vf	LS	2 d pf/po	-
	JAC 10	0-12	Ap	10 YR 2/2	m f sbk	<10	ss/ps - fr	2f 3vf	3f 3vf	SL	-	a s/w
		12-30	Bw	10 YR 4/6	m m abk	<10	ss/ps - fr	1f 2vf	1f 2vf	SL	1 f po	a s

30-56	B	10 YR 4/6	1 fm sbk	<10	s/p - fr/fi	2f 3vf	2m 2f 2vf	SCL	1 f pf/po	a s
56-106	B1	10 YR 5/6	m f abk	<10	ss/ps - fr	2f 3vf	1f 3vf	SL	-	g s
106-134	B2	10 YR 5/6	m fm abk	10	ss/ps - vfr	2f 3vf	2vf	SL	-	a s
134-	B3	10 YR 5/8	m m abk	<10	s/p - fr	2f 3vf	1f 3vf	SL	-	-

Sub Horizon Designation: p = disturbance, w = weak development, t = clay accumulation, b = buried horizon, r = weathered rock
Structure: Grade: m = massive, 1 = few, 2 = common, 3 = many; Size: f = fine, m = medium, c = coarse, vc = very coarse
Structure: Type: abk = angular blocky, sbk = sub-angular blocky
Wet Consistence: so = non-sticky, ss = slightly sticky, s = sticky, vs = very sticky, po = non-plastic, ps = slightly plastic, p = plastic, vp = very plastic;
Moist Consistence: lo = loose, vfr = very friable, fr = friable, fi = firm, vfi = very firm, efi = extremely firm
Pores & Roots: Grade: 1 = few, 2 = common, 3 = many; Size: vf = very fine, f = fine, m = medium, c = coarse
Texture: SL = sandy loam, SCL = sandy clay loam, SICL = silty clay loam, SIL = silty loam, SC = sandy clay, SIC = silty clay, L = loam, LS = loamy sand, CL = clay loam
Clay Films: Grade: v1 = very few, 1 = few, 2 = common, 3 = many; Prominence: f = faint, d = distinct, p = prominent; Location: po = pores, pf = ped faces
Boundaries: Distinctness: a = abrupt, c = clear, g = gradual, d = diffuse; Topography: s = smooth, w = wavy, i = irregular

Figure 4.2: Photograph of cobbles and pebbles on Qt4 tread, Catawba Indian Reservation, Rock Hill, SC.

Figure 4.3: Qt3 exposure (JAC 11) off SC Highway 9 in Fort Lawn, SC. Star represents IRSL – 1 sample Dr. Eppes (~2m) pictured for scale.

Figure 4.4: Qt3 exposure (JAC 15) Mason's Bend neighborhood Riverview, SC. Lines represents the gravel – bedrock contact, dashed lines represent other gravels found in the profile, and the star represents IRSL – 4 sample location. Ladder (~3.8 m) pictured for scale.

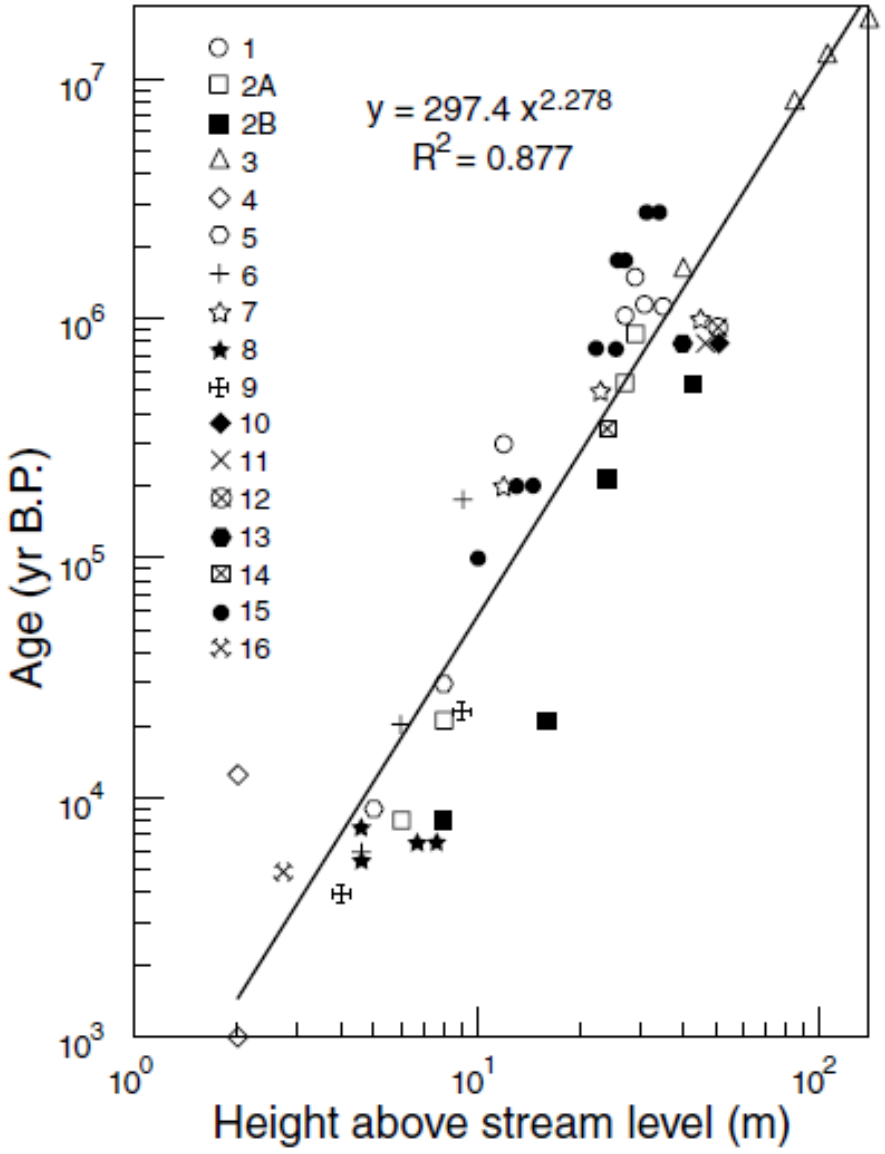

Figure 4.5: Log-log plot surface age vs. elevation curve developed in Mills (2000) using tread heights and ages from 16 different studies along the US east coast. The equation developed with this data was utilized for terrace heights measured in this study.

Figure 4.6: A) RCN – 1 sample location depth below surface (JAC 10); B) RCN – 2 sample location depth below surface (JAC 1); and C) RCN – 3 sample location depth below surface (JAC 3).

Figure 4.7: A) OSL – 1 depth below surface, Riverview, SC – upper reach, B) OSL – 1 height above gravels, and C) OSL – 2 Sample location depth below surface, Fort Lawn, SC – lower reach. Note that streaks in each photo are a result of excavation.

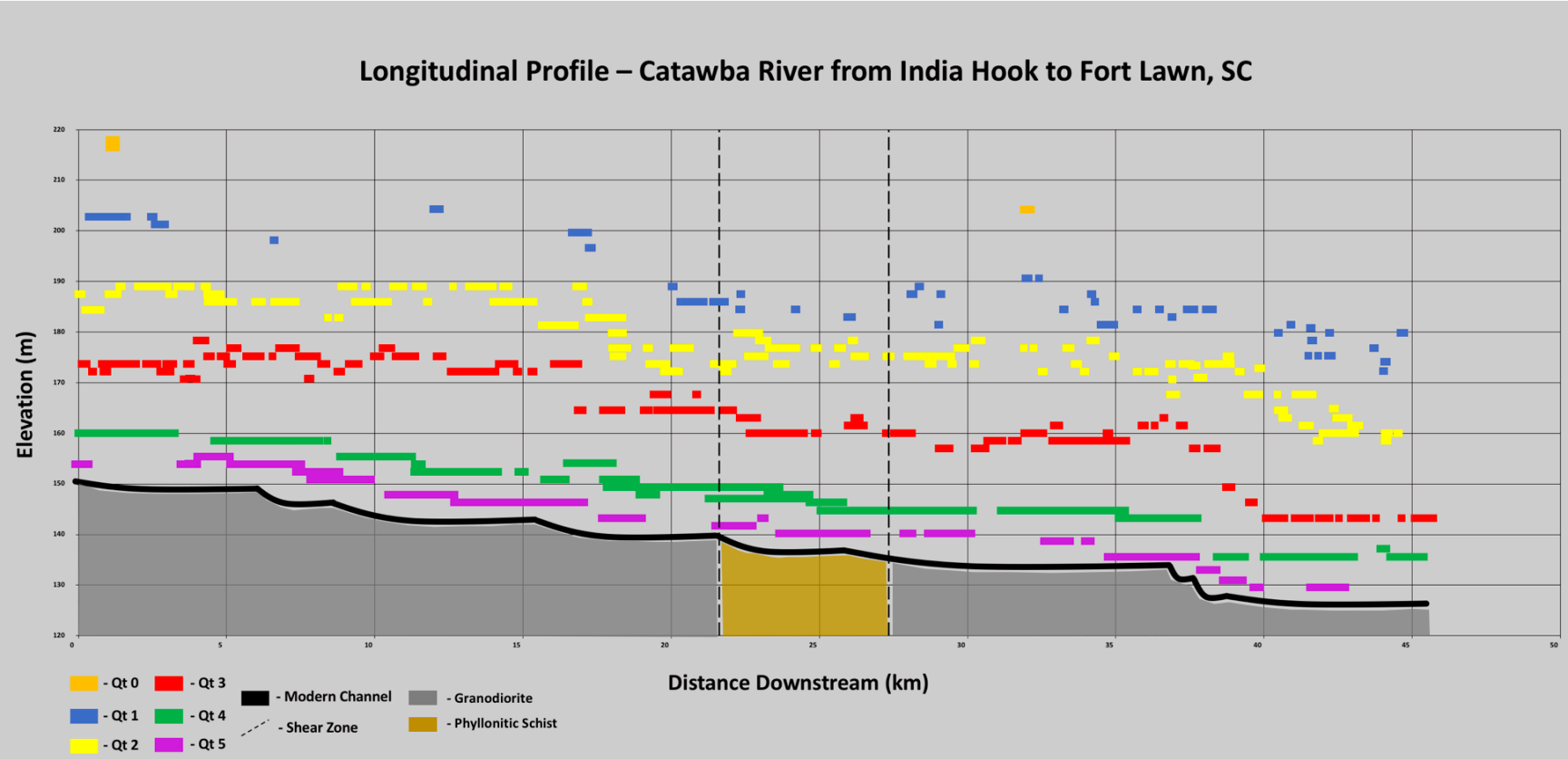

Figure 4.8: Longitudinal Profile of terrace units (Qt0-5) and the modern channel. The Gold and Silver Hill shear zones are indicated by the dashed lines.

Table 4.3: Summary of Lab Analysis data, where BD is bulk density (g/cm^3), and Depletion represents the change in base cation *x* from horizon to parent material as it relates to change in Titanium from horizon to parent material.

Unit	Pit ID	Depth (cm)	Parent Material	% clay	% silt	% sand	Fe_H (wt%)	Fe_D (wt%)	Fe Activity	BD (g/cm^3)	Depletion Ca	Depletion Fe	Depletion Si	Depletion Al
Qt2	JAC 7	0-1	-	6.69	32.29	61.35	0.60	1.31	0.46	-	0.44	0.36	0.88	0.42
		1-12	rock	6.32	45.67	48.30	0.33	1.81	0.18	1.74	0.60	0.38	0.80	0.61
		12-34	rock	10.64	62.57	27.19	0.23	8.02	0.03	1.50	0.85	1.08	0.80	0.86
		34-56	rock	10.02	59.47	30.87	0.32	8.00	0.04	1.38	0.85	1.11	0.80	0.95
		56-	rock	8.05	53.82	38.45	0.24	5.65	0.04	1.46	1	1	1	1
Qt3	JAC 2	0-11	fluvial sed	6.98	30.00	63.42	0.32	0.36	0.90	1.21	0.37	0.24	0.86	0.43
		11-35	fluvial sed	6.22	37.82	56.29	0.10	0.36	0.26	1.66	0.36	0.21	0.85	0.44
		35-40	fluvial sed	10.22	50.94	39.40	0.10	0.77	0.13	1.63	0.36	0.32	0.73	0.56
		40-60	fluvial sed	11.50	57.57	31.37	0.04	2.29	0.02	1.36	0.21	0.87	0.60	0.73
		60-80	fluvial sed	9.57	47.34	43.36	0.03	2.34	0.01	1.49	0.46	1.06	0.67	0.88
		80-100	rock	8.47	46.35	45.44	0.06	2.34	0.03	1.45	0.49	1.08	0.74	0.90
		100-	rock	5.53	38.44	56.20	0.00	1.71	0.00	1.44	1	1	1	1
	JAC 4	0-1	rock	7.06	58.38	34.91	0.49	0.32	1.55	1.29	0.51	0.47	1	0.43
		1-12	rock	9.34	75.48	15.62	0.44	0.39	1.14	1.44	0.32	0.39	0.96	0.62
		12-21	rock	10.42	78.82	11.26	0.32	0.81	0.39	1.43	0.15	0.63	0.78	0.68
		21-32	rock	10.04	80.02	10.41	0.52	4.81	0.11	3.38	-0.05	0.85	0.32	0.35
		32-51	rock	8.88	77.85	13.66	0.25	1.76	0.14	1.70	0.17	1.35	0.84	0.99
		51-	rock	6.92	75.76	17.59	0.44	0.42	1.05	2.00	1	1	1	1
	JAC 8	0-5	fluvial sed	6.67	40.00	53.68	0.53	1.38	0.39	2.83	-2.84	0.55	1.03	0.45
		5-15	fluvial sed	8.48	50.68	41.25	0.76	2.85	0.27	1.48	0.73	0.51	0.84	0.66
		15-30	rock	13.02	66.62	20.91	0.62	7.39	0.08	1.49	1.30	1.31	1.25	1.15
		30-45	rock	9.05	57.92	33.38	0.60	7.82	0.08	1.74	1.49	1.51	1.42	1.31
		45-70	rock	7.05	50.13	43.12	0.67	7.96	0.08	1.31	1.24	1.26	1.19	1.05
		70-95	rock	5.86	39.47	54.91	0.36	5.35	0.07	1.44	1.24	1.20	1.17	1.03
		95-112.5	rock	4.05	30.61	65.52	0.63	4.34	0.15	1.13	1.07	1.08	1.01	0.87
		112.5-	rock	3.57	28.70	67.89	0.50	3.61	0.14	1.25	1	1	1	1

JAC 11	0-25	fluvial sed	26.46	33.49	41.01	0.37	5.20	0.07	-	1.28	-0.01	1.40	1.55
	25-70	fluvial sed	23.48	47.40	30.15	0.36	4.37	0.08	-	1.25	0.90	1.36	1.42
	70-150	fluvial sed	21.67	63.22	16.03	0.50	6.13	0.08	1.57	1.15	1.05	1.16	1.29
	150-200	fluvial sed	20.55	63.68	16.66	0.53	6.26	0.08	1.53	1.07	1.01	1.07	1.15
	200-250	fluvial sed	18.91	64.75	17.18	0.54	6.03	0.09	1.53	0.99	0.97	1	1.02
	250-300	fluvial sed	19.41	60.30	21.15	0.66	8.32	0.08	1.43	1	0.96	1	1.11
	300-	fluvial sed	18.60	57.51	24.70	0.70	5.58	0.13	1.49	1	1	1	1
JAC 13	0-5	rock	6.17	32.98	61.20	0.90	0.82	1.10	1.39	1.36	0.66	2.07	0.77
	5-13	rock	6.54	32.87	60.95	1.48	1.03	1.44	1.56	1.65	0.79	1.87	0.70
	13-40	rock	7.96	41.80	50.58	0.48	1.42	0.34	1.50	0.35	1.32	0.76	0.77
	40-85	rock	5.57	35.33	59.30	0.71	1.55	0.46	1.46	-	1.69	1.16	1.01
	85-108	rock	4.38	28.67	67.14	0.53	1.45	0.36	1.48	-	1.48	1.01	0.87
	108-	rock	2.69	22.03	75.40	0.00	0.86	0.00	1.40	1.00	1.00	1.00	1.00
JAC 14	0-11	rock	5.95	36.88	57.48	1.97	1.02	1.92	-	-	0.66	0.73	0.39
	11-36	rock	10.94	55.08	34.52	0.78	1.27	0.62	-	-	0.91	0.97	0.75
	36-52	rock	9.89	56.96	33.61	0.53	1.77	0.30	-	-	1.08	0.94	0.82
	52-76	rock	5.94	49.75	44.57	0.47	1.61	0.29	-	-	1.17	0.99	0.96
	76-96	rock	4.48	37.41	58.30	0.31	0.50	0.62	-	-	1.04	0.99	1.04
	96-	rock	3.84	27.93	68.39	0.44	0.94	0.47	-	-	1.00	1.00	1.00
JAC 15	0-10	fluvial sed	6.50	21.34	72.50	0.30	0.60	0.50	1.46	-	0.12	1.04	0.82
	10-30	fluvial sed	10.66	34.74	55.14	0.20	1.26	0.16	1.59	0.49	0.17	0.76	1.03
	30-63	fluvial sed	12.34	35.87	52.24	0.36	2.62	0.14	1.56	0.34	0.35	0.72	1.36
	63-96	fluvial sed	13.37	30.58	56.51	0.37	2.45	0.15	1.52	0.38	0.34	0.75	1.33
	96-130	fluvial sed	13.41	29.24	57.82	0.34	2.46	0.14	1.62	0.60	0.36	0.78	1.39
	130-175	fluvial sed	12.07	27.23	61.14	0.46	2.08	0.22	1.59	0.59	0.32	0.77	1.32
	175-220	fluvial sed	11.41	29.37	59.68	0.46	2.62	0.17	1.55	0.60	0.35	0.79	1.33
	220-315	fluvial sed	12.54	45.09	42.97	0.40	3.30	0.12	1.57	0.57	0.39	0.74	1.28
	315-397.5	fluvial sed	8.81	37.66	53.95	0.50	4.04	0.12	1.50	0.64	0.52	0.83	1.25
	297.5-480	fluvial sed	7.15	34.21	58.98	0.53	2.63	0.20	1.57	0.53	0.36	0.69	1.12

		480-	rock	12.43	58.64	29.53	1.18	9.15	0.13	1.17	1.00	1.00	1.00	1.00
Qt4	JAC 1	0-9	fluvial sed	4.68	33.83	61.72	0.99	1.44	0.69	1.11	1.79	0.72	1.47	1.29
		9-24.5	fluvial sed	5.05	53.36	41.83	0.52	1.45	0.36	1.48	1.45	0.66	1.02	1.33
		24.5-35	fluvial sed	6.45	63.42	30.45	1.32	1.26	1.05	1.49	1.38	0.71	1.00	1.39
		35-108	fluvial sed	10.85	71.18	18.52	1.29	0.92	1.41	1.58	0.69	0.96	0.90	1.30
		108-	fluvial sed	8.97	55.43	36.06	1.22	0.84	1.45	1.66	0.78	0.92	1.17	1.39
	JAC 5	0-12	fluvial sed	4.42	32.90	62.90	0.53	0.70	0.76	1.16	0.33	0.67	1.16	1.36
		12-30	fluvial sed	3.34	31.40	65.41	0.67	0.88	0.76	1.27	0.30	0.74	1.16	1.59
		30-51	fluvial sed	3.62	29.51	67.04	0.59	0.53	1.11	1.33	0.36	0.55	1.06	1.31
		51-68	fluvial sed	4.03	33.43	62.74	0.67	0.50	1.35	1.35	0.35	0.55	1.12	1.29
		68-85	fluvial sed	4.73	39.19	56.31	0.65	0.51	1.28	1.59	0.36	0.55	1.12	1.42
		85-110	fluvial sed	5.04	38.86	56.35	1.13	0.80	1.40	1.67	0.27	0.66	0.98	1.29
		110-	fluvial sed	5.35	39.58	55.33	0.90	1.02	0.89	1.56	0.22	0.71	0.93	1.30
	JAC 9	0-9	fluvial sed	5.31	18.61	76.36	0.33	0.40	0.83	-	0.16	0.31	1.22	0.59
		9-19	fluvial sed	5.43	24.67	70.16	0.33	0.43	0.76	1.62	-	0.24	1.33	0.82
		19-35.5	fluvial sed	10.92	34.65	55.01	0.47	0.89	0.53	1.62	-	0.38	0.95	0.90
		35.5-52	fluvial sed	10.85	33.47	56.23	0.55	1.08	0.51	1.72	-	0.45	0.98	0.99
		52-68.5	fluvial sed	10.43	29.58	60.53	0.37	1.20	0.31	1.64	-	0.47	0.99	1.05
		68.5-85	fluvial sed	10.24	26.54	63.73	0.36	1.13	0.32	1.75	-	0.45	1.02	0.97
		85-95	fluvial sed	9.97	26.01	64.52	0.46	1.15	0.40	1.70	-	0.49	1.04	1.01
		95-122.5	fluvial sed	10.78	28.15	61.61	0.27	1.42	0.19	1.63	-	0.56	1.04	1.04
		122.5-	fluvial sed	10.48	26.55	63.47	0.24	1.49	0.16	1.80	-	0.63	1.03	1.10
	JAC 12	0-3	fluvial sed	5.69	40.26	54.34	1.51	1.58	0.96	2.55	1.66	0.70	1.36	1.20
		3-22	fluvial sed	5.56	46.08	48.64	0.86	1.51	0.55	1.53	1.42	0.69	1.11	1.24
		22-50	fluvial sed	9.50	66.52	24.47	1.00	1.05	0.95	1.58	0.93	0.87	0.87	1.37
		50-88	fluvial sed	9.44	60.84	30.19	1.06	0.32	3.26	1.65	0.95	0.92	0.94	1.35
		88-	fluvial sed	6.48	49.33	44.50	1.29	0.85	1.51	1.63	1.13	0.95	1.10	1.36
Qt5	JAC 3	0-9	fluvial sed	5.13	28.34	66.78	0.64	0.80	0.80	-	0.34	0.66	1.18	1.36
		9-32	fluvial sed	3.19	30.16	66.80	0.53	0.81	0.66	1.33	0.26	0.64	1.20	1.48

	32-48	fluvial sed	2.22	17.08	80.80	0.65	0.81	0.80	1.27	0.27	0.71	1.28	1.66
	48-62	fluvial sed	3.60	32.87	63.70	0.85	1.20	0.71	1.25	0.19	0.82	0.98	1.58
	62-82	fluvial sed	3.09	26.78	70.28	0.77	0.96	0.80	1.23	0.18	0.75	1.11	1.57
	82-108	fluvial sed	6.80	63.12	30.43	1.05	1.96	0.54	1.32	0.08	0.86	0.76	1.25
	108-125	fluvial sed	4.23	33.09	62.89	0.84	1.53	0.55	1.21	0.19	0.71	0.86	1.27
	125-	fluvial sed	5.07	32.79	62.40	1.08	1.31	0.82	1.14	0.19	0.75	0.82	1.28
JAC 6	0-10	fluvial sed	9.49	58.16	32.83	1.48	1.57	0.94	1.30	0.41	0.94	0.90	1.11
	10-29.5	fluvial sed	6.42	48.31	45.59	1.04	1.84	0.57	1.41	0.15	0.91	0.85	1.44
	29.5-49	fluvial sed	7.32	52.37	40.68	1.23	2.32	0.53	1.34	0.10	0.94	0.79	1.34
	49-60	fluvial sed	4.14	33.75	62.31	0.80	1.10	0.72	1.17	0.21	0.76	1.10	1.48
	60-80	fluvial sed	7.46	58.47	34.45	1.19	2.19	0.54	1.35	0.06	0.88	0.73	1.27
	80-105	fluvial sed	3.44	22.40	74.32	0.72	0.88	0.82	1.24	0.26	0.68	1.07	1.44
	105-130	fluvial sed	4.85	32.37	63.03	1.32	1.50	0.88	1.34	-	-	-	-
	130-	fluvial sed	8.13	50.03	42.26	1.36	1.79	0.76	1.25	0.13	0.80	0.75	1.45
JAC 10	0-12	fluvial sed	5.14	39.23	55.86	1.76	0.47	3.77	1.23	5.67	0.63	1.32	1.03
	12-30	fluvial sed	4.35	41.56	54.31	1.18	0.82	1.44	1.27	0.30	0.61	1.14	1.27
	30-56	fluvial sed	5.17	46.99	48.11	1.22	1.07	1.14	1.40	0.22	0.69	0.90	1.26
	56-81	fluvial sed	4.72	36.27	59.25	0.89	0.67	1.32	1.64	0.29	0.57	0.92	1.35
	81-106	fluvial sed	3.66	28.90	67.62	0.72	0.51	1.40	1.49	0.34	0.52	1.07	1.27
	106-120	fluvial sed	2.62	22.32	75.18	0.72	0.40	1.80	-	0.38	0.50	1.28	1.31
	120-134	fluvial sed	3.14	25.11	71.90	0.89	0.51	1.73	-	0.36	0.55	1.23	1.23
	134-	fluvial sed	4.64	39.22	56.36	1.34	0.90	1.49	1.62	0.24	0.65	0.91	1.23

Fe_H = Iron extracted via Hydroxylamine Method
Fe_D = Iron Extracted via Citrate – Dithionite Method (Mehra and Jackson, 1960)
Fe Activity = Iron Activity ratios, calculated by dividing Fe_H/Fe_D
BD = Bulk Density
Depletion Ca, Fe, Si, Al: Values < 1 = depletion, Values > 1 = enrichment

CHAPTER 5: Results

5.1: Mapping, Stratigraphy and General Morphological Data

Mapping revealed five consistent terrace treads (Qt5 – Qt1) throughout the field area and in some areas a sixth terrace surface (Qt0) was mapped (Fig. 4.1A and D, see above). The area of remnant treads varies with height above the channel, with larger remnants preserved on lower terraces. Overall remnants range in area from 0.01 km^2 – 0.33 km^2. Average height above the channel for all surfaces ranged from 3.43 (Qt5) – 68.96 m (Qt0); absolute height of remnants for each terrace unit varied by ~2 – 9 m within any one 5 km reach. Lateral distance away from (perpendicular to) the modern channel ranges from ~0 – 2 km (Qt5 – Qt1), with the oldest surface (Qt0) averaging ~1.6 km from the channel. Other surfaces average distance from the channel are as follows; Qt2 averages ~1.3 km, Qt3 averages 0.7 km, and Qt4 averages 0.3 km from the modern channel.

Vegetative canopy cover at pit locations ranged from 0 – 90%, with most uncovered areas occurring on Qt4 surfaces (2/3 pit locations had 0%, where these surfaces were used for agricultural purposes) and Qt5 being the most covered areas with an average of 65.83% canopy coverage, due to lack of human development on this surface. Qt2 and Qt3 pit location surfaces never exceeded 20% vegetative cover, with homes and businesses frequently occupying these surfaces. Vegetative ground cover ranges from 0-100%, with Qt4 surfaces containing the most ground cover overall. Vegetation regimes include various grasses, spruce and pine species, and is primarily dominated by deciduous species, such as red maple, sweet gum, white and pignut

hickory, and white oak. Many remnants throughout the study area were developed, with commercial, residential and agricultural land uses.

Qt0 – Average 69 m elevation above the modern channel

The oldest and highest terrace (Qt0) is present in two locations in the field area, with three mapped terrace remnants (Fig. 4.1, 4.1A and 4.1D). It includes the highest surfaces in the study area, as it stands approximately 69 m above the modern channel. At the surface of all of these Qt0 remnants was evidence of unweathered bedrock or saprolite with weathered vein quartz fragments present in some areas indicating a strath surface (Fig. 5.1). Nevertheless, this tread contains occasional sub-rounded gravel sized quartzite clasts, providing evidence of its fluvial origins (Fig. 5.2). Surface clasts average 2.25 cm in diameter.

Qt1 – Average 46 m elevation above the modern channel

The Qt1 terrace is present throughout the study area, and lies between 45 and 58 m above the channel on average. These terrace treads have also been extensively eroded, as evidenced by frequent exposures of saprolite or relatively weathered bedrock with vein quartz at their surface (Fig. 5.3). This unweathered bedrock and/or saprolite likely represents the strath surface for the Qt1 terrace unit. The strath surfaces of the Qt1 also include, however, rounded to sub-rounded (rounding average of 0.73 and sphericity average of 0.72) quartzite cobbles and gravels were relatively common on these Qt1 remnants. These surface clasts range from 1-14 cm, and have an average diameter of 7 cm (Table 5.1).

Qt2 – Average 38 m elevation above the modern channel

The Qt2 terrace lies between 34 to 44 m above the modern channel on average. In most locations, this surface is also characterized by saprolite and weathered bedrock at or very near the surface, with common intact vein quartz and bedrock float found on treads. This unweathered bedrock and/or saprolite likely represents the carved strath of the Qt2 terrace unit. Qt2 remnant treads consistently exhibit rounded to sub-rounded (rounding average of 0.74, sphericity average of 0.66) quartzite surface clasts that range from 1 to 22.5 cm, averaging approximately 5.2 cm (Table 5.1). Large patches of coarse gravels were common on Qt2 surfaces, with clasts from more detailed clasts counts averaging 2.3 cm in length and 1.6 cm in width. The maximum diameter clast measured during clast counts on this unit was 7.8 cm long and 4.3 cm wide.

The one soil pit (Table 4.2) examined on the Qt2 surface was characterized by A/B/Bt horizonation with clear evidence of bedrock proximity (such as white kaolinite streaks) beginning at the surface (within ~1 cm) in the pit. Most weathered B horizons were based on field observations of structure, texture and presence of clay films. Soil profile B horizons are dominated by strong, deep red hues, ranging from 7.5 YR 3/4 to 2.5 YR 4/8 with depth. Soil structure in B horizons is characterized by fine to medium angular blocky peds. Wet consistence of the soil is mostly sticky and plastic, while moist consistence varies from very friable near the surface to firm/very firm with depth (~1 – 56 cm). The Qt2 soil decreased in texture with depth from sandy loams to sandy and silty clays. Clay films increase with depth from faint in B horizons to distinct/prominent in Bt horizons along ped faces and in pores (Table 4.2). Clay content of the Qt2 soil increases with depth with a maximum measured of 10.64%. The dominant grain size was silt in the

most weathered B horizon of the pit, at 62.57%. Iron content of the most weathered B horizon for this terrace unit's single pit was measured at 0.23% Fe_H and 8.01% Fe_D, with an iron activity ratio of 0.03 (Table 4.3). Total iron for the Qt2 surface is 0.094 g/cm^2.

Qt3 – Average 24 m elevation above the modern channel

The Qt3 terrace unit is a well-expressed terrace unit along the entire study area, and lies approximately between 16 and 29 m above the modern channel. In many locations, it appears the Qt3 terrace sediments have been eroded, as evidenced by bedrock float and vein quartz at the surface. This unweathered bedrock and/or saprolite found at the surface is likely the remnants of the strath surface of the Qt3 unit. Thus, all soils pits dug on this surface encountered the underlying granodiorite bedrock.

In contrast to older terraces, some cobbles and gravels comprised of the local granitic bedrock were found on this terrace in addition to those composed of quartzite. On average, all surface clasts on Qt3 are rounded (rounding average of 0.76 and sphericity of 0.72) and range in size from 2 – 51 cm in length (Table 5.1; Fig. 5.4). For this terrace unit, in addition to 5 soil pits, we documented the gravel content of two construction exposures and one of the soil pits which contained gravel facies, at 3m, 0.1, and 0.05 m, respectively (Fig. 5.5 A, B; Fig. B2, Appendix B). These *in situ* clasts range from 2 to 40 cm, with an average maximum diameter of 11 cm. Three additional clast counts from the Qt3 surface reveal averages of 2.62 cm in length and 1.88 cm in width.

Soils of the Qt3 exhibit Ap/B/Bt/2Bt/2Cr horizonation, with most pits reaching C horizons in bedrock. Soils of the Qt3 unit are characterized by red coloration ranging from 10YR 3/3 in its upper A horizons to 2.5YR 4/8 in the most weathered B horizons. Soil structure is described as fine/medium to coarse peds with angular to sub-angular

shape. Moist consistence ranges from firm to very firm (~19.5 – 157.9 cm), and sticky to plastic for wet consistence in B horizons. Qt3 soil texture decrease with depth from sandy loams and sandy clays to sandy clay loams and clay loams. Clay films range from distinct to prominent among ped faces and pores in the most weathered B horizons (~7 – 169.71 cm) (Table 4.2). Clay content for the most weathered B horizons of this terrace unit ranged from 10.42 to 13.41%, with the majority of grain sizes for the fine fraction being dominated by silt, ranging from 57.57 to 78.82%, with the exception of the most complete exposure (JAC 15) which was dominated by sand (57.82%) in the most weathered B horizon. Iron content for the most weathered B horizons ranged from 0.1 to 0.62% for Fe_H, while Fe_D weight percent ranged from 0.42 to 9.15%. Iron activity ratios ranged from 0.11 to 0.18 in the most weathered B horizons (Table 4.3). Total iron calculated averaged at 0.066 g/cm^2 among five profiles, with a range of total iron from 0.017 to 0.151 g/cm^2.

In the center of the study area, a change in bedrock from granodiorite to phyllonitic schist appears to result in textures that include more silty clays and silt loams than those of the granodiorites, with very weak structure and clay films (Pits JAC 4, 5 and 6) (Table 4.2). Also, two pits dug on this terrace unit in the upper reaches of the study area were lacking overlying sediments, with bedrock clearly evident within ~10 cm of the surface. These soils are markedly different in their morphology, characterized by hues ranging from 7.5YR 4/4 to 5YR 5/6, coarse peds, and slightly sticky and slightly plastic to plastic for wet consistence (Table 4.2). Thus, these latter soils represent minimum weathering characteristics relative to the age of this surface and are not included in the discussion below.

Qt4 – Average 9.5 m elevation above the channel

The Qt4 terrace unit lies between 9 and 11 m above the modern channel. This unit manifests as broad, planar remnants with some relief, but with little evidence of erosional degradation in the soil profiles. The parent material of this unit is well-sorted, medium to fine grained sands with intermixed silt and clay, with a range of 80 – 95% quartz. Radiocarbon dating from a sample collected at a depth of 100 cm of the Qt4 in the upper reach area yielded a 6,484 ± 41 ypb age. However, this terrace is consistently topped by a sand unit with minimum soil development, showing that extreme modern floods can reach Qt4 elevations.

Cobble and gravel facies of the Qt4 unit are comprised of quartzite and bedrock. No cobbles are found in the soil pits examined on the surface. Instead, cobbles were found at depth in the Qt4 deposits and in small drainages adjacent to treads. Surface clast measurements range from 3 to 25.5 cm, with an average maximum diameter of 9.5 cm, and rounding and sphericity averages of 0.73 and 0.75, respectively (Table 5.1). Clast counts on the Qt4 terrace unit average 2.93 cm in length and 2.04 cm in width. Exposure of the basal contact between Qt4 and its strath was observed only once in the field area (Fig. 5.6), while being mapped in the study area. This evidence suggests that Qt4 may lie on its own strath surface that sits ~2.7 m above the modern channel, while the Qt5 shares a strath surface with the current channel floor. However, all mapped units exhibit about 3 m of relief on their mapped treads.

Qt4 soil profiles are characterized by A/Ap/B/Bb/Btb/Cb horizonation, with a common buried A horizon at approximately 0.25 m, ranging from 0.2 to 0.3 m in thickness. This buried A horizon is present throughout the study area; and likely

represents the pre-1916 flood surface. Soils on this unit are characterized by yellowish-red to tan coloration, ranging from 10YR 4/4 in A horizons to 10YR 5/8 - 7.5YR 4/6 in B and buried horizons. Soil structure is not as well-formed as older surfaces with medium angular blocky peds. Wet consistence changes from slightly sticky and slightly plastic to sticky and plastic (~47.25 – 150 cm) with depth. Qt4 soil texture decrease with depth from sandy loams and loamy sands to sandy clay loams and silty clays. Clay films in the soils of the Qt4 unit are seldom, with faint coatings in pores and some ped faces (Table 4.2). Clay content varies from 5.35 to 10.92% in the most weathered B horizons. Iron content of the Qt4 terrace unit ranged from 0.24 to 1.51% for Fe_H, from 0.32 to 1.58% for Fe_D, and iron activity ratios that range from 1.4 to 1.51, with an outlier of 0.35 for a pit located at Lansford Canal State Park, where disturbance from a man-made canal may have influenced this value (Table 4.3). Average total iron for Qt4 soils was deemed to be 0.016 g among four different pits, with a range from 0.011 to 0.018 g.

Qt5 – Average 3 m elevation above the channel

The Qt5 unit is the lowest unit in the Catawba River valley, and lies approximately between 3 and 5 m above the modern channel. This unit is generally a paired terrace, with several long stretches of unpaired treads throughout the study area. This unit can be considered the flood plain, as it lies adjacent to the modern channel throughout most of the study area and is characterized by evidence of active flooding, such as cumulic designations in all soil profiles. This unit shows little to no evidence of erosion. The parent material of this terrace is very similar to the parent material of the Qt4, and is comprised mostly of medium to fine grained sands intermixed with silts and clays. Cobble and gravel facies of this unit are comprised of quartzite and bedrock and

are found in small drainages and in the main channel of the Catawba River. Surface clasts range in size from 6.25 to 25.5 cm, with an average maximum diameter of 15.86 cm (Table 5.1). Clast counts, where large well-sorted patches of gravels are present, revealed an average length and width of 3.21 cm and 2.22 cm, respectively.

Soils of the Qt5 terrace unit reveal A/Ap/B/C horizonation and exhibit characteristics of cumulic soils – that is an accumulation of materials that leads to thickened epipedons – as would be expected of a floodplain. Qt5 soils are characterized by yellowish to red coloration, with Munsell colors ranging from 10YR 3/4 and 10YR 4/2 in A horizons and 7.5YR 5/8 and 10YR 5/6 in B horizons. Soil structure remains uniform throughout Qt5 profiles with peds ranging from fine to medium in size and angular blocky in shape. Moist consistence of the Qt5 soils generally varies from slightly sticky and slightly plastic to sticky and plastic. Soil textures range from sandy loams in the upper horizons to sandy clay loams, sandy loams and silt loams in B horizons. Clay films for this terrace unit vary from faint to distinct in pores and on ped faces (Table 4.2). Clay content of the most weathered B horizons range from 4.72 to 7.46%, with the highest value coming from the surface located in the middle reach of the field area (JAC 6). Iron content for the Qt5 terrace unit ranges from 0.53 to 1.77% Fe_H, 0.40 to 2.32% Fe_D, and iron activity ratios that range from 0.70 to 1.48 (Table 4.3). Total iron was averaged from three pits at 0.013 g/cm^2, and ranged from 0.004 to 0.022 g/cm^2.

5.2: Age Control

Using the Mills (2000) surface age/elevation curve, surface ages of mapped terrace units on the Catawba River are calculated as follows: 4,590 ± 404 ka for the Qt0 (69 m), 1,851 ± 365 ka for the Qt1 (46 m), 1,181 ± 194 ka for the Qt2 (38 m), 407 ± 143

ka for the Qt3 (24 m), 50 ± 8 ka for the Qt4 (9.5 m), and 5 ± 2 ka for the Qt5 (3 m) (Fig. 5.7; Table 5.2). Reported errors are calculated using the standard deviation of the height above the channel for all terrace remnants mapped in the field area.

Radiocarbon samples were collected from both the Qt4 and Qt5 terrace units at approximately 1 m depth (Fig. 4.6A, B and C; Table 5.2). Previously, samples taken from the lower extent of the Catawba River's bank, just above the modern water level, revealed dates that reflect the most recent 100-year flood event that occurred in 1916, where record flood levels were recorded ~12 m above the current level of the river. Analysis for sample RCN – 3 collected from the Qt5 surface at 1 m depth reported a calendric age of 144 +/- 95 ybp. Sample RCN – 2 collected from the Qt4 surface at 1 m depth was dated at a calendric age of 6,484 +/- 41 ypb. A total of two Infrared Stimulated Luminescence samples were collected from the JAC 11 and JAC 15 on the Qt3 unit. Sample IRSL – 1 collected from the JAC 11 exposure at a depth ~2.5 m from the surface yielded an age of 100.7 ± 27.4 ka (Fig. 4.7C). Sample IRSL – 4 from the JAC 15 exposure at a depth of ~4 m reported an age of 182.7 ± 36.4 ka (Fig. 4.7A and B; Table 5.2). These samples were both collected from approximately 14 m height above the channel, which when plugged into Mills (2000) surface age vs. elevation curve, yield a comparable age at ~128 ka (Table 5.2).

Soil chemical and morphological properties (i.e. color hue and pedogenic iron) of Catawba River terraces are comparable to other regional chronosequence studies conducted in the eastern United States (Mills and Allison, 1995; Engel et al., 1996; Eaton et al., 2003; Layzell et al., 2012). However, few studies in the eastern US Piedmont provide reliable age control for Cenozoic landforms. McGavick et al. (2016) present a

series of Infrared stimulated luminescence (IRSL), optically stimulated luminescence (OSL), and terrestrial cosmogenic nuclide (TCN) erosion rate ages for eight fluvial landforms on the South Anna River, Virginia. Surface heights of this study, for instance those ~24 m above the modern channel exhibit ages of approximately 400 ka. This height is similar to the Qt3 surface on the Catawba River, and is consistent with Mills (2000) dates applied here (~407 ka) (Table 5.2). Soil morphological properties of the South Anna River terrace (24 m) exhibit 2.5 YR hues and silty clay to clay loam textures, which are consistent with properties observed in Qt3 soil profiles of this study (Table 4.2). Terrace units approximately 4 m above the modern channel on the South Anna River ranged from 16.9+/-3 – 18+/-4.9 ka (McGavick et al., 2016). These ages are approximately 12 ka older than those derived from the Mills (2000) curve applied to the Qt5 unit of this study. Morphologically, soils of terraces ~4 m above the modern channel on the South Anna River and the Catawba River share similar hues, at 10YR, however, textures on South Anna terraces exhibit finer textures (clay loam) than the Catawba (sandy loam). Older terraces of the South Anna River do not sit as high the oldest surfaces on the Catawba River, >27 m compared to 38 – 68 m, respectively (McGavick et al., 2016) (Table 5.2).

Another comparable system, the James River, VA, located ~400 km north of the field area; exhibits well-preserved terraces, in the upper portion of the valley, ~60 m and 75 – 90 m above the modern channel. Cosmogenic Super^{10}Be dates for these surfaces range from ~1.0 – 1.1 Ma for the lower terraces at 60 m, and 1.1 – 1.3 Ma for the higher terraces at 75 – 90 (Hancock et al., 2004; Hancock et al., 2002). Heights above the modern channel are comparable with this study's Qt0 surface at approximately 69 m

above the modern channel, however, ages estimates using Mills (2000) curve are much older for the Catawba Qt0 (~4.6 Ma). No other soil data from the James River terraces were collected. Studies of smaller systems in the Piedmont, such as Ivester et al. (2009) study on the North Tyger and North Pacolet River, SC, present ages for floodplain/lowest terrace formation to range from 4500 – 1500 ybp based on artifacts found in buried A horizons of the terrace unit. This is comparable to ages applied to Qt5 via Mills (200) in this study (5 ka) (Table 5.2).

Lastly, the Susquehanna River is a system where fluvial stratigraphy is well preserved on high strath terrace units in the Piedmont of Pennsylvania. These deposits have been correlated to similar deposits of fluvial systems in the Piedmont and upper Coastal Plain of the Mid-Atlantic region (Pazzaglia and Gardner, 1993; Engel et al., 1996; Pazzaglia et al., 1997). These fluvial deposits, palynologically dated to the mid- to late- Miocene (~23 Ma) (Pazzaglia and Gardner, 1993), lie much higher above the channel than the highest terraces of this study. This varies from older terrace units of this study that lack preservation of fluvial deposited materials. Terraces of the low Piedmont on the Susquehanna, reflect comparable heights above the modern channel comparisons to strath surfaces of the Catawba; however, only a couple of units share similar heights. The highest low Piedmont Qt strath surface (Qtg) recorded in Pazzaglia and Gardner (1993), correlates to Qt1 terrace units in terms of height above the modern channel, however Qt terrace units of the Susquehanna are well-preserved in sedimentology that allows correlative analysis between other Wisconsinan and Illinoian glacial deposits. Other terrace units that correlate to mapped Qt units by Pazzaglia and Gardner (1993) include terraces at 22 m (Qt2), 10 m (Qt3), and 3 m (Qt6) above the modern channel. Soil

color and general textural descriptions of these terraces match descriptions of Qt3, Qt4, Qt5 units of this study, respectively. Stratigraphically, strath surfaces on the Susquehanna are more frequent, with extra strath surfaces falling in between 22 and 10 m, as well as in between 10 m and 3 m. Pazzaglia and Gardner (1993) attribute the preservation of straths to base-level fluctuation response during interglacial periods.

5.3.1: Chronofunctions of Soil Properties

Catawba terrace soil properties vary with respect to their time-trends. Hurst color index and clay films appear to change relatively predictably as a function of terrace age (Fig. 5.8 and 5.9). Weathering threshold trends are observed in these soils with respect to color, with hues reaching a maximum of 2.5YR and a Hurst Index value of 6.25, at around Qt3 time (~400 ka). Hurst Index Values are plotted against surface ages for most weathered B horizons (Fig. 5.8). This relationship is seen, as values decrease from ~12 – 15 index values in younger units (Qt5 – 4) to 6.25 in older units (Qt3 – 2). Maximum color hue generally increases from 10YR in Qt5 unit (~5 ka) to 2.5 YR in Qt3 – Qt2 units (~ 141.5 – 1181 ka) with surface age. Annotated soil pit photographs showcase this trend in color data, as yellowish-tan colors (10YR) transition into deep reds (2.5 – 5YR), from younger to older landforms (Appendix B).

In terms of other soil morphological characteristics, Birkeland (1999) showed that soil structure, clay films, and B horizon thickness, increase in development with increasing surface age. Clay films was the only one of these to show a meaningful trend with respect to increasing surface age in the Catawba terraces (Fig. 5.9). Clay films are present only as faint coatings on ped faces in younger soils (ex. JAC 5 and 3, Table 4.2), but are distinct and prominent on ped faces and in pores in older terraces (ex. JAC 11 and

15, Table 4.2). Upon analysis, average maximum clay film index values increase predictably with age with values reaching a plateau near Qt2 surface age (~1.2 Ma) (Fig. 5.9). Values at this maximum weathering threshold represent clay films that are common to many in their amount, and either distinct or prominent in their distinctness. Other soil morphological characteristics, such as texture (Fig. 5.10) and wet consistence (Fig. 5.11) did not change predictably with surface age

5.3.2: Grain Size analysis

Generally, soils are also known to increase in clay content with increasing surface age (e.g. Eppes et al., 2008, Engel et al., 1996), as finer particles are translocated down by water infiltrating the weathering profile, and as primary minerals weather into clay minerals. For this study, percent clay does increase with age in the most weathered B horizons of pits (Fig. 5.12). In general, older surfaces (Qt3 – Qt2), clay content also increases with depth, ranging from 6 – 7% in A horizons to 10 – 20% in Bt horizons. Ternary plots (Fig. 5.13; Appendix C) show that the soils on the Qt2 and Qt3 within the study reach of the Catawba River are primarily dominated by the sand and silt sized fraction, with silt being a prominent component of most weathered B horizons in older surfaces, with a range from 35.87 – 80.02%, and a total average of 46.51% (Fig. 5.13). While sand is the dominant particle size in the younger Qt4 and Qt5 terrace units with a majority of pits ranging from 50 – 80% sand for all horizons. A few pits on the Qt4 and Qt5 (JAC 1, 12, 3, and 6) exhibit B horizons with sand percentages of ~20 – 30% in the weathering profile, with younger terraces, primarily Qt5, exhibiting coarser textures than older terraces (Table 4.3).

To further evaluate the differences between the particle size distribution of different terrace units in this study a T-Test statistical analysis was performed on the d10, d50 and d90 distributions of each soil sample (Table 5.3A, B and C, respectively). The d10, d50 and d90 distributions show where 10, 50 and 90% of the mass of the sample is comprised of particles smaller than the reported size. Averages for d10, d50, and d90 for terrace units Qt5 – Qt2 are presented in Table C1 in Appendix C. What the T-Test results determine is if there is a statistical difference (p-value < 0.05) in the recorded value (average of all horizons in all pits) for each d10, d50 and d90 analysis between different terrace units. For d10, we see that the Qt5 separates itself from older surfaces as being significantly coarser (Table 5.3A). Whereas, there is no statistical difference in d10 for the Qt4 – Qt2, which are much finer. For d50, Qt4 is no longer statistically different from the Qt5, while Qt3 – 2 remain significantly different from Qt5 (Table 5.3B). In the d90 analysis Qt3 highlights itself as significantly distinct from Qt5 and Qt4 (Table 5.3C). These differences and similarities can, again, be explained by coarse textures in younger surfaces, where older surfaces contain higher percentages of clay and silt. Qt2 does not show any statistical difference in the d90 analysis between younger surfaces. This is likely due to a sampling of saprolitic materials in older surfaces compared to younger surfaces.

5.3.3: Pedogenic Fe Analysis

The analysis of pedogenic iron via iron activity ratios in soil weathering profiles has been shown to decrease as surface age increases (McFadden and Hendricks, 1985; Vinson et al., 2005; Eppes et al., 2008; Layzell et al., 2012). Iron activity ratios are a way to evaluate iron formed only via weathering processes as opposed to iron bound in

unweathered materials (Birkeland, 1999). Overall, the lowest iron activity ratios for most weathered B horizons were found in older surfaces (Qt3 – Qt2). Iron activity ratios for most weathered B horizons in this study show an overall decline with relative surface age, where Qt5 and Qt4 surfaces average at 0.97 and 1.17, respectively, and Qt3 and Qt2 average at 0.13 and 0.17, respectively (Fig. 5.14). These averaged values do not show declines between Qt5 – Qt4 and Qt3 – Qt2, however the Qt2 terrace is represented by only one soil pit and is thus not reflective of weathering of the original terrace deposit.

5.3.4: Elemental Analysis (XRF)

Elemental analysis of the percentage of large base cations, such as Ca, K and Mg, contained in a soil profile decrease as soils weather (e.g. Taylor and Blum, 1995). An index, or depletion factor ($X_{i,j}$), can be calculated as a ratio of the difference in quantity of the base cation of interest in each horizon and its quantity in the parent material, to titanium – assumed to be immobile – in the same horizon and in the parent material using the equation below, where $C_{i,j}$ is the concentration of the element (*i*) in a particular horizon (*j*), $C_{i,p}$ is the concentration of that same element (*i*) in the parent material (*p*), and Ti_j, Ti_p are the concentration of titanium in the same horizon (*j*) and parent material (*p*) (Taylor and Blum, 1995).

$$X_{i,j} = (C_{i,j}/C_{i,p})/(Ti_j/Ti_p)$$

Values less than 1.00 show depletion, whereas values greater than 1.00 show enrichment of that base cation. In order to assess base cation depletion in fluvial terrace on the Catawba River, sands from the modern-day channel were collected to compare to soils in the terraces. The base cation iron progressively decreases with soil age, decreasing from 0.9 to a low of 0.24 near the surfaces of soils, from 5 – 142 ka (Fig. 5.15). Aluminum,

also decreases with soil age, as values change from ~1.3 to 0.4 at the surface of soils from 50 – 1181 ka respectively. These observations are consistent with results seen in Taylor and Blum (1995). In each profile, (Appendix C), the base cation iron appears to accumulate in the subsurface of older surface (>= 50 ka), a visual representation of accumulation of pedogenic iron as a result of weathering.

5.4 Channel Morphology and Longitudinal Profiles

The modern channel of the Catawba River is characterized by a very shallow stream gradient, with an average of 0.0005. Based on field observations, the channel depth of this system is extremely shallow, with bedrock visible or breaking the water surface nearly throughout the study reach, depending on the water level. The steepest gradient change on the modern Catawba channel is located ~38 km from the Lake Wylie Dam (Fig. 4.8), where the channel drops 6.09 m over 1.91 km, or a stream gradient of ~0.003. This is the location of Lansford Canal State Park, and this location will be referred to as Lansford Canal knickpoint for the rest of this paper (LCKP). This is the last major knickpoint on the river before the Fall Zone.

Longitudinal profiles of terraces were generated from river distance 0 (35.021237°; -81.005722°), near Lake Wylie Dam to 45.71 km, or the beginning and end, respectively, of the study area. This plot (Fig. 4.8) shows missing data for the Qt0 surface, as it is only present at the beginning (1.05 – 1.27 km) and middle (31.89 – 32.14 km) of the study area. Gaps in the presence of Qt1 exposures are also present from 2.94 to 6.6 km, 6.7 to 11.98 km, and 12.2 to 16.65 km (Fig. 4.8). In these areas, Qt2 is the highest surface above the channel in the valley. In older surfaces (Qt1 – Qt3) along the profile, there is significant (2 – 9 m) variability in elevation among treads and tread

remnants of the same unit, within the same small area. This variability could be attributed to the Quaternary erosion of terrace treads that is apparent in older surfaces in the Catawba River valley or natural topographic relief along the strath surface. This may also be explained as a possible preservation of braided channel morphology, where stacked terraces in the profile represent stretches of the channel where multiple channels previously existed.

Elevation difference between different terrace units at the same distance downstream is roughly uniform in older surfaces (Qt1 – Qt4) with the greatest vertical offset between treads occurring between Qt3 and Qt4, with a maximum difference of 22.86 m at ~16 km downstream, and an average of 14.46 m for the entire study area. Differences in height between the two youngest surfaces in this study, the Qt4 and Qt5 units, are much smaller. The smallest vertical height between these two surfaces is 3.05 m in several locations in the upstream reaches of the study area, with an average difference of 6.07 m throughout the entire study area.

Overall the Catawba has been a fluvial system marked by net down-cutting during the mid- to late Pleistocene, if the Mills (2000) chronology applies to the Catawba. Mapping of terraces and terrace remnants and longitudinal expressions of terraces herein support overall channel narrowing between ~ 1851 – 50 ka, and total vertical incision of ~ 69 – 46 m over the course of ~ 2 m.y. Generally incisional rates based on Mills (2000) generated ages for each terrace unit does not exceed 0.1 mm/yr. Incision rates between each major terrace unit are as follows: Qt2 – Qt1 ~0.02 mm/yr., Qt3 – Qt2 ~0.02 mm/yr., Qt4 – Qt3 ~0.04 mm/yr., and Qt5 – Qt4 ~0.1 mm/yr. Qt3 incision rate based on the average of IRSL ages presented in Table 5.2 are calculated to be 0.1mm/yr.

Figure 5.1: Photograph of relatively unweathered granodiorite bedrock on the highest surface (Qt0) of the study area (216.4 m). Field Assistant Pamela Mefferd (1.7 m) pictured for scale.

Figure 5.2: Photograph of Qt0 pebbles found adjacent to saprolitic material.

Figure 5.3: Exposure of Qt1 profile weathered into granodiorite bedrock located at the southern corner of the intersection of Fort Mill Southern Bypass and Holbrook Rd, Fort Mill, SC. Lanyard (~44 cm) pictured for scale.

Table 5.1: Summary table of clast data collected on Catawba River terraces. Ages presented for Qt5, 4, 2, 1, and 0 are based on Mills (2000) surface age vs. elevation curve. Qt3 age is the average of IRSL – 1 (101 ± 27 ka) and IRSL – 4 (183 ± 36 ka).

Terrace Unit	Surface Age (ka)	Height above the channel (m)	Max Diameter (cm)	Min Diameter (cm)	Average Diameter (cm)	Average Rounding	Average Sphericity
Qt0	4590± 404	69	2.25	2.25	2.25	0.5	0.5
Qt1	1852 ± 365	46	14	1	6.69	0.73	0.72
Qt2	1181 ± 194	38	22.5	0.81	5.27	0.74	0.66
Qt3	141 ± 32	24	51	0.51	11.02	0.76	0.72
Qt4	50 ± 8	9	25.5	0.66	9.54	0.73	0.75
Qt5	5 ± 2	3	25.5	0.71	15.88	0.90	0.80

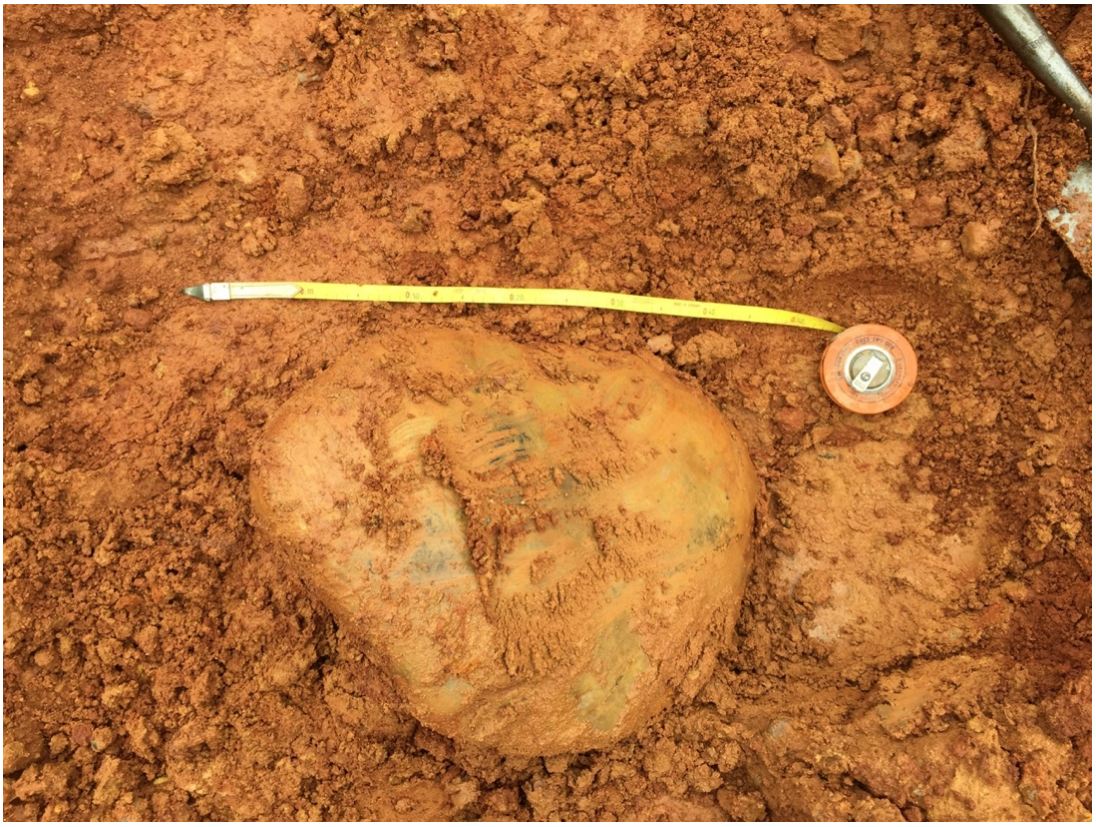

Figure 5.4: Photograph of the largest rounded boulder found in the study area (51 cm length). Located at JAC 15 (Qt3) exposure, Riverview, SC.

Figure 5.5: A) Photograph of gravels found *in situ* at JAC 15 (Qt3) Riverview, SC and B) Photograph of gravels found *in situ* at JAC 11(Qt3) Fort Lawn, SC.

Figure 5.6: Photograph of the basal contact of the Qt4 terrace unit, Riverview, SC. The bedrock is located in the bottom left hand corner of the photograph.

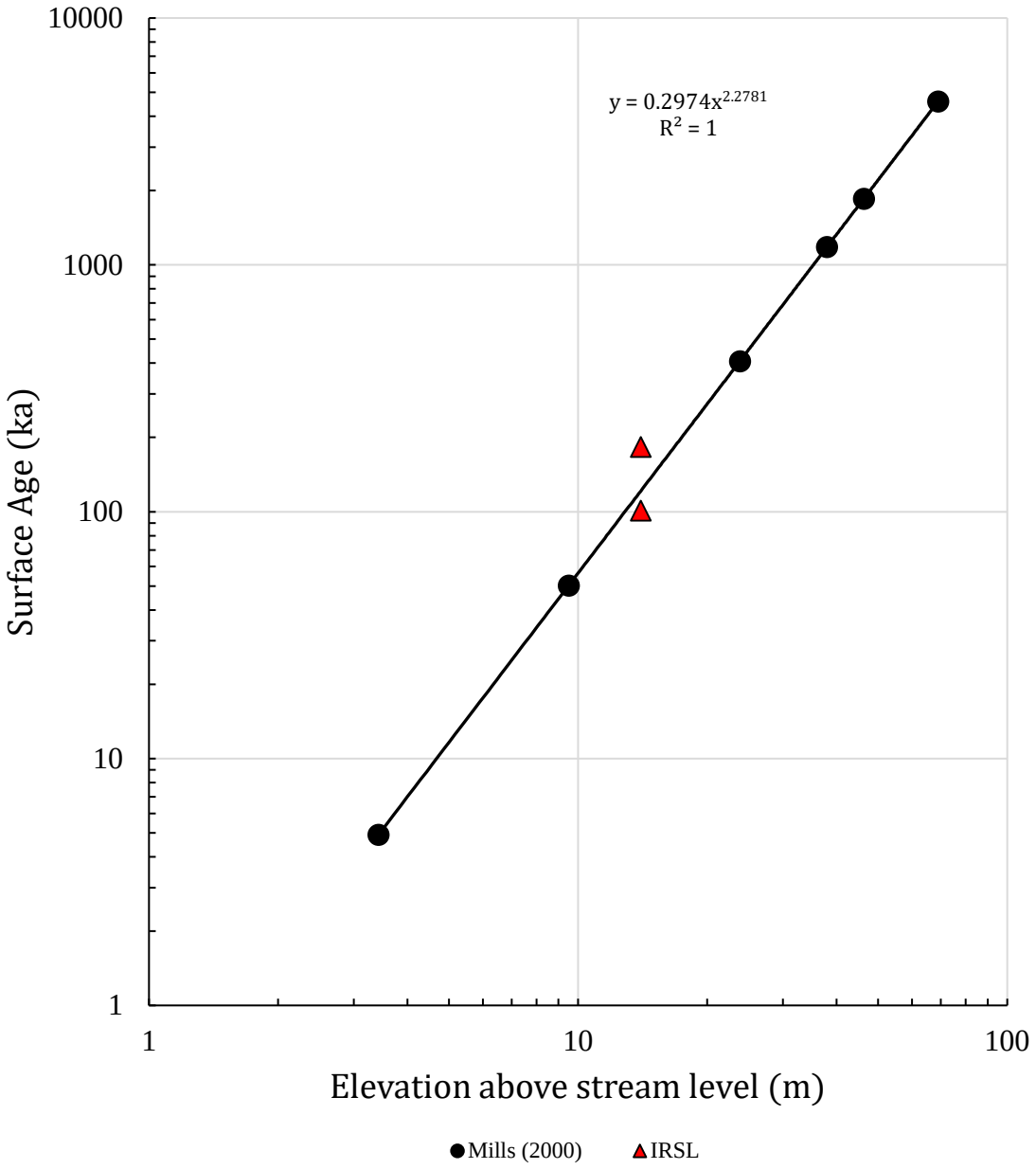

Figure 5.7: Log-log plot of terrace heights above stream level for Qt5 – Qt0 terraces of this study using Mills (2000) equation. IRSL ages obtained from this study are portrayed in red.

Table 5.2: Summary table of age control, where HATC is height above the channel.

Study	River	Unit	HATC (m)	Feature	Age (ka)	Dating Method
This Study	Catawba	Qt0	69	Qt0	4591 ± 404	Mills (2000)
		Qt1	46	Qt1	1852 ± 365	Mills (2000)
		Qt2	38	Qt2	1181 ± 194	Mills (2000)
		Qt3	24	Qt3	407 ± 143	Mills (2000)
		Qt4	9	Qt4	50 ± 8	Mills (2000)
		Qt5	3	Qt5	5 ± 2	Mills (2000)
		Qt4 RCN-2	8	Qt4	6484 ± 41	^{14}C
		Qt5 RCN-3	2	Qt5	0.144 ± 95	^{14}C
		Qt3 IRSL-1	14	Qt3	100.7 ± 27.4	IRSL
		Qt3 IRSL-4	14	Qt3	182.7 ± 36.4	IRSL
Layzell (2012)	Catawba	Qt1	42	Terrace	1470 ± 180	Mills (2000)
		Qt2	28	Terrace	610 ± 75	Mills (2000)
		Qt3	14	Terrace	128 ±16	Mills (2000)
		Qt4	10	Terrace	50 ±6	Mills (2000)
		Qt5	3	Terrace	4 ± 0.5	Mills (2000)
McGavick (2016)	S. Anna	-	24	Terrace	400	OSL
		-	4	Terrace	16.9 - 18	
Hancock (2002 & 2004)	James	-	60	Terrace	1000-1100	^{10}Be
		-	75-90	Terrace	1100-1300	^{10}Be
Ivester (2009)	N. Tyger & N. Pacolet	-	-	FP	4.5-1.5	^{14}C

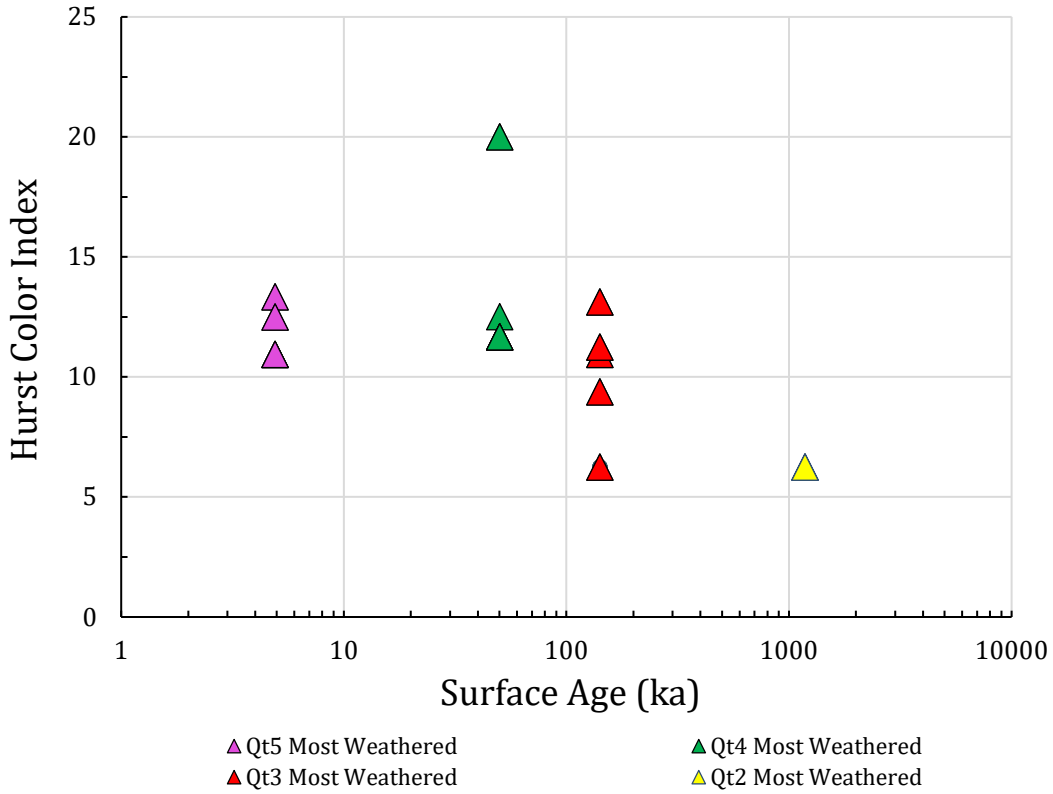

Figure 5.8: A lin-log plot highlighting the decrease in Hurst color index for most weathered B horizons with surface age (Mills, 2000). Low values in the Qt5 are interpreted as inheritance of previously weathered materials from older surfaces. Higher values in the Qt3 are weathered into granodiorite bedrock.

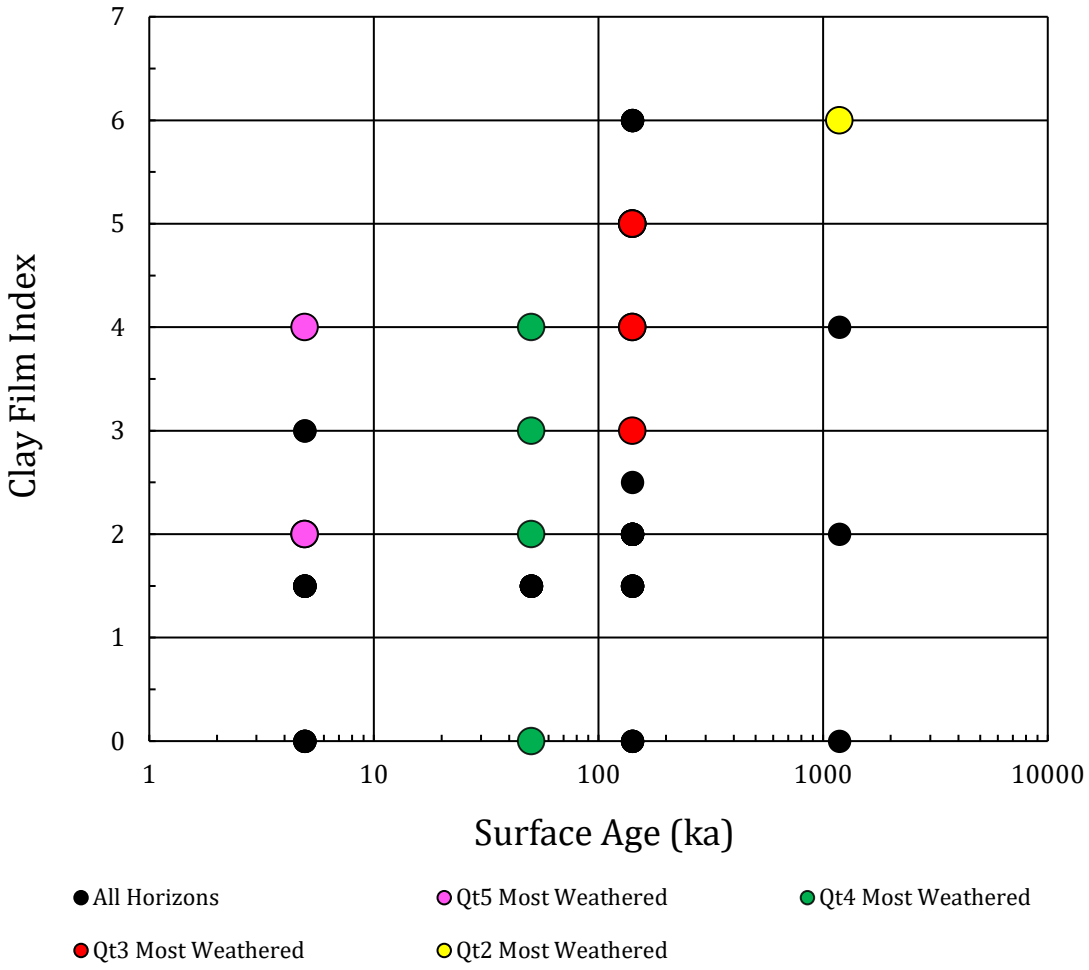

Figure 5.9: A lin-log plot depicting increases in amount and distinctness of clay films with surface age (ka). Increased values in Qt5 soils are attributed to inheritance of previously weathered materials due to hillslope erosion upstream.

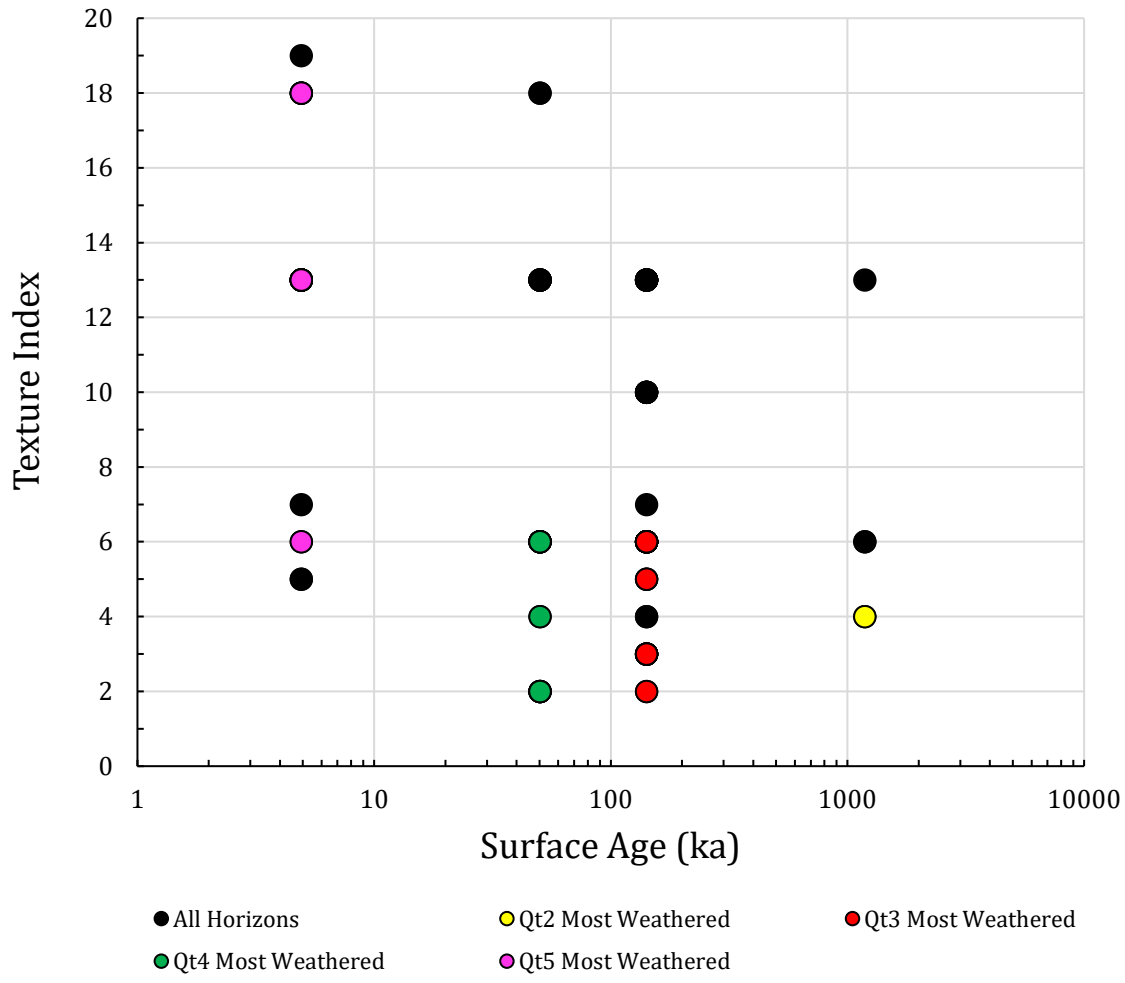

Figure 5.10: Lin-log plot showing no correlation between soil texture and surface age (ka).

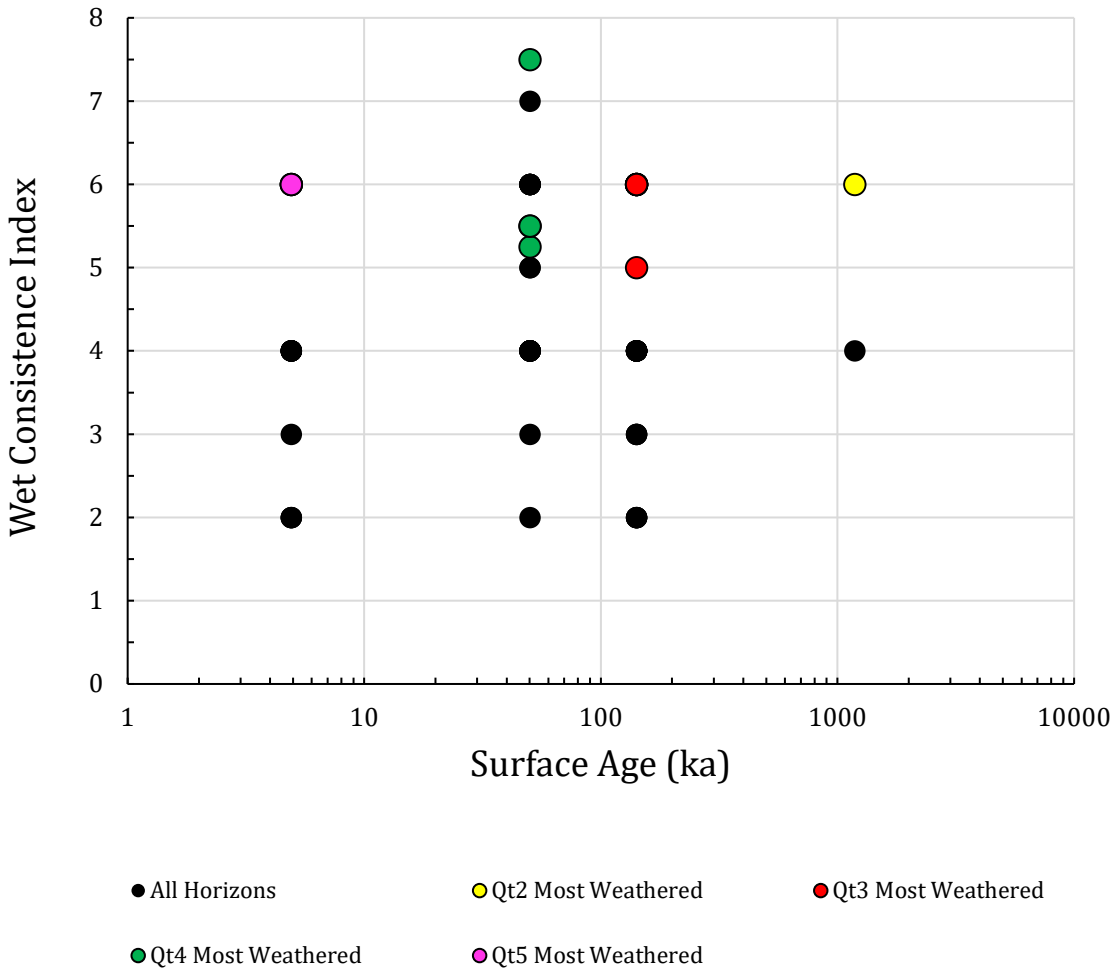

Figure 5.11: Lin-log plot showing no correlation between wet consistence and surface age (ka).

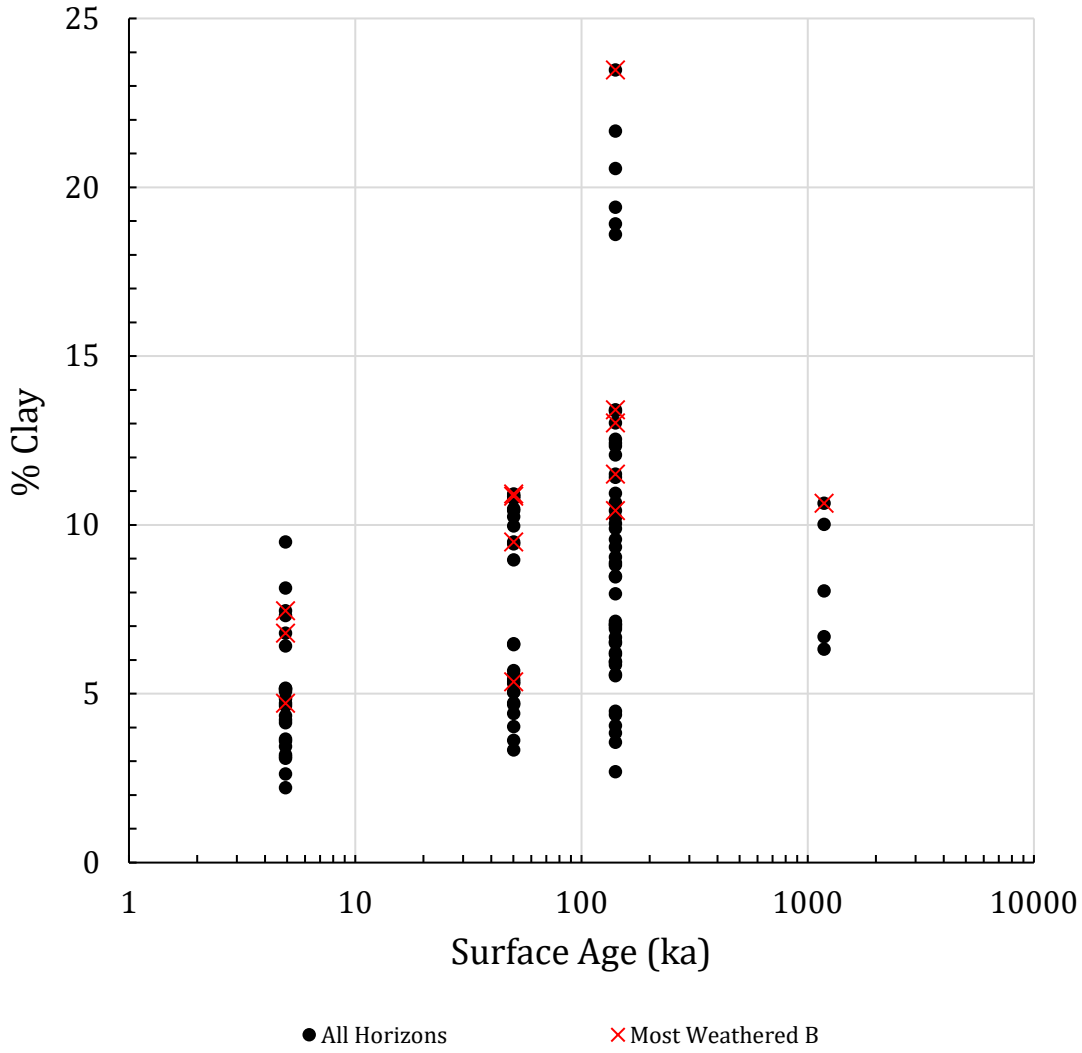

Figure 5.12: A lin-log plot highlighting the relationship between surface age (ka) and increases in clay content in most weathered B horizons (error < 0.3).

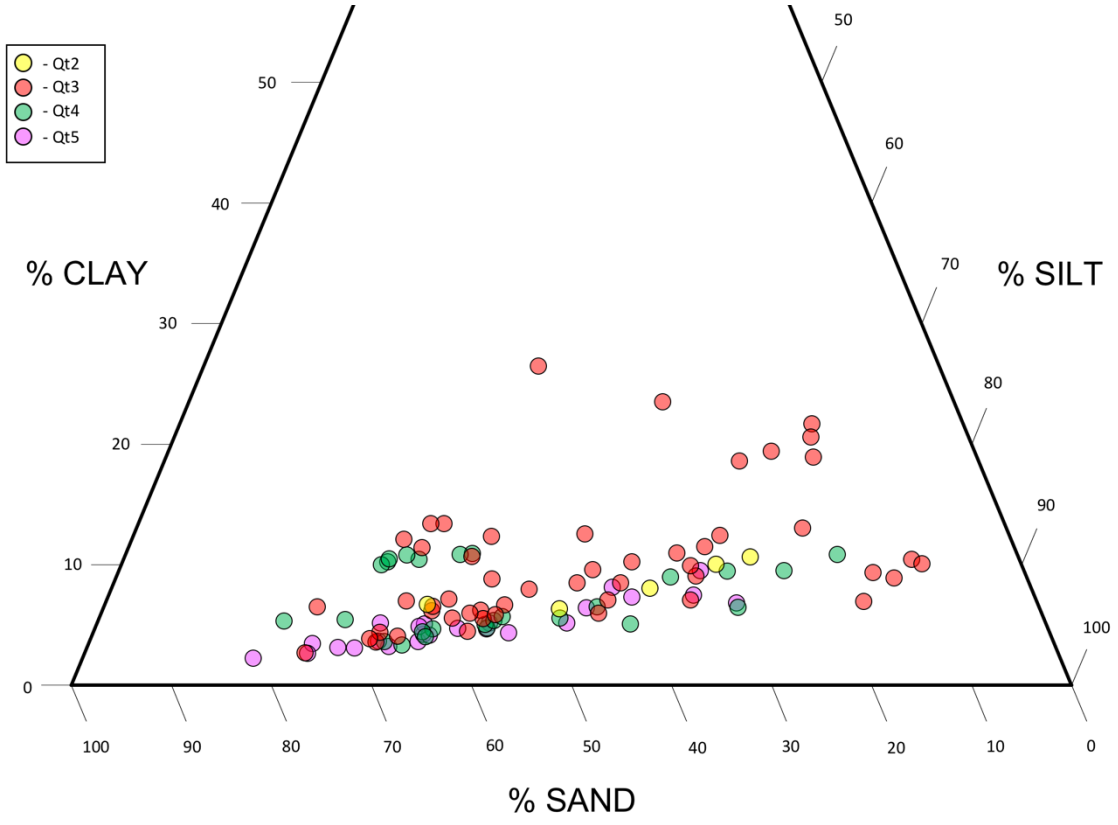

Figure 5.13: Ternary plot diagram of particle size analysis for all horizons for this study. Soils on the Catawba River are dominated by sand and silt.

Table 5.3A: Statistical T-Test for d10 particle size distribution (p-value < 0.05).

T-Test d10	Qt5	Qt4	Qt3	Qt2
Qt5	-	0.004	0.000	0.036
Qt4	0.004	-	0.270	0.226
Qt3	0.000	0.270	-	0.508
Qt2	0.036	0.226	0.690	-

Table 5.3B: Statistical T-Test for d50 particle size distribution (p-value < 0.05).

T-Test d50	Qt5	Qt4	Qt3	Qt2
Qt5	-	0.453	0.018	0.048
Qt4	0.453	-	0.093	0.102
Qt3	0.018	0.093	-	0.508
Qt2	0.048	0.102	0.508	-

Table 5.3C: Statistical T-Test for d90 particle size distribution (p-value < 0.05).

T-Test d90	Qt5	Qt4	Qt3	Qt2
Qt5	-	0.766	0.016	0.508
Qt4	0.766	-	0.030	0.759
Qt3	0.016	0.030	-	0.402
Qt2	0.508	0.759	0.402	-

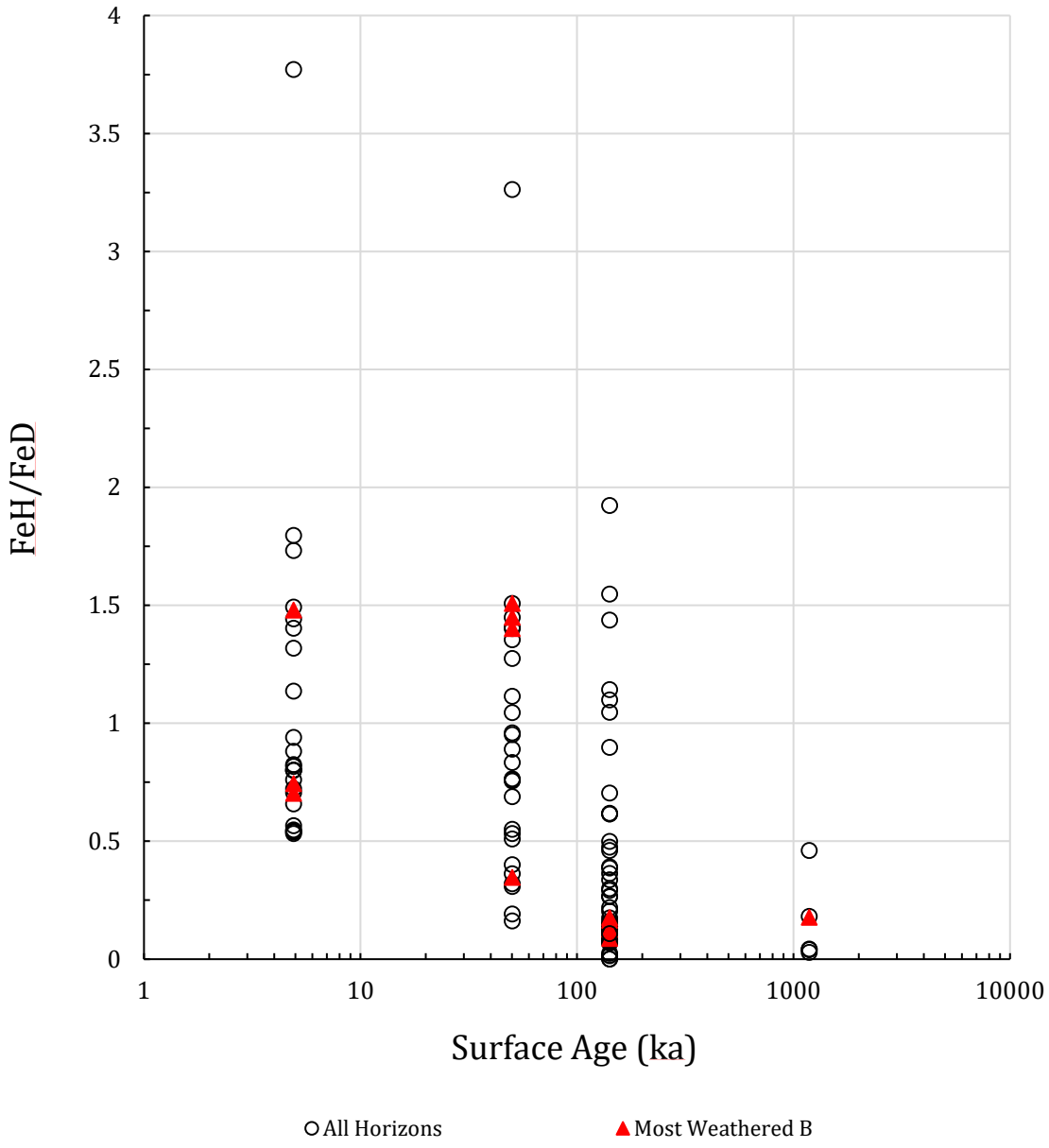

Figure 5.14: Pedogenic iron chronofunction of iron activity ratios for all soil samples from 15 locations. Most weathered B horizons are plotted in red. Analytical error are < 0.2 for both Fe_H and Fe_D.

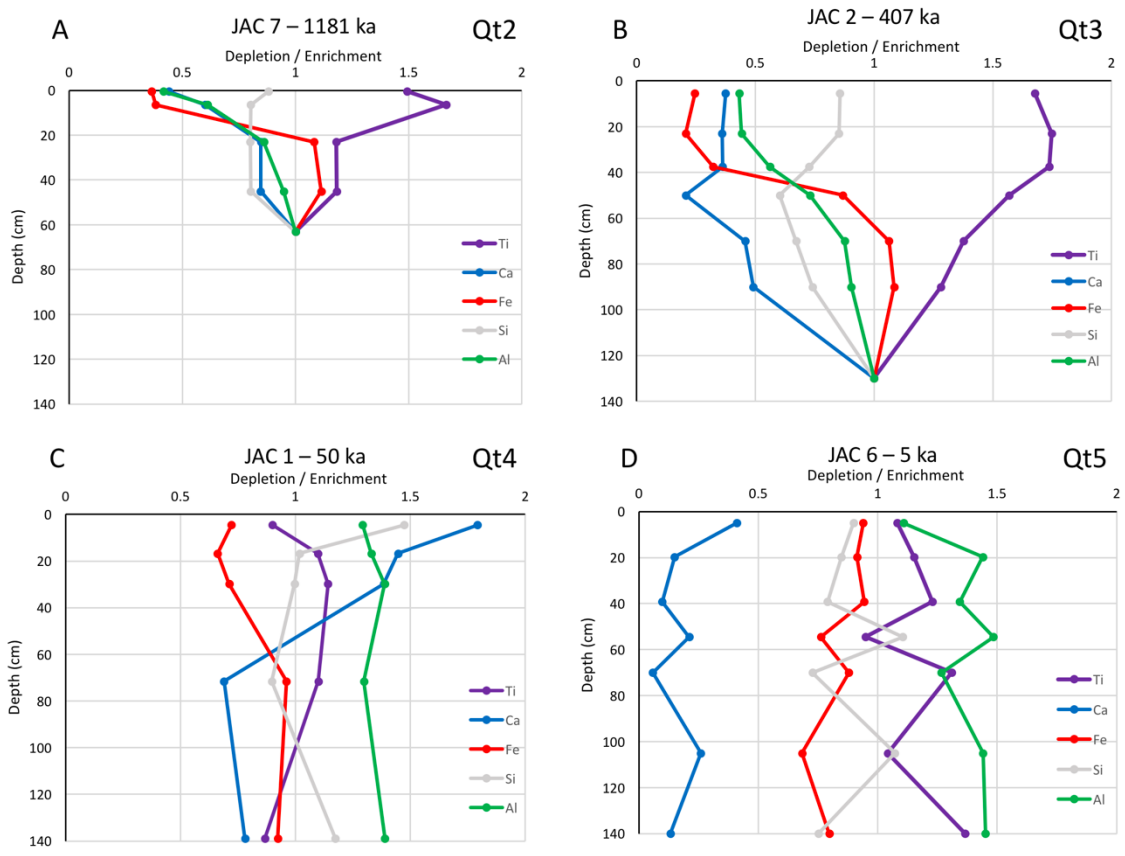

Figure 5.15: Depletion/Enrichment vs. depth plots for 5 base cations of different aged surfaces of the Catawba; A) Qt2 – 38 m, B) Qt3 – 24 m, C) Qt4 – 9.5 m, and D) Qt5 – 3 m. Depletion shows changes in base cation concentration in the profile compared to its concentration in the parent material. Ti is assumed to be immobile. Cations in A and B move towards 1 with depth because this represents saprolite at the bottom of the profile. C and D depletion were measured against 1916 flood sand deposit. Analytical error: Ti = 0.04; Ca = 0.04; Fe = 0.25; Si = 1.0; and Al = 0.51.

CHAPTER 6: Discussion

6.1: Soil Chronosequence:

Many studies have shown that soils weathering *in situ*, will exhibit morphological properties that change predictably over time until a threshold is achieved (e.g. Eppes et al., 2008). The soils of the Catawba exhibit similar trends as other studies in many cases (Fig. 5.8, 5.9, 5.13, 5.14, 5.15), however, there are several exceptions that can be explored. Some of the lack of time trends with soil ages in the Catawba terraces is likely due to the erosion of the terraces subsequent to their abandonment. For example, outlier high Hurst Index color values in the JAC 4, JAC 13 and JAC 14 pits of the Qt3 terrace can be attributed to the fact that there was evidence of bedrock at the ground surface of these soils. In contrast, the pits dug on the Qt3 in what is interpreted as fluvial deposited sediments exhibit some of the lowest values in the field area (Fig. 5.8). Thus, these latter values are interpreted to more representative of weathered alluvial materials. Similarly, relatively low values (10.93 and 11.67) were occasionally present in both Qt5 and Qt4 units in buried horizons. These values may reflect erosion and re-deposition of previously weathered sediments from older surfaces. Nevertheless, the overall reddening trends observed herein are similar to those of other studies with reddening reaching its maximum as surfaces reach ~100 ka (Foss et al., 1981; Markewich and Pavich, 1991; Layzell et al., 2012).

Another example of possible inheritance evident in the chronofunctions of the Catawba terraces is in the particle size analysis (Fig. 5.12). The Qt4 surface exhibits similar clay composition to the older units Qt3 and 2, with clay content spiking at ~10%

around 20 – 50 cm depth (Fig. 6.1). This zone coincides with a buried paleosol that is present in all Qt4 pits of this study. Given that clay accumulation in the form of clay films is not as well developed in this soil than in the older terrace soils, however, it is likely that the high clay content reflects a change in the size of sediment load for the Catawba. Similarly, the Qt5 soils also exhibit variability in percent clay with depth, as clay content in A horizons is initially high before fluctuating with depth (Fig. 6.1). This variability in texture is likely a result of sedimentological difference between flood events during the Holocene.

Percent clay does not exceed 26.46% (JAC 11 1, Qt3) in the study area (Fig. 5.12). This varies drastically from previous study on the Catawba River, where Layzell et al. (2012) documented ~25% clay in the youngest surface (Qt5, ~4 ka), with older surfaces exhibiting a maximum limit of ~60% clay. Layzell et al. (2012) were able to correlate these upper clay content values to similar soil textures (53% clay) for terraces of Mid-Atlantic Piedmont (Engel et al., 1996). The difference may provide additional evidence that even Qt3 terraces in the current study area have been significantly modified by erosion. Those at the Layzell et al. (2012) study site may be better preserved given their location in the interior of large meander bend, which would have cut off the remnants from runoff and erosion from the surrounding landscape.

Iron activity ratios show the strongest trends with time, and predictably decrease with surface age, with values plateauing at approximately Qt3 time (~142 ± ka) (Fig. 5.14). Slight increases in averages of iron activity between Qt3 – Qt2 (from 0.13 to 0.17, respectively) are consistent with the observation that Qt2 soil is developing in saprolite. The occasional lower iron activity values, such as 0.53 and 0.16, observed in Qt5 and Qt4

surfaces, respectively, have been observed in previous studies (Layzell et al., 2012), and have been attributed to inheritance of previously weathered materials from eroded remnants upstream.

In addition to age trends in the iron values, there is also a pattern in their variability relative to their location within the field area. Iron activity ratios are higher in Qt4 unit (~1.45) in the upper and middle reaches pit locations, and are drastically lower for the Qt4 terrace unit (0.34) downstream from these locations. Conversely, Qt5 values are relatively low (~0.7) at the beginning and central locations of the study area, and are higher (1.45) at the distal sample location. At the lower reach study site (Lansford Canal), iron activity ratios behave more predictably as values decline from 1.47 (Qt5) to 0.17 (Qt2) (Fig. 6.2). This change between Qt4 and Qt5 values based on location may be explained by the dynamics of the channel at Lansford Canal, where Qt5 surface lies no more than a meter above the channel in most portions of LCKP (~3.2 km in length). This steeper gradient may have some effect on the retention of materials during flood events. In the lower reach Qt4 exhibits its lowest ratio in the data set at 0.35. Values of the Qt4 most weathered B horizons at the upstream locations exhibit values that exceed 1.0, possibly reflecting the fact that in the upstream portion of the study area the Qt4 unit is still affected by occasional modern flooding. For example, these low values could be representative of relatively young sediments being deposited during flooding events, i.e. the historic 1916 flood that broke state rainfall and flooding records. In contrast, in the distal downstream, down-cutting in the lower reach has preserved Qt4 deposits, allowing for weathering processes to occur, thus a lower iron activity ratio.

Results, presented in (Fig. 5.15; Table 4.3; Appendix C) show that, in general, the base cation Fe decreases, or is depleted, upward through the weathering profiles. This could be explained by the translocation of iron-bearing clay mineral in profiles. In younger surfaces (Qt4 – Qt5) Fe and Si seem to be relatively static, suggesting renewal of the primary weathering surfaces during flood events. Trends regarding Si seem to be consistent throughout the study area, which may speak towards the dominating presence of sand in the stratigraphy of these soils.

6.2: Channel Morphology:

Maps and long profiles of the Catawba River terraces reveal that each of these terraces are generally paired fluvial features (Fig. 4.1 and 4.8; Appendix A) with several reaches where terraces are unpaired. Thus, their plan-view outcropping is likely a feature of lateral migration of the channel back and forth across the strath during eustatic high stands, whereas, the long profiles of the terraces reveal periods of vertical down-cutting throughout the river's history (Pazzaglia and Gardner, 1993; Merritts et al., 1994). Mapping also reveals an overall narrowing of the river valley through time, reducing by approximately half its width between Qt2 and Qt3 time (1181 – 142 ka), from an average of 3.03 to 1.52 km, respectively (Fig. 4.8). This general narrowing of the river valley suggests that the history of the Catawba River has been marked by net vertical down-cutting. Longitudinal profiles of terraces also exhibit this vertical incision through time as vertical height in between treads and strath surfaces increases from Qt1 – Qt4 time (Fig. 4.8); but care must be taken in this interpretation (Gallen et al., 2015).

Mapping suggests that plan-view morphology of Qt4 and Qt5 terrace units are slightly meandering, more or less with the same sinuosity as the current channel

morphology of the Catawba River. Dissection of older remnants due to erosion makes it difficult to assess channel sinuosity or morphology in older terrace units. Excellent exposures of the Qt3 at Riverview, SC (Fig. 5.4A) and Fort Lawn, SC (Fig. 5.4B) exhibit poorly-sorted basal gravels above saprolite. However, sedimentary structures consistent with meandering morphology, i.e. trough cross-bedding and climbing ripples, etc., are not present in soil stratigraphy subsurface profiles, but weathering state of the deposits likely precludes their preservation.

Evidence of fluvial deposited gravels on each mapped surface, as well as in the modern channel suggests that the bed load of the Catawba has been relatively consistent throughout its existence (Fig. 6.3). Previously, Layzell et al. (2012) had inferred that gravel sized clasts had been removed from the bed load of the Catawba River in between Qt3 and Qt4 time, with medium to fine sands taking over the sediment load. This increase in sand sized materials is observed in similar terrace units in the study area, however, the plots of gravels against surface age (Fig. 6.3), suggests a slight reduction in size, as opposed to removal, of clasts between ~142 – 50 ka, possibly due to decrease in stream discharge.

6.3: Causes of Catawba River incision and terrace formation

The data collected in this study provide strong evidence that the Catawba River is marked by an overall history of net incision that was punctuated for periods of time by lateral planation of broad bedrock straths. In this section, I discuss possible external factors that may have contributed to this history. Terrace formation – i.e. pauses in vertical incision – is often attributed to climatic periods of increased sediment supply or decreased discharge (e.g. Eppes et al., 2008). On the Catawba, assuming Mills (2000)

chronology, periods of terrace formation occur at 4,590 ± 404 ka for the Qt0, 1,851 ± 365 ka for the Qt1, 1,181 ± 194 ka for the Qt2, 407 ± 143 ka for the Qt3, 50 ± 8 ka for the Qt4, and 5 ± 2 ka for the Qt5 (Fig. 5.7) A comparison with global climate records reveals that terrace formation for Qt5 – Qt1seem to align with interglacial periods. The match-ups are as follows: Qt1 possibly during the MIS 63 and 61 periods (~1.8 – 1.77 Ma), Qt2 during the MIS 35 period (~1.18 – 1.16 Ma), Qt3 during the MIS 11 period (~450 – 350 ka), Qt4 during the MIS 3 period (~60 – 24 ka), and Qt5 matching up with the current interglacial stand of the Holocene (~11.6 ka – present) (Fig. 6.4). Thus, it seems that the Catawba terraces' straths are carved during interglacial periods, when temperatures are warmer, sea-level and regional base-level are rising, and discharge reduced. Ages constrained for the Qt3 terrace unit via IRSL dating reveal strath formation between 101 ± 27 and 183 ± 36 ka. This time period lines up with the MIS 5e interglacial period (124 – 119 ka).

There are several factors that are known to lead to a stream incising into its channel: 1) base level fall – a) due to sea level changes, or b) due to tectonic offset via faulting; 2) increased discharge, or 3) uplift in the headwaters. In terms of a change in eustasy as a driver for terrace abandonment on the Catawba River, it is unlikely that changes in sea level would cause incisional events this far inland from the coast. The shallow continental shelf off the southeast coast of the US would have caused the shoreline to retreat 10 – 100 km offshore from its current position today, limiting eustatic influence in the Quaternary to the Coastal Plain (Leigh and Freeney, 1995, Leigh, 2008).

Tectonic induced base level change could be a cause of incisional events on the Catawba River. In the lower reach of the study area, the LCKP is the steepest channel

convexity in the modern profile, and is present in Qt5 – Qt1 terraces (Fig. 4.8). This knickpoint does not appear to be related to change in rock type or related to any local structural feature. Knowledge of basement fault reactivation in the southeastern Coastal Plain, such as the buried East Coast fault system, could be possible explanations for this knickpoint. However, the event that created this convexity would have had to pass through the Fall Zone to reach its current location. In the middle reach of study area the presence of the Gold Hill and Silver Hill shear zones, which have been shown to be tectonically quiescent since Alleghanian shortening during the late Paleozoic (Hibbard et al., 2012), do not appear to have influence on incisional events on the Catawba River. Expression of an older knickpoint in Qt3 – 1 is present from ~16.5 – 19 km (Fig. 4.8), just prior to the Gold/Silver Hill shear zones, could possibly be an older en echelon fault that has been quiescent since Qt3 time. Offset on this fault could have been responsible for incisional events during Qt2 – 1 time.

Increased discharge during periods of glacial advancements, i.e. in between strath carving interglacial periods, could be a cause of terrace abandonment on the Catawba River, particularly in younger terrace units (Qt4 – Qt5). It has been suggested that during colder periods streams have increased sediment load due to hillslope instability via lack of vegetation coverage (Eaton et al., 2003, Leigh, 2008). Presence of braided channel deposits (~80 – 35 ka) in the upper Coastal Plain indicate much higher discharge rates during this cooling period of MIS 4 around Qt4 time (Leigh, 2008).

Terraces on the Catawba River do not show evidence for divergence towards the headwaters or Fall Zone. However, the study reach is a considerable distance from either extremity in the system. Gallen et al. (2013) have explored possible tectonic rejuvenation

caused by epeirogenic uplift in the Southern Appalachians, beginning in the Miocene, as a cause for such high relief in the region. Further study of terraces in the headwaters and Coastal Plain of the Catawba – Wateree – Santee system may lend a diverging of terraces trend in the headwaters and toward the Fall Zone to support this claim as a cause for incision on the Catawba.

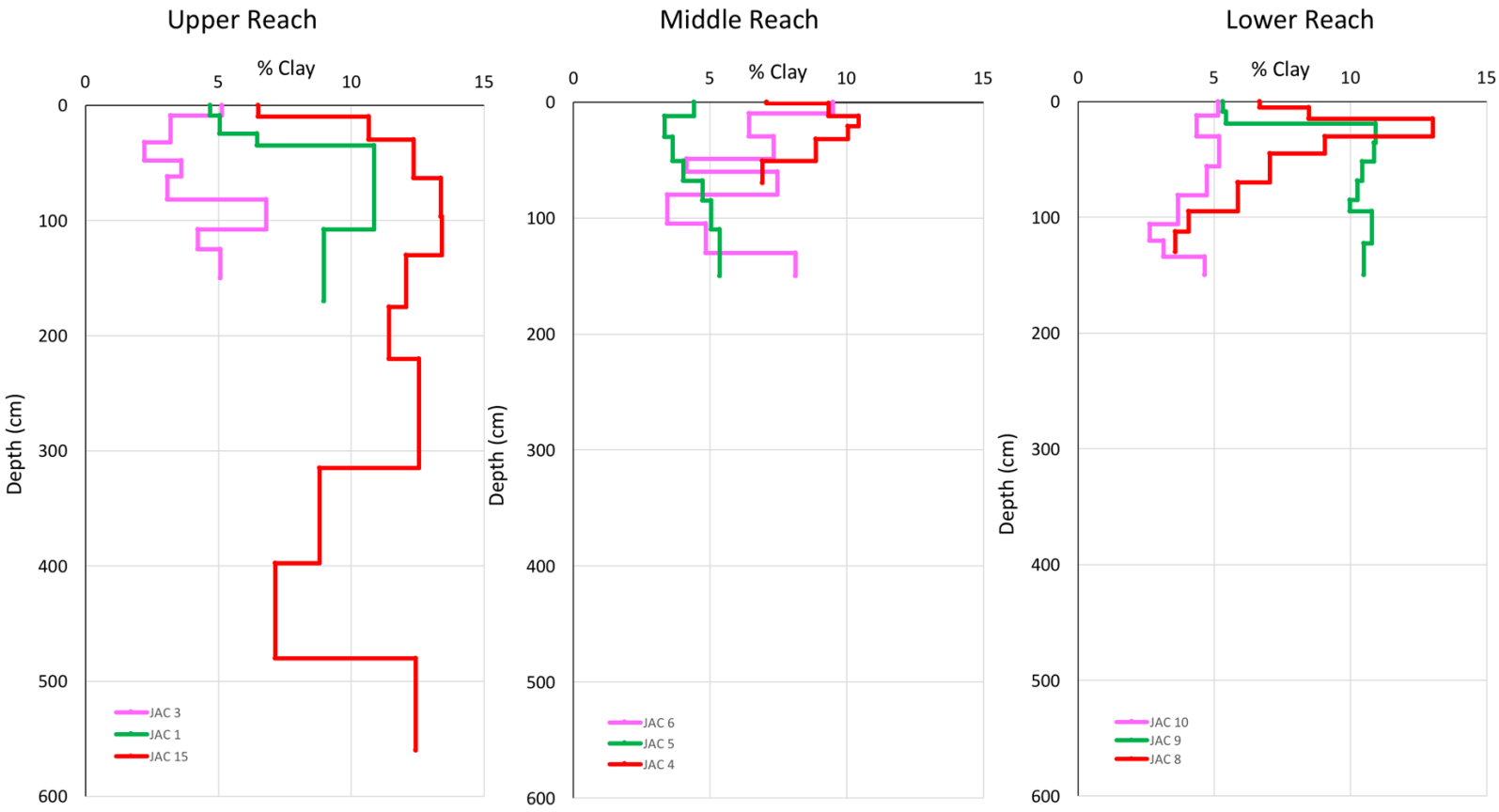

…….

Figure 6.1: Soil depth profile of clay content (%) for each major reach of the study area. Colors of depth profiles correspond to terrace unit, where pink is the Qt5 (5 ± 2 ka), green is the Qt4 (50 ± 8 ka), and red is the Qt3 (142 ± 32 ka). Average error for percent clay is 0.26.

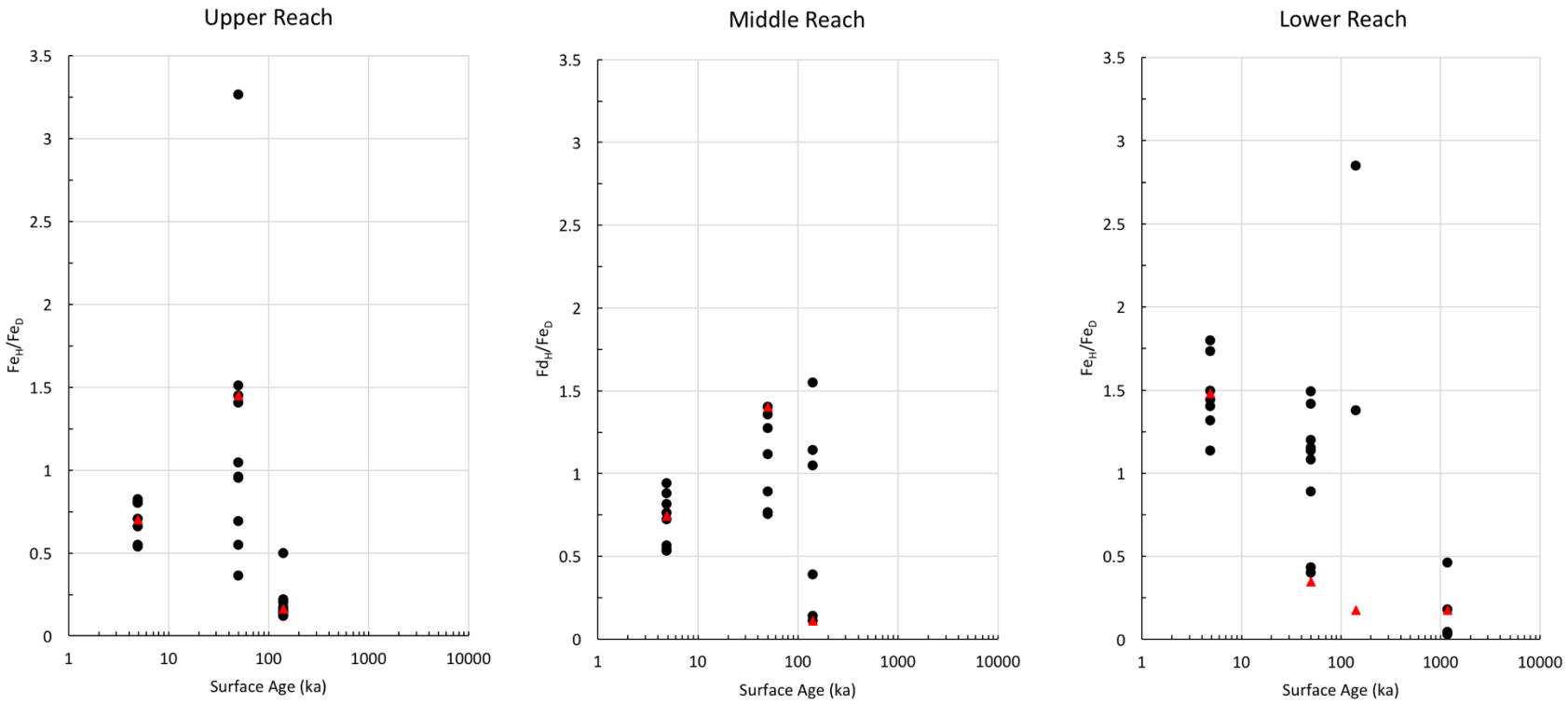

Figure 6.2: Lin-log, iron activity ratio chronofunction plot for the three major reaches of the study area. Low values in Qt5 in the upper and middle reach, and Qt4 in the lower reach have been attributed to inheritance of previously weathered materials from upstream.

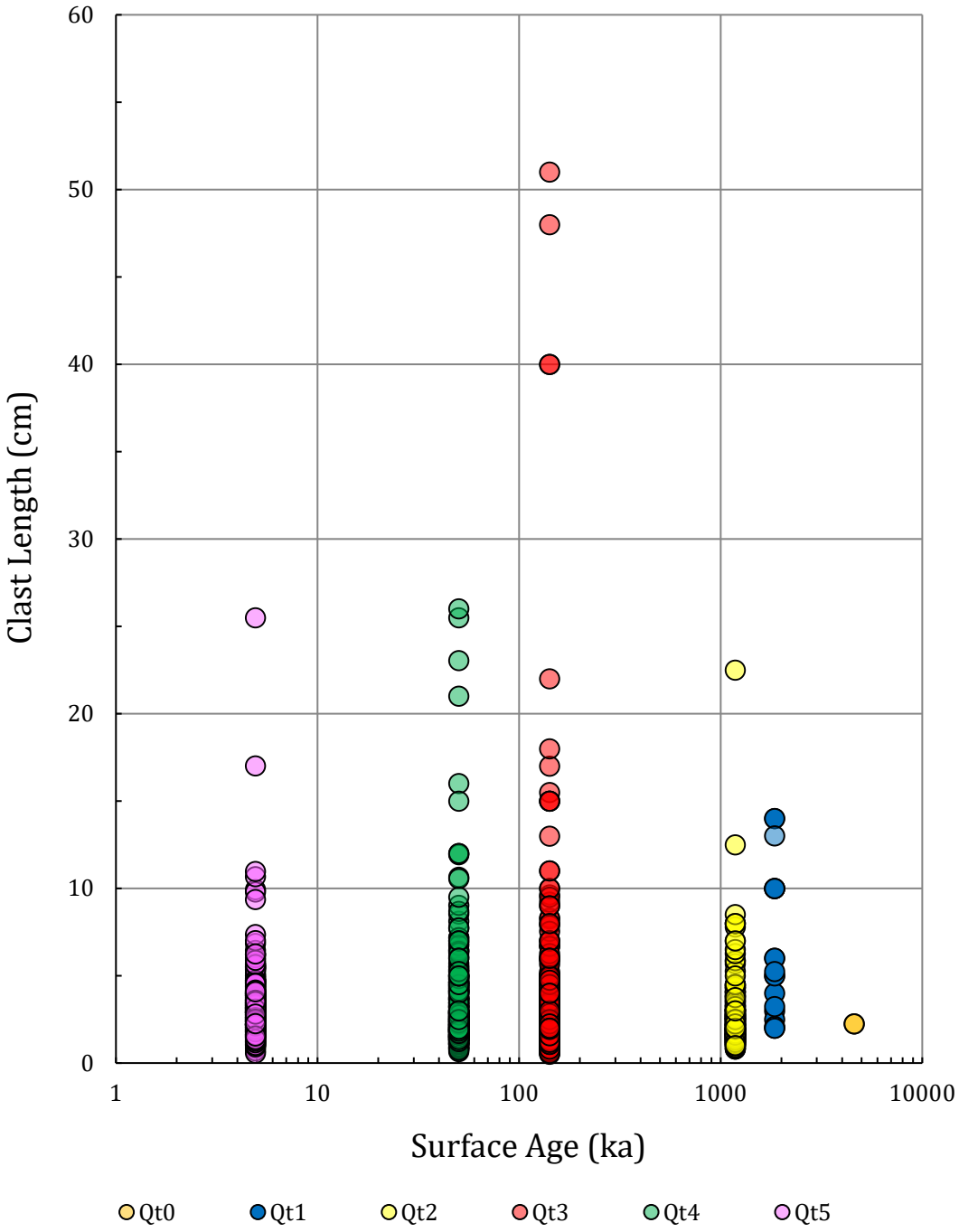

Figure 6.3: Lin-log plot of the length all clasts measured in the study (both in mapping and in clast counts) vs. surface age (ka).

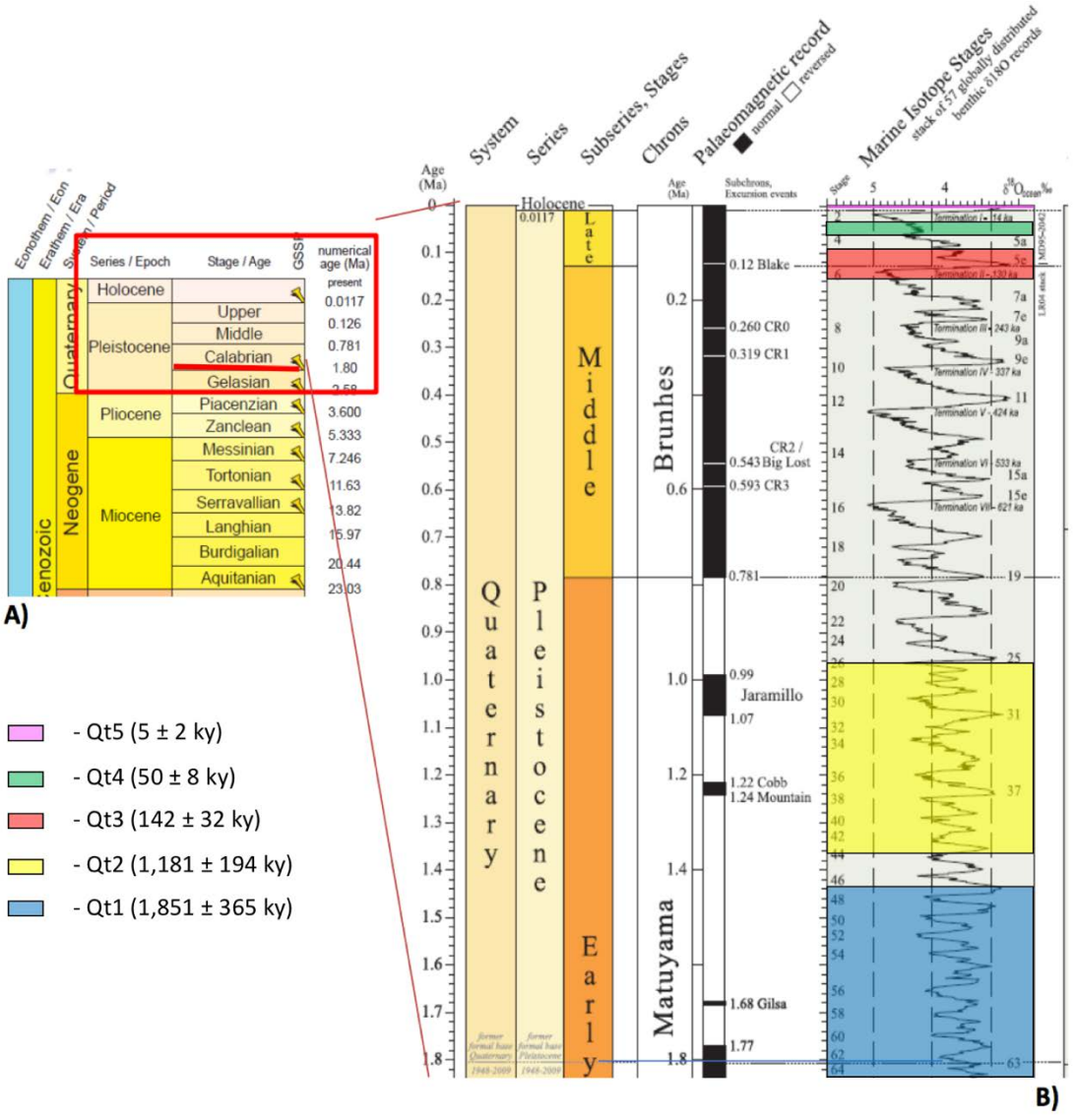

Figure 6.4: A) Chronostratigraphic chart of the Neogene to present (23.03 Ma – present). B) Inset Marine Isotopic Stages (MIS) curve from Calabria stage to present (1.8 Ma – present) with Mills (2000) surface ages for Qt5 – Qt1. Figure modified from Bustamante (2016), Chronostratigraphic chart taken from the International Commission on Stratigraphy (v2015/01), MIS curve from Lisiecki and Raymo (2005).

CHAPTER 7: Conclusions

In the Catawba River Valley in the Piedmont of North and South Carolina, terrace remnants and soils provide a strong basis for examining landscape evolution in the southeastern Piedmont during the Quaternary. Soils of terraces of the Catawba River show some trends with respect to increasing surface age, the most meaningful being an approach to the weathering threshold around 100 ka In terms of chronology of terraces, IRSL ages obtained from exposures on the Qt3 unit are consistent with those of Mills (2000), with both samples collected ~14 m above the channel estimated to ~142 ± 32 ka Overall, there have been 5 periods of significant lateral planation (as evidenced by the 5 terrace units) that have punctuated by down-cutting of the channel. These terrace-forming periods loosely coincide with warmer climatic conditions suggesting a possible climatic control on terrace formation on the Catawba River. The origins of the down-cutting on this system are, at this stage, unknown and could be attributed to overall eustatic fall during the Quaternary, climatic transitions to glacial periods, and/or epeirogenic uplift of the Piedmont and Blue Ridge in the Late Cenozoic (Gallen et al., 2013). In any case, the data presented in this study provides a foundation through which drivers of landscape evolution in the Piedmont of the southeastern United States may be further explored.

REFERENCES:

Antoine, P., et al. (2007). Pleistocene fluvial terrace from northern France (Seine, Yonne, Somme): synthesis and new results from interglacial deposits. *Quaternary Science Reviews*, v. 26, doi: 10.1016/j.quascirev.2006.01.036.

Aquino, K. (2014). Continuing a chronosequence on the Catawba River: Insights into America's "fifth most endangered river". Department of Geography and Earth Sciences, University of North Carolina at Charlotte. Master: p. 1-82.

Bailey, C.M. (2000). Major faults and high strain zones in Virginia. Department of Geology, College of William and Mary.

Bank, G.C. (2001). Testing the origins of the Blue Ridge Escarpment. Department of Geological Sciences, Virginia Polytechnical and State University. Master: p. 1 107.

Berger, P., and A.M. Johnson. (1980). First-order analysis of deformation of a thrust sheet moving over a ramp. *Tectonophysics*, v. 70, p. T9-T24.

Birkeland, P.W. (1999). *Soils and Geomorphology*, 3rd edition. Oxford University Press, New York, p. 430.

Bustamante, C.M. (2016). Stratigraphic record of the glacio-eustatic cycles and the deformation during the Pleistocene along the central Ecuadorian margin: using the ATACAMES data campaign. Université Nice Sophia Antipolis. tel.archives ouvertes.fr/tel-01358673/document.

Blake, G.R. (1965). Bulk density. p. 374-390. *In:* C.A. Black (ed.) Methods of soil analysis, Part 1, Physical and mineralogical properties including statistics of measurement and sampling. No.9, Agronomy. American Society of Agronomy., Madison, WI.

Castelltort, S., Whittaker, A., and J. Vergés. (2015). Tectonics, sedimentation and surface processes: from the erosional engine to basin deposition. *Earth Surface Processes and Landforms*, v. 40, p. 1839-1846, doi:10.1002/esp.3769.

Cook, F.A., Albaugh D.S., Brown, L.D., Kaufman, S., Oliver, J.E. and R.D. Hatcher Jr. (1979). Thin-skinned tectonics in the crystalline southern Appalachians; COCORP seismic reflection profiling of the Blue Ridge and Piedmont. *Geology*, v.7, p. 563-567.

Dallmeyer, R.D., Wright, J.E., Secor Jr., D.T. and A.W. Snoke. (1986). Character of the Alleghanian Orogeny in the Southern Appalachians; Part II, Geochronological constraints on the tectonothermal evolution of the eastern Piedmont in South Carolina. *Geological Society of America Bulletin*, v. 97, p. 1329-1344.

Day, P.R. (1965). Particle fractionation and particle-size analysis. *In:* Blake, C.A., Evans, D.D., White, J.L., Ensminger, L.E., and F.E. Clark eds. *Methods of Soil Analysis*, Part 1, no. 9, p. 545-567.

Diemer, J., Bobyarchick, A.R., Aquino, K., Greer, B., Henke E., et al. (2010). Evidence for Quaternary channel incision and migration of the Catawba River near Charlotte, NC. *Abstracts with Programs - Geological Society of America*, v. 42, i. 5, Abstract 241.

Earthquake track. 11/04/15. United States Geological Survey. April 9, 2016. http://earthquaketrack.com/quakes/2015-11-04-11-00-52-utc-2-6-7.

Eaton, S.L., Morgan, B.A., Kochel, R.C., and A.D. Howard. (2003). Quaternary deposits and landscape evolution of the central Blue Ridge of Virginia. *Geomorphology*, v. 56, p. 139-154. doi: 10.1016/S0169-555X(03)00075-8.

Eppes, M.C., Bierma, R., Vinson, D., and F.J. Pazzaglia. (2008). A soil chronosequence study of the Reno valley, Italy: Insights into the relative role of climate versus anthropogenic forcing on hillslope processes during the mid-Holocene. *Geoderma*, v. 147, p. 97 – 107. doi:10.1016/j.geoderma.2008.07.011.

Foss, J.E., Wagner, D.P., and F.P. Miller. (1981). Soils of the Savannah River Valley; Russell Papers 1985. National Park Service, Atlanta, p. 57 plus appendices.

Gallen, S.F., et al. (2011). Hillslope response to knickpoint migration in the Southern Appalachians: Implications for the evolution of post-orogenic landscapes. *Earth Surface Processes and Landforms*, v. 36, p. 1254-1267. doi: 10.1002/esp.2150

Gallen, S.F., Wegmann, K.W., and D.R. Bohnenstieh. (2013). Miocene rejuvenation of topographic relief in the southern Appalachians. *GSA Today*, v. 23, i. 2, p. 4-10.

Gallen, S.F., Pazzaglia, F.J., Wegmann, K.W., Pederson, J.L., and T.W. Gardner. (2015). The dynamic reference frame of rivers and apparent transience in incision rates. *Geology*, v. 43, p. 623-626. doi: 10.1130/G36692.1.

Goldstein, A.G., and L.L. Brown. (1988). Magnetic susceptibility anisotropy of mylonites from the Brevard Zone, North Carolina, U.S.A. *Physics of the Earth and Planetary Interiors*, v. 51, p. 290-300. doi: 10.1016/00319201(88)90070-2.

Hancock, G.S., and D. Harbor. (2002). Cosmogenic isotope dating of rapid, disequilibrium incision of the James River in central Virginia. *Abstracts with Programs - Geological Society of America*, v. 34, i. 2.

Hancock, G., and Harbor, D., and Felis Johnson. (2003). Knickpoint retreat and landscape disequilibrium on the James River from the Piedmont through the Valley and Ridge, central Virginia, USA. *Eos Trans. AGU*, 84(46), Fall Meet. Suppl., Abstract H52A-114.

Hancock, G.S., Harbor, D.J., Felis, J., Turcotte, J. and Anonymous. (2004). (super 10) Be dating of river terraces reveals Piedmont landscape disequilibrium in the central James River basin, Virginia *Abstracts with Programs - Geological Society of America*, v. 36, i. 2.

Hibbard, J., Miller, B.V., Hames, W.E., Standard, I.D., Allen, J.S., Lavallee, S.B., and I. Boland. (2012). Kinematics, U-Pb geochronology, and Ar/Ar thermochronology of the Gold Hill shear zone, North Carolina: the Cherokee orogeny in Carolinia, southern Appalachians: *Geological Society of America Bulletin*, v. 124, p. 643-656.

Horton, J.W., and R.A. Williams. (2012). The 2011 Virginia Earthquake: What are scientists learning? *EOS, Transactions American Geophysical Union*, v. 93, p. 317-324. doi: 10.1029/2012EO330001.

Ivester, A., Ferguson, T., Butler, S., and Anonymous. (2009). Holocene floodplain and terrace formation in Piedmont river valleys of northwestern South Carolina. *Abstracts with Programs - Geological Society of America*, Vol. 41, Iss.7, Abstract 615.

Jackson, M.L. (1969). Soil Chemical Analysis, Advanced course, published by author (2nd edition), Madison, WI, p. 44-51.

Krumbein, W.C., and L.L. Sloss. (1956). Stratigraphy and Sedimentation. Freeman and

Company, San Francisco, CA.
Layzell, A.L., Eppes, M.C., and R.Q. Lewis. (2012). A soil chronosequence study on terraces of the Catawba River near Charlotte, NC: Insights into the long-term evolution of a major Atlantic piedmont drainage basin. *Southeastern Geology*, v. 49, p. 13-24.
Leigh, D.S., Srivastava, P., and G.A. Brook. (2004). Late Pleistocene braided rivers of the Atlantic Coastal Plain, USA. *Quaternary Science Reviews*, v. 23, p. 65–84.
Leigh, D.S. (2008). Late Quaternary climates and river channels of the Atlantic Coastal Plain, Southeastern USA. *Geomorphology*, v. 101, p.90-108, doi:http://dx.doi.org/10.1016/j.geomorph.2008.05.024.
Lisiecki, L.E., and M.E. Raymo. (2005). A Pliocene-Pleistocene stack of 57 globally distributed benthic $\delta^{18}O$ records. *Paleoceanography*, 20. PA1003, doi: 10.1029/2004PA001071
Markewich, H.W., Pavich, M.J., and G.R. Buell. (1990). Contrasting soils and landscapes of the Piedmont and Coastal Plain, eastern United States. *Geomorphology*, v. 3, p. 417-447.
Markewich, H.W., and M.J. Pavich. (1991). Soil chronosequence studies in temperate to subtropical, low-latitude, low-relief terrain with data from the eastern United States U.S. Geological Survey, Doraville, GA and Reston, VA, USA. *Geoderma*, v. 51, p. 213-239.
Marple, R.T., and Pradeep Talwani. (2000). Evidence for a buried fault system in the Coastal Plain of the Carolinas and Virginia—Implications for neotectonics in the southeastern United States. *Geological Society of America Bulletin*, 112 (2): 200 220. doi: 10.1130/0016-7606(2000)112<200:efabfs>2.0.co;2.
McDonald, E., et al. (2015). Iron Extraction (Hydroxylamine Method). *The Desert Research Institute Soil Characterization and Quaternary Pedology Laboratory Methods Manual*, v. 3.3, p. 58-59.
McFadden, L.D. and D.M. Hendricks. (1985). Changes in the Content and Composition of Pedogenic Iron Oxyhydroxides in a Chronosequence of Soils in Southern California. *Quaternary Research*, v. 23, p. 189-204.
McGavick, M., Pazzaglia, F.J., Carter, M.W., Mahan, S.A., Counts, R., and et al. (2016). Landscape evolution on the Virginia Piedmont; a new soil chronosequence, luminescence (OSL and IRSL) and cosmogenic (TCN) dating, and intraplate seismicity-driven river incision. *Abstracts with Programs - Geological Society of America***,** v. 48, i. 7.
McKeague, J.A., and J.H. Day. (1966). Dithionite and oxalate extractable Fe and Al as aids in differentiating various classes of soils. *Canadian Journal of Soil Science*, v. 46, p. 13-22.
McKeon, R.E., Zeitler, P.K., Pazzaglia, F.J., Idleman, B., and E. Enkelmann. (2014). "Decay of an old orogen: inferences about Appalachian landscape evolution from low-temperature thermochronology". Geological Society of America Bulletin, 126, 1-2, p. 31-46. doi: 10.1130/B30808.1.
Mehra, O.P., and M.L. Jackson. (1960). Iron oxide removal from soils and clay by a dithionite citrate system buffered with sodium bicarbonate. *Clays and Clay Minerals*, v. 7, p. 313-317.
Merritts, D.J., Vincent, K.R., and Ellen E. Wohl. (1994). Long river profiles, tectonism,

and eustasy: A guide to interpreting fluvial terraces. *Journal of Geophysical Research: Solid Earth*, v. 99, p. 14031-14050. doi: 10.1029/94JB00857.

Miller, S.R., Sak, P.B., Kirby, E., and Paul R. Bierman. (2013). Neogene rejuvenation of central Appalachian topography: Evidence for differential rock uplift from stream profiles and erosion rates. *Earth and Planetary Science Letters*, v. 369-270, p. 1-12. doi: http://dx.doi.org/10.1016/j.epsl.2013.04.007.

Mills, H.H. (2000). Apparent increasing rates of stream incision in the eastern United States during the late Cenozoic. *Geology*, v. 28, p. 955-957. doi: 10.1130/0091 7613(2000)28<955:AIROSI>2.0.CO;2.

Mills, H.H., and J.B. Allison. (1995). Weathering and soil development on fan surfaces as a function of height above modern drainage ways, Roan Mountain, North Carolina. *Geomorphology*, v. 14, p. 1-17.

O'Hara, K., and Thomas P. Becker. (2004). Tectonic assembly of the Brevard-Chauga belt, South Carolina: Fluid inclusion evidence from the Appalachian Deep Core Site investigation hole 2 (ADCOH-2). *Journal of Geodynamics*, v. 37, p. 565-581.

Pavich, M.J., Brown, L., Klein, J., and R. Middleton. (1984). ^{10}Be accumulation in a soil chronosequence. *Earth and Planetary Science Letters*, v. 68, p. 198-204.

Pavich, M.J., Brown, L., Valette-Silver, J.N., Klein, J., and R. Middleton. (1985). ^{10}Be analysis of a Quaternary weathering profile in the Virginia Piedmont. *Geology*, v. 13, p 39-41.

Pazzaglia, F. J. and T.W. Gardner. (1993). Fluvial terraces of the lower Susquehanna River. *Geomorphology*, v.8, p.83-113. doi: http://dx.doi.org/10.1016/0169 555X(93)90031-V.

Pazzaglia, F.J., Robinson, R.A.J., and A. Traverse. (1997). Palynology of the Bryn Mawr Formation (Miocene): insights on the age and genesis of Middle Atlantic margin fluvial deposits. *Sedimentary Geology* v. 108, p. 19-44.

Pazzaglia, F.J. and M.T. Brandon. (2001). A fluvial record of long-term steady state uplift and erosion across the Cascadia forearc high. *American Journal of Science*, v. 301, p. 385.

Pazzaglia, F.J., Carter, M.W., Rittenour, T., Malenda, H. F., Anonymous. (2015). Fluvial responses to base level, climate, and active tectonics; south Anna River, Central Appalachian Piedmont, Louisa County, Virginia. *Abstracts with Programs Geological Society of America*, v. 47, i. 7, Abstract 219.

Picotti, V., Ponza, A., and Frank J. Pazzaglia. (2009). Topographic expression of active faults in the foothills of the Northern Apennines. *Tectonophysics*, v. 474, p. 285 294, doi: http://dx.doi.org/10.1016/j.tecto.2009.01.009.

Price, K. and D.S. Leigh. (2006). Morphological and sedimentological responses of streams to human impact in the southern Blue Ridge Mountains, USA. *Geomorphology*, v. 78, p. 142–160. doi: 10.1016/j.geomorph.2006.01.022.

Price, J.R. (2011). Summary of geologic mapping of the Redlair property, Gastonia North Carolina. *North Carolina Plant Friends Organization*. http://www.ncplantfriends.org.

Prince, P.S., Spotila, J.A., and Williams S. Henika. (2011). Stream capture as driver of transient landscape evolution in a tectonically quiescent setting. *Geology*, v. 39, p. 823-826. doi: 10.1130/G32008.1.

Prince, P.S., and James A. Spotila. (2013). Evidence of transient topographic

disequilibrium in a landward passive margin river system: Knickpoints and paleo landscapes of the New River basin, southern Appalachians. *Earth Surface Processes and Landforms*, v. 38, p. 1685-1699. doi: 10.1002/esp.3406.

Reusser, L.J., Bierman, P.R., Pavich, M.J., Zen, E., Larsen, J., and Robert Finkel. (2004). Rapid late Pleistocene incision of Atlantic passive-margin river gorges. *Science (Washington)*, v. 305, p. 499-502. doi: http://dx.doi.org/10.1126/science.1097780

Roper, P.J., and Philip S. Justus. (1973). Polytectonic evolution of the Brevard zone. *American Journal of Science*, v. Cooper 273-A, p. 105-132.

Schanz, S.A., and D.R. Montgomery. (2016). Lithologic controls on valley width and strath terrace formation. *Geomorphology*, v. 258, p. 58-68. doi: 10.1016/j.geomorph.2016.01.015.

Shepard, C., Schaap, M.G, Rasmussen, C., and Anonymous. (2015). Probabilistic modeling of soil development variability with time. *American Geophysical Union Fall Meeting*, Vol. 2015, Abstract EP31B-1009.

Singer, M.J. (1986). Bulk Density-paraffin clod method, *In:* Singer, M.J. and P. Janitzky, compilers, Field and Laboratory Procedures used in a Soil Chronosequence Study: U.S. Geological Survey Bulletin 1648, p. 18-19.

Stanford, S.D., Witte, R.W., Braun, D.D., and J.C. Ridge. (2016). Quaternary fluvial history of the Delaware River, New Jersey and Pennsylvania, USA: The effects of glaciation, glacioisostasy, and eustasy on a proglacial river system. *Geomorphology*, v. 264, p.12-28. doi: 10.1016/j.geomorph.2016.04.002.

Taylor, A. and J.D. Blum. (1995). Relation between soil age and silicate weathering rates determined from the chemical evolution of a glacial chronosequence. *Geology*, v. 23; no. 11, p. 979–982.

Wegmann, K.W. and Frank J. Pazzaglia. (2009). Late Quaternary fluvial terraces of the Romagna and Marche Apennines, Italy: Climatic, lithologic, and tectonic controls on terrace genesis in an active orogen. *Quaternary Sciences Reviews*, v. 28, p. 137-165. doi: http://dx.doi.org/10.1016/j.quascirev.2008.10.006.

Wheeler, R.L. (2006). Quaternary tectonic faulting in the Eastern United States. *Engineering Geology*, v. 82, p. 165-186. doi: 10.1016/j.enggeo.2005.10.005.

Vinson, D.S., Eppes, M.C., and R.M. Bierma. (2005). Iron oxide crystallinity in fluvial terraces, Reno River valley, Italy. *Abstracts with Programs - Geological Society of America*, v. 37, i. 6.

Zaprowski, B.J., Pazzaglia, F.J., and E.B. Evenson. (2005). Climatic influences on profile concavity and river incision. *Journal of Geophysical Research*, v. 110, F03004, doi:10.1029/2004JF000138.

APPENDIX A: Detailed Surficial Geology Maps of the Catawba River.

Note: Maps are descending in order from the beginning of the study area at Lake Wylie Dam (Fig. 4.1A) all the way down to SC Highway 9 Bridge (Fig. 4.1E).

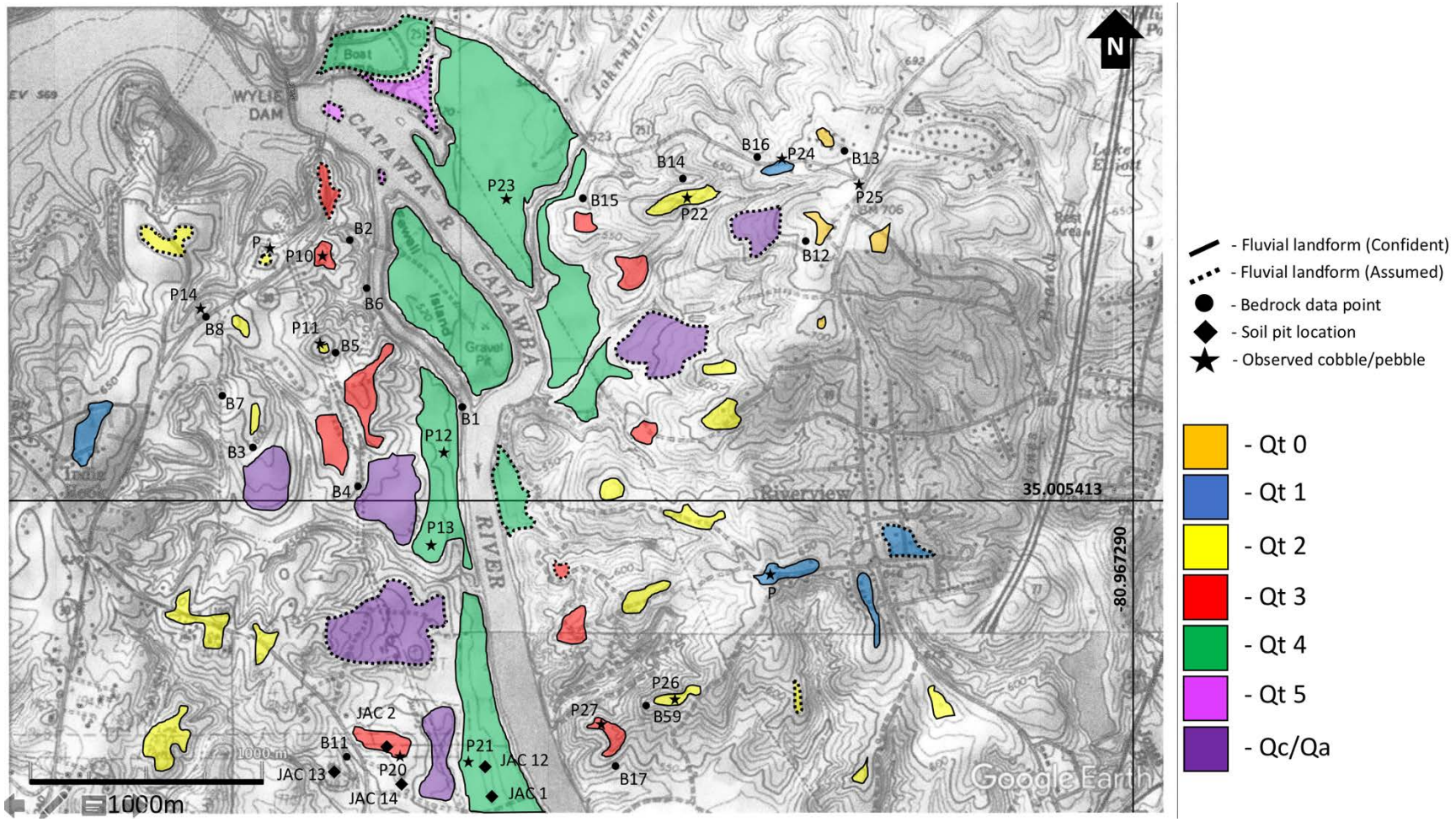

Figure A1: Detailed surficial geologic map of the Catawba River at the start of the study area.

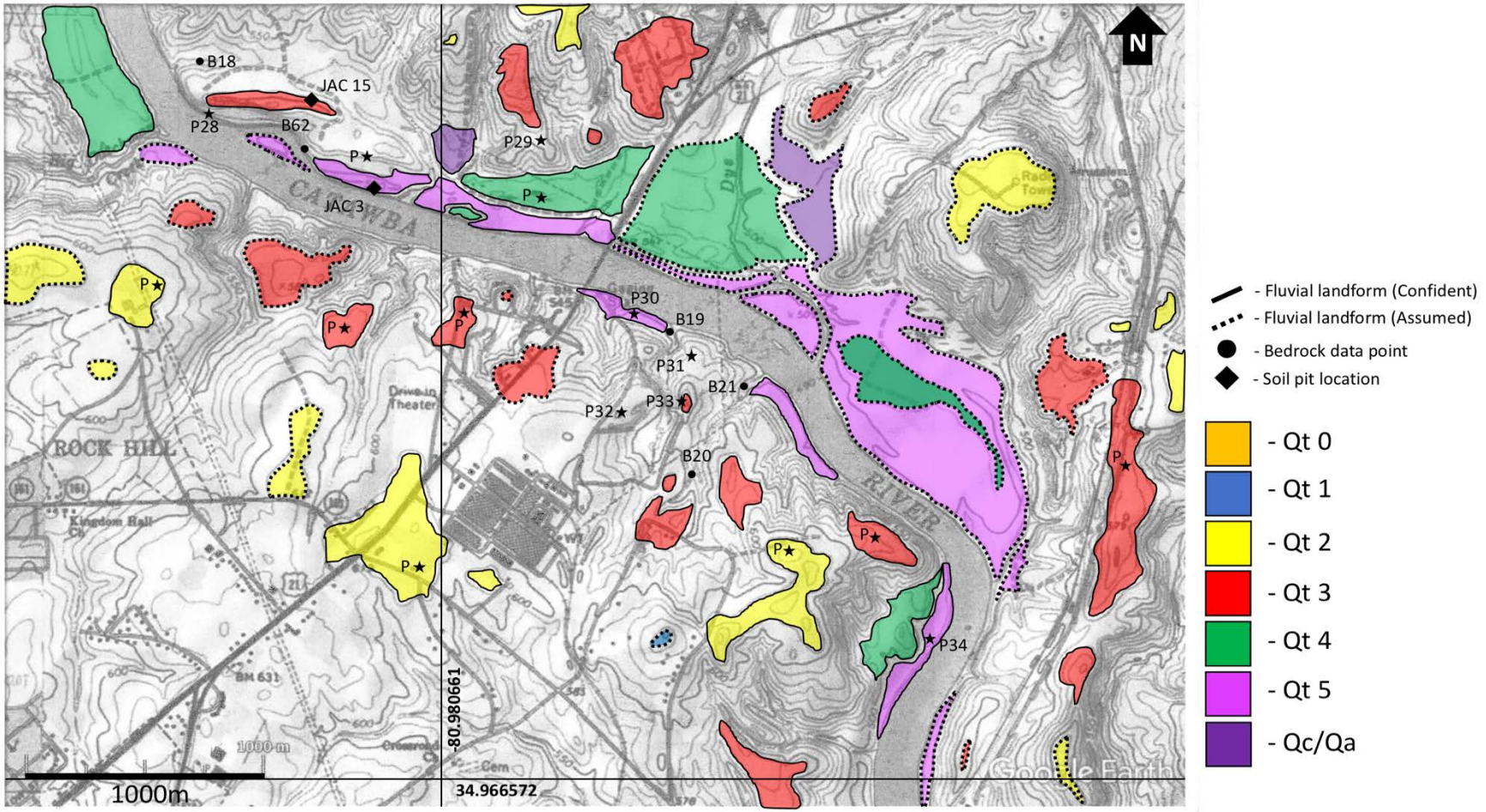

Figure A2: Detailed surficial geologic map of the Catawba River. Bridge crossing is US – 21 (Cherry Rd.) Rock Hill, SC.

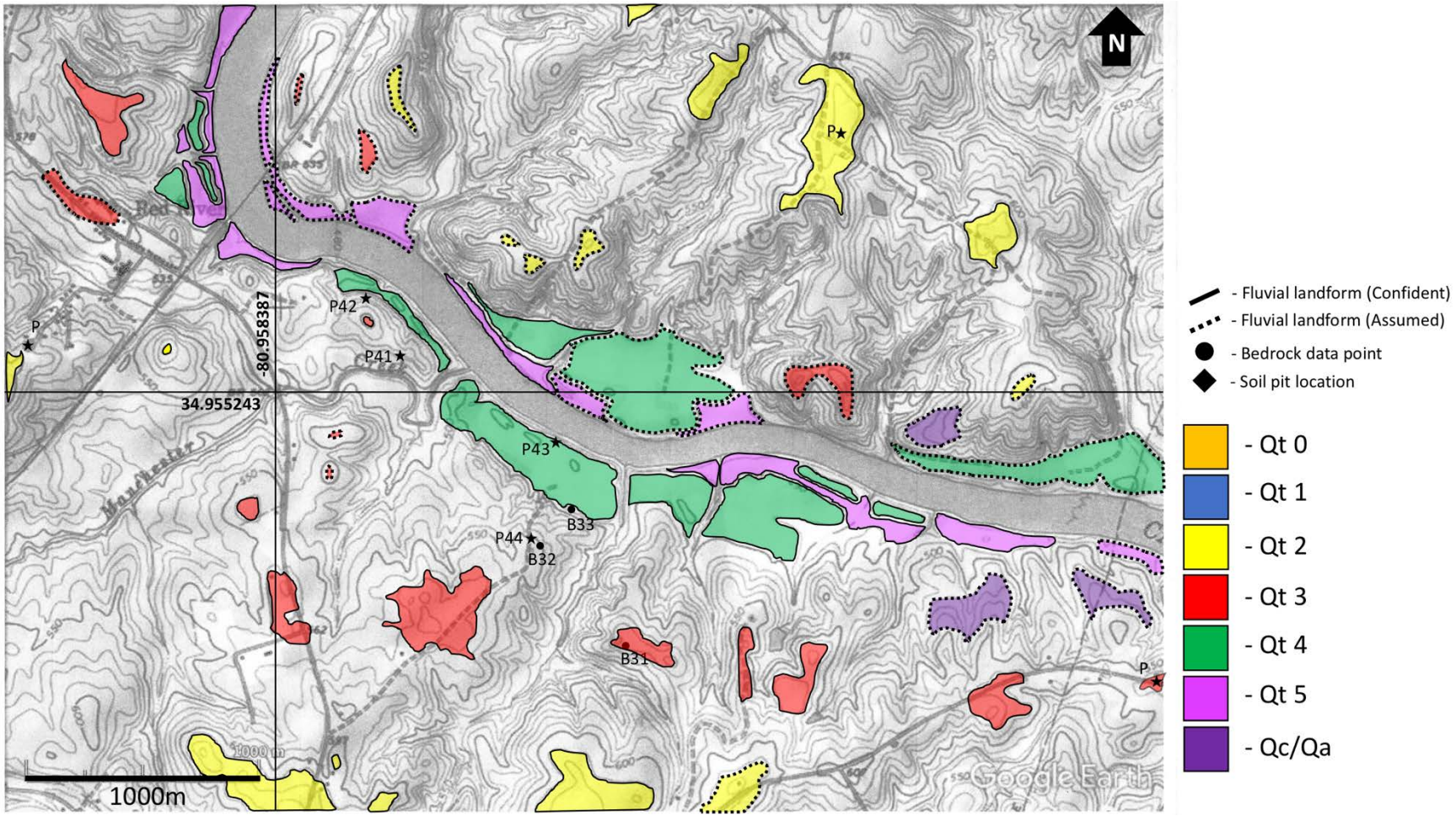

Figure A3: Detailed surficial geologic map of the Catawba River, Red River, SC.

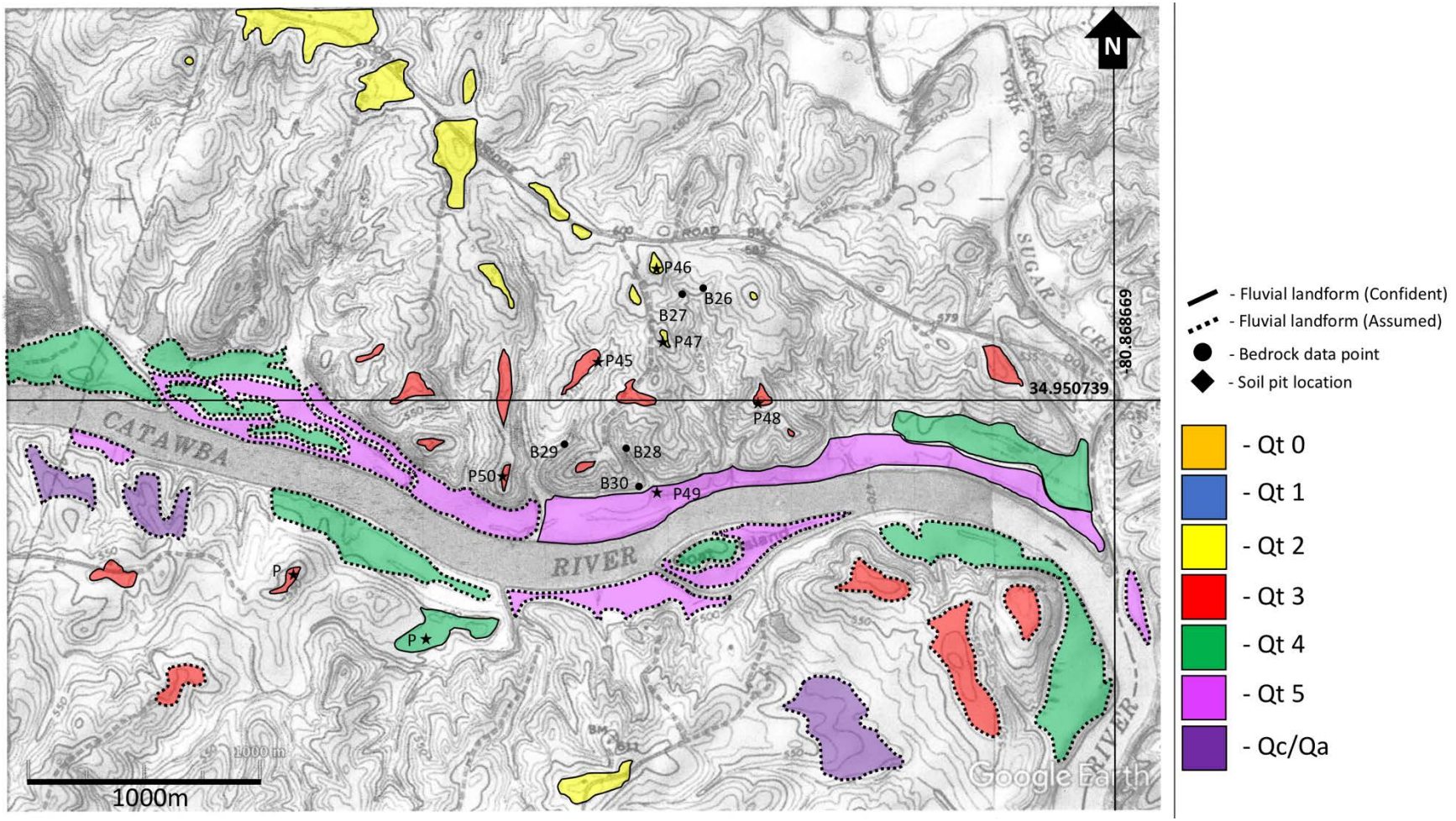

Figure A4: Detailed surficial geologic map of the Catawba River, just east of US – 521, south of Indian Land, SC.

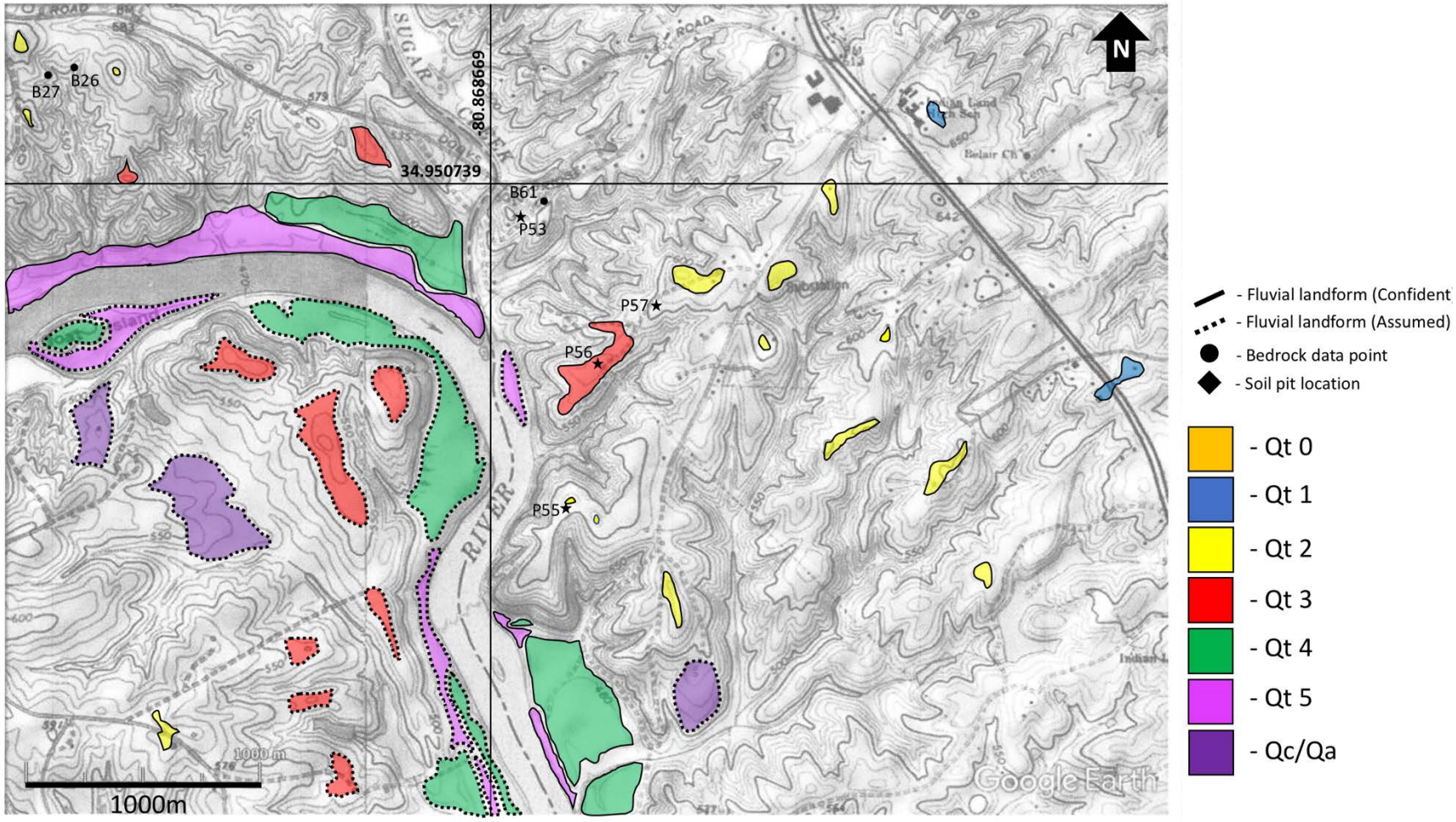

Figure A5: Detailed surficial geologic map of the Catawba River. Main road is US – 521, Indian Land, SC.

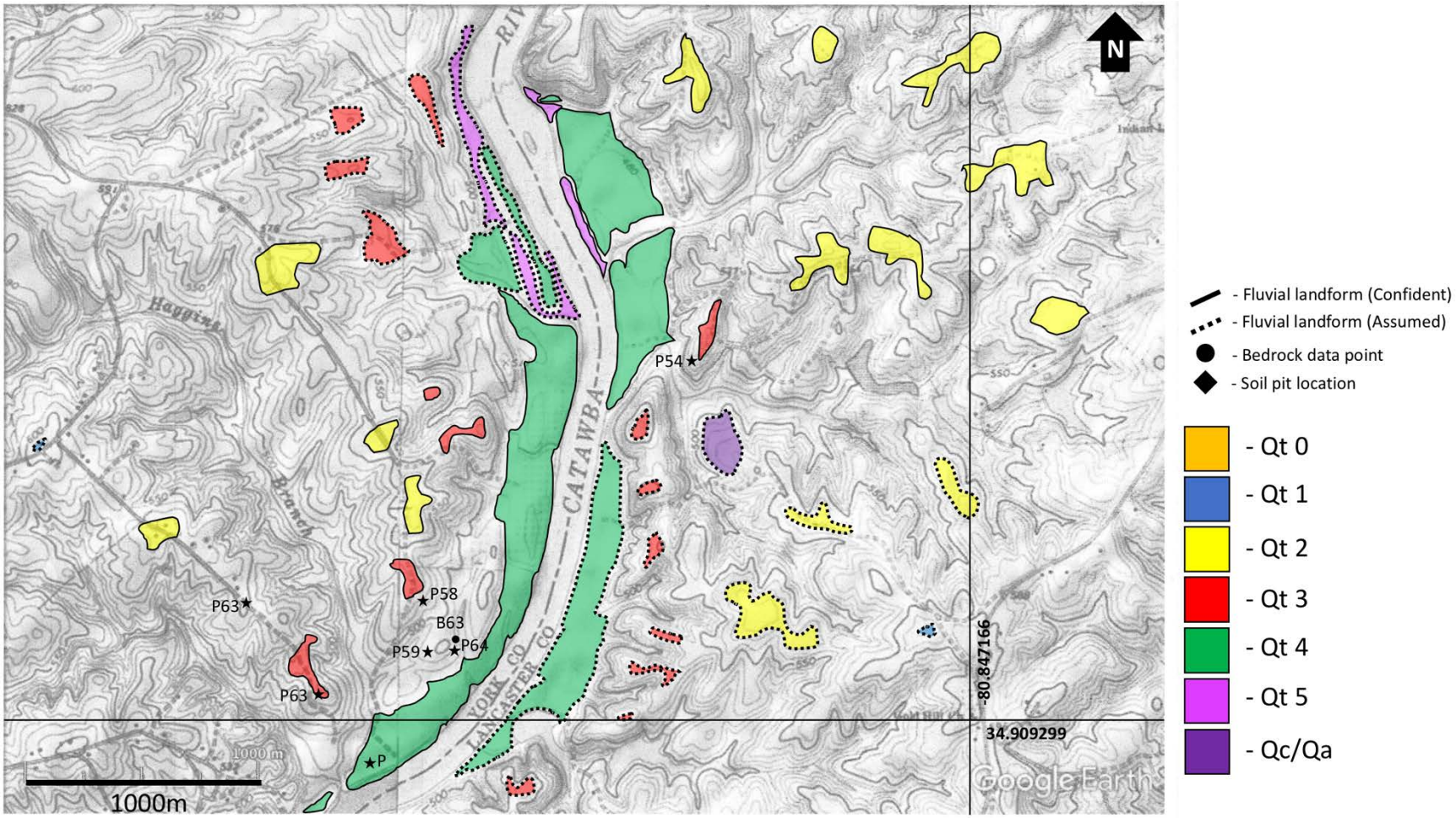

Figure A6: Detailed surficial geologic map of the Catawba River. West side of the valley is the Catawba Indian Reservation.

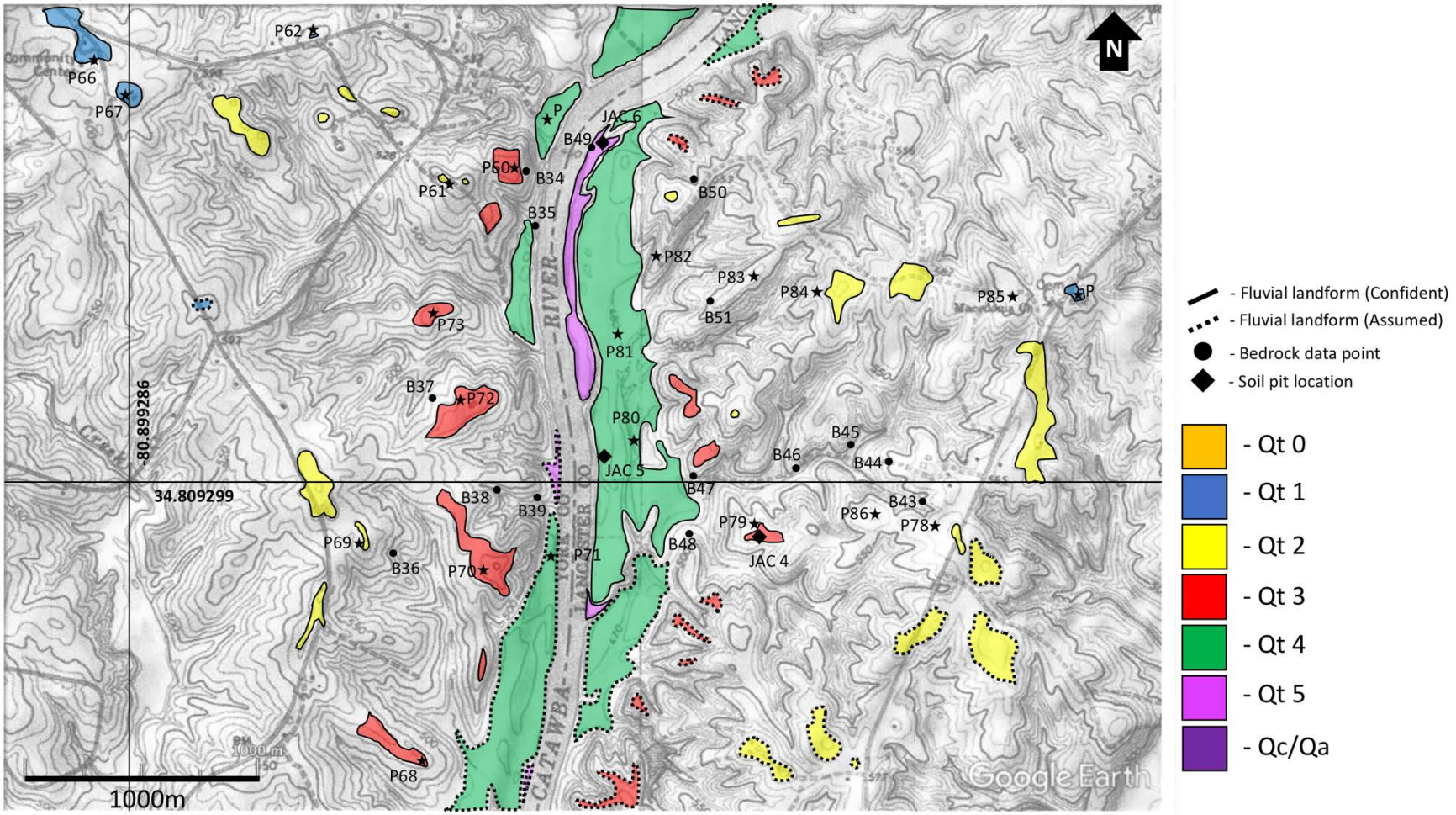

Figure A7: Detailed surficial geologic map of the Catawba River of the middle reach of the study area, Van Wyck, SC.

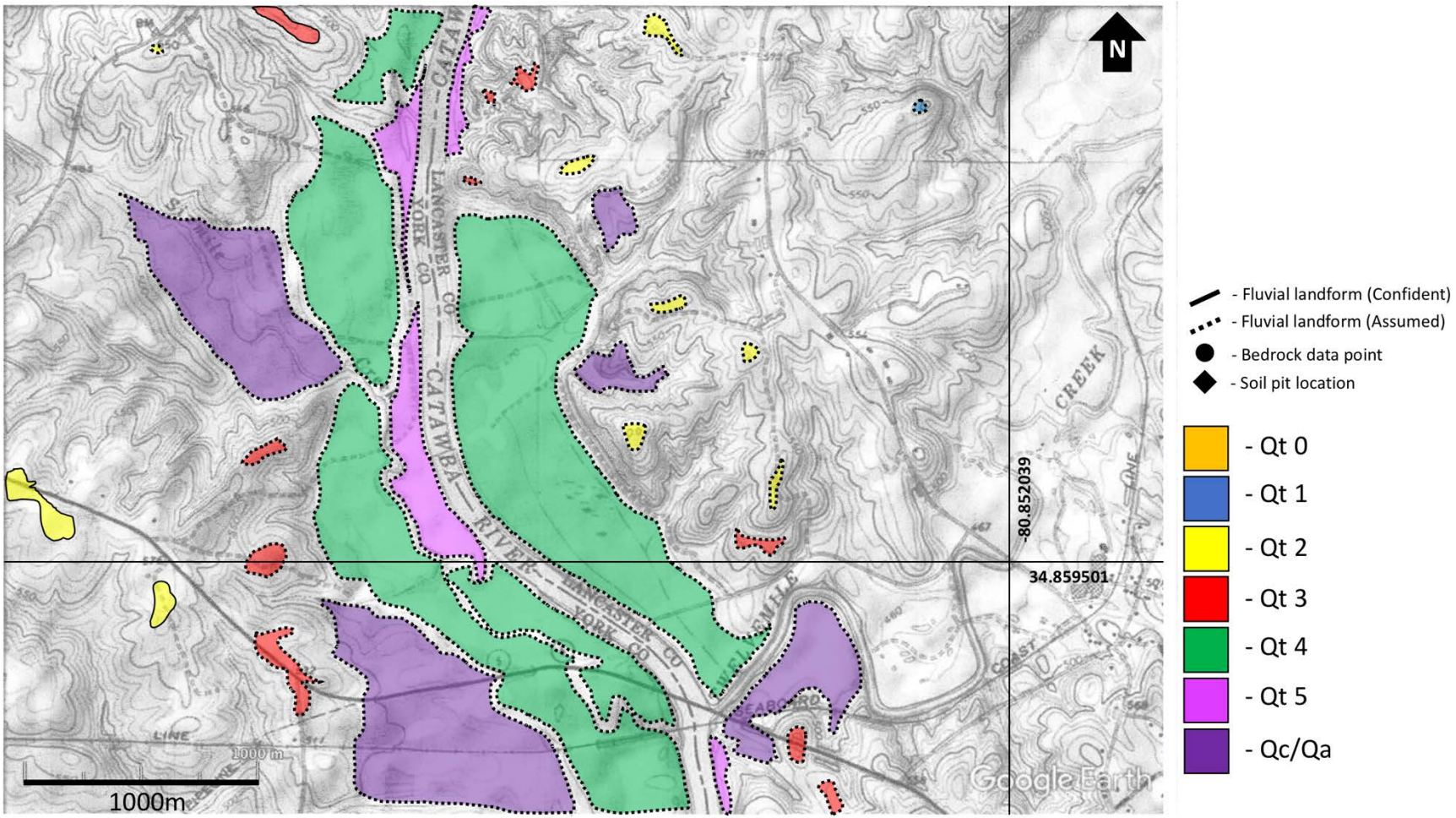

Figure A8: Detailed surficial geologic map of the Catawba River. Bridge crossing is SC Highway 5, between Catawba and Van Wyck, SC.

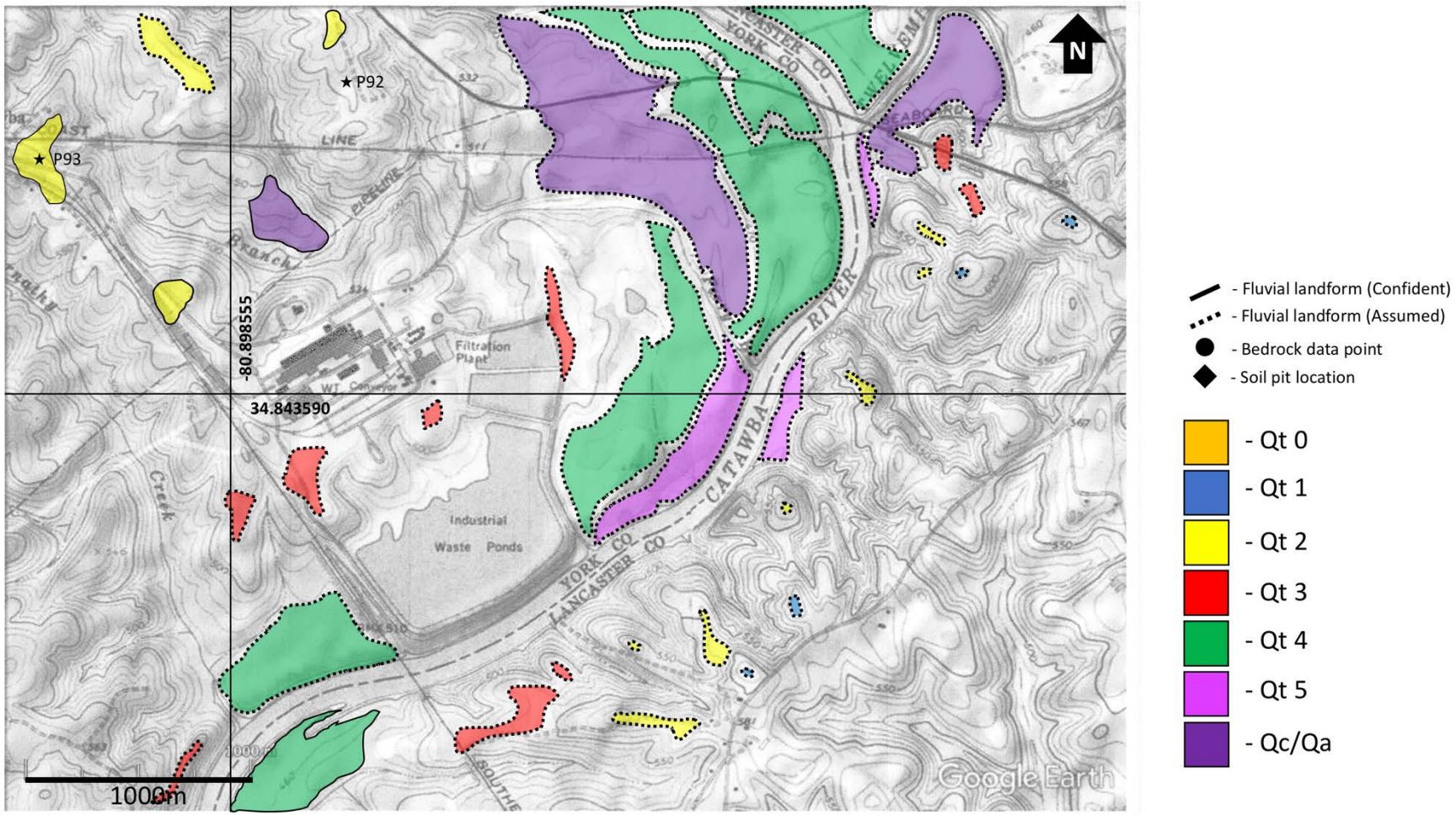

Figure A9: Detailed surficial geologic map of the Catawba River, south of SC Highway 5. West side of the valley is Chemtrade water chemical and liquid ammonium – sulfate production plant and Resolute Forest Products paper plant.

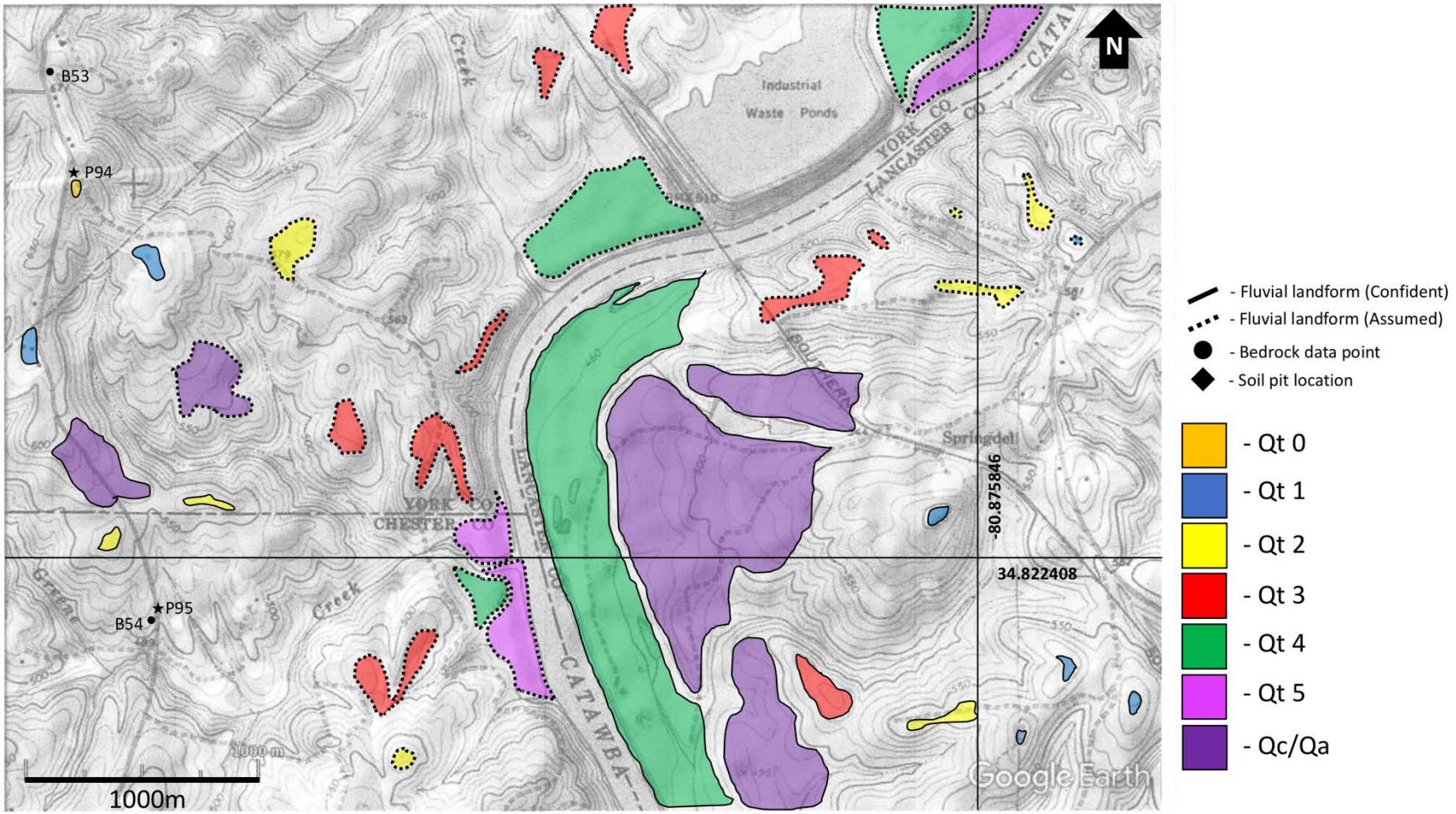

Figure A10: Detailed surficial geologic map of the Catawba River between State Road 465 and Riverside Rd.

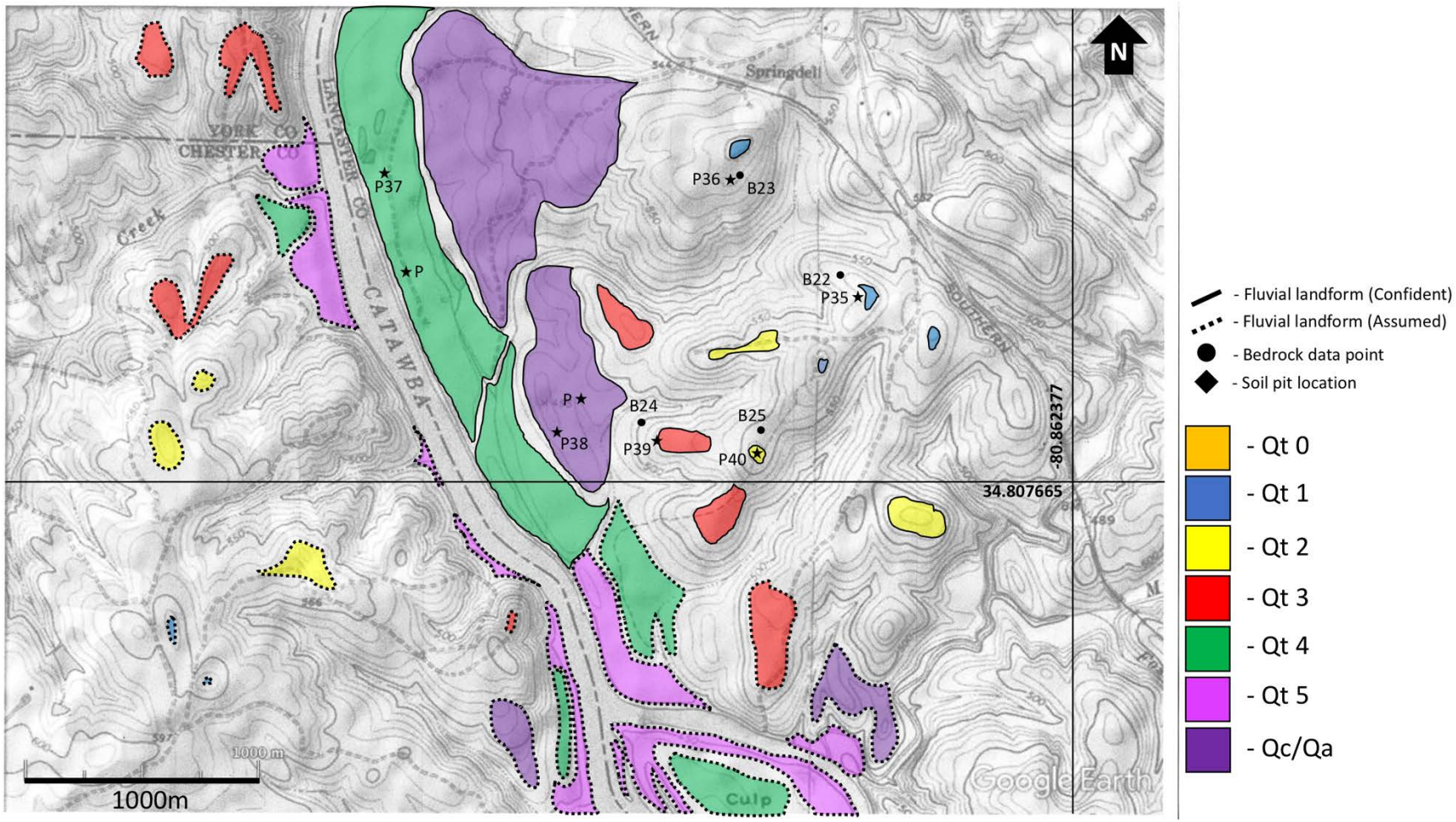

Figure A11: Detailed surficial geologic map of the Catawba River, north of Landsford, SC.

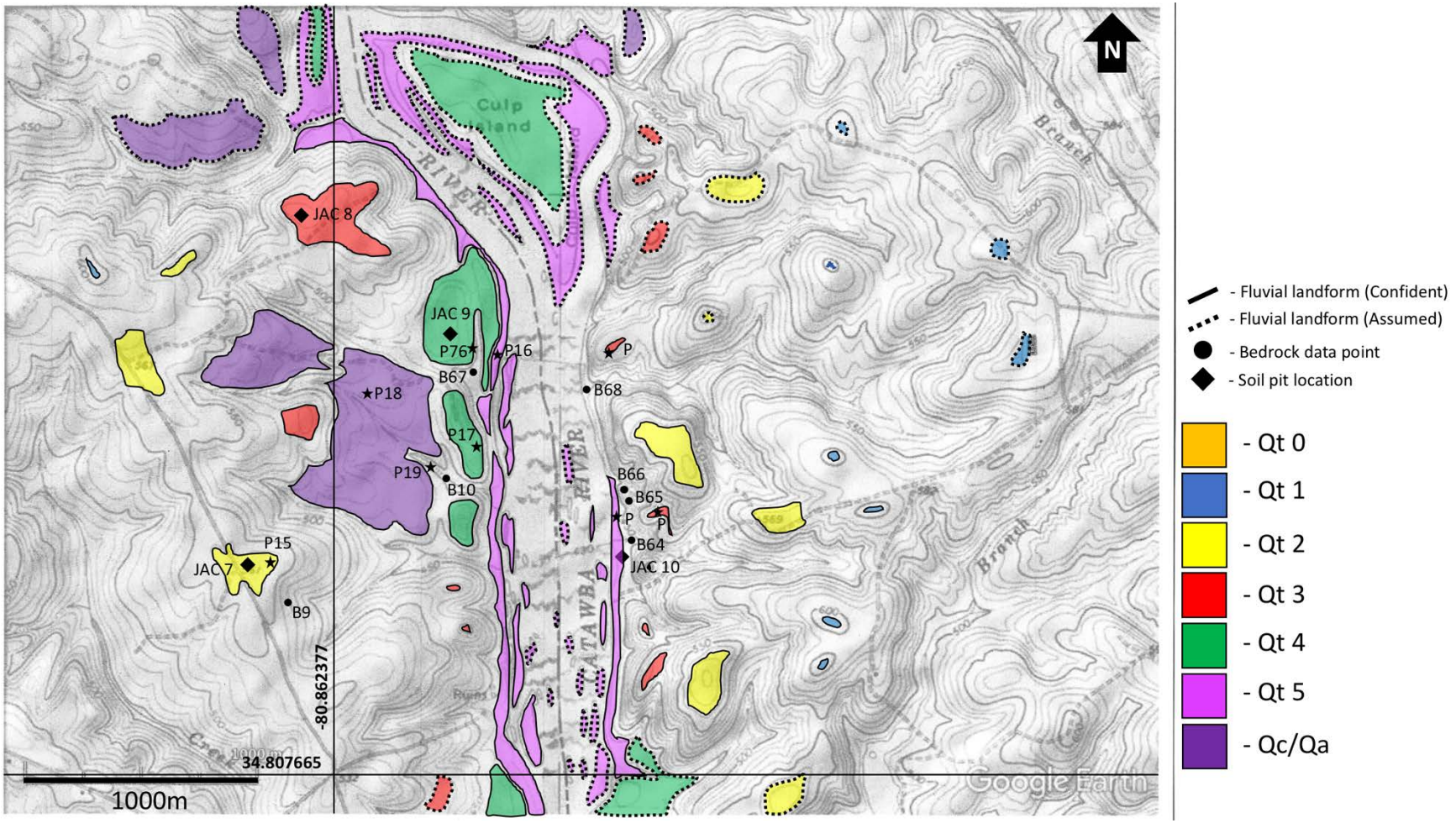

Figure A12: Detailed surficial geologic map of the Catawba River in the lower reach of the study area, Landsford Canal State Park.

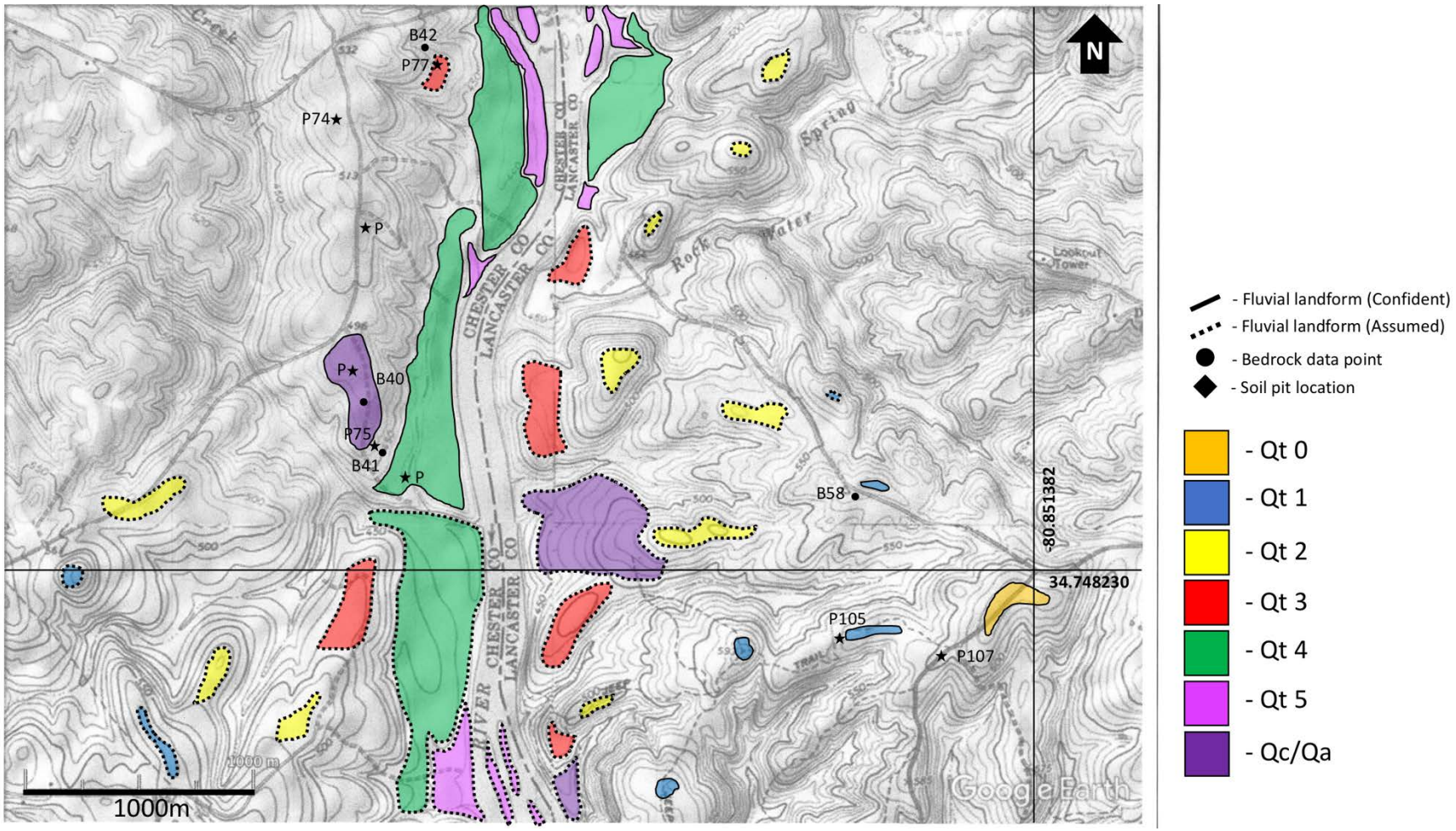

Figure A13: Detailed surficial geologic map of the Catawba River, south of Landsford, SC.

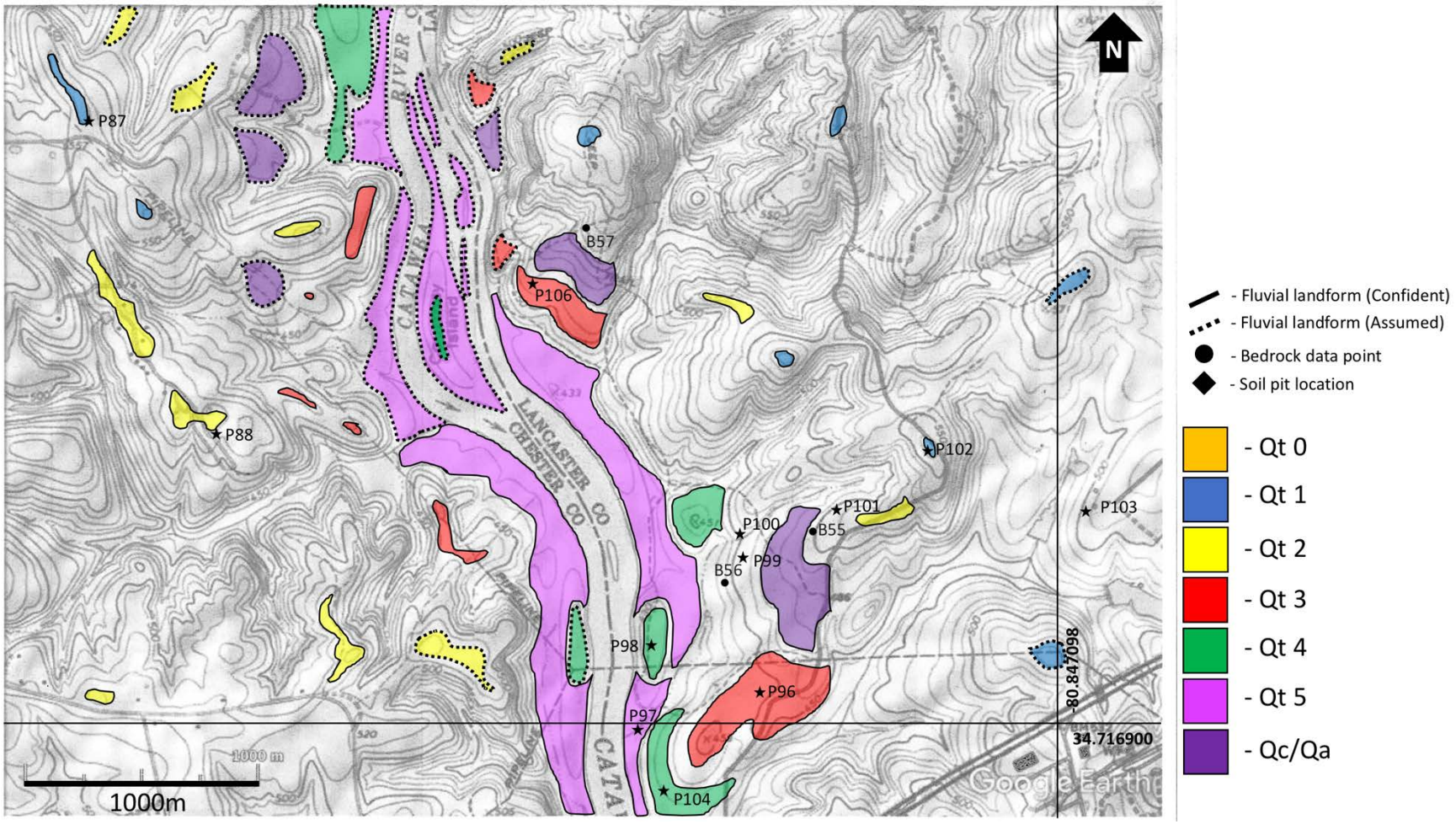

Figure A14: Detailed surficial geologic map of the Catawba River. Road in SE corner is SC Highway 9.

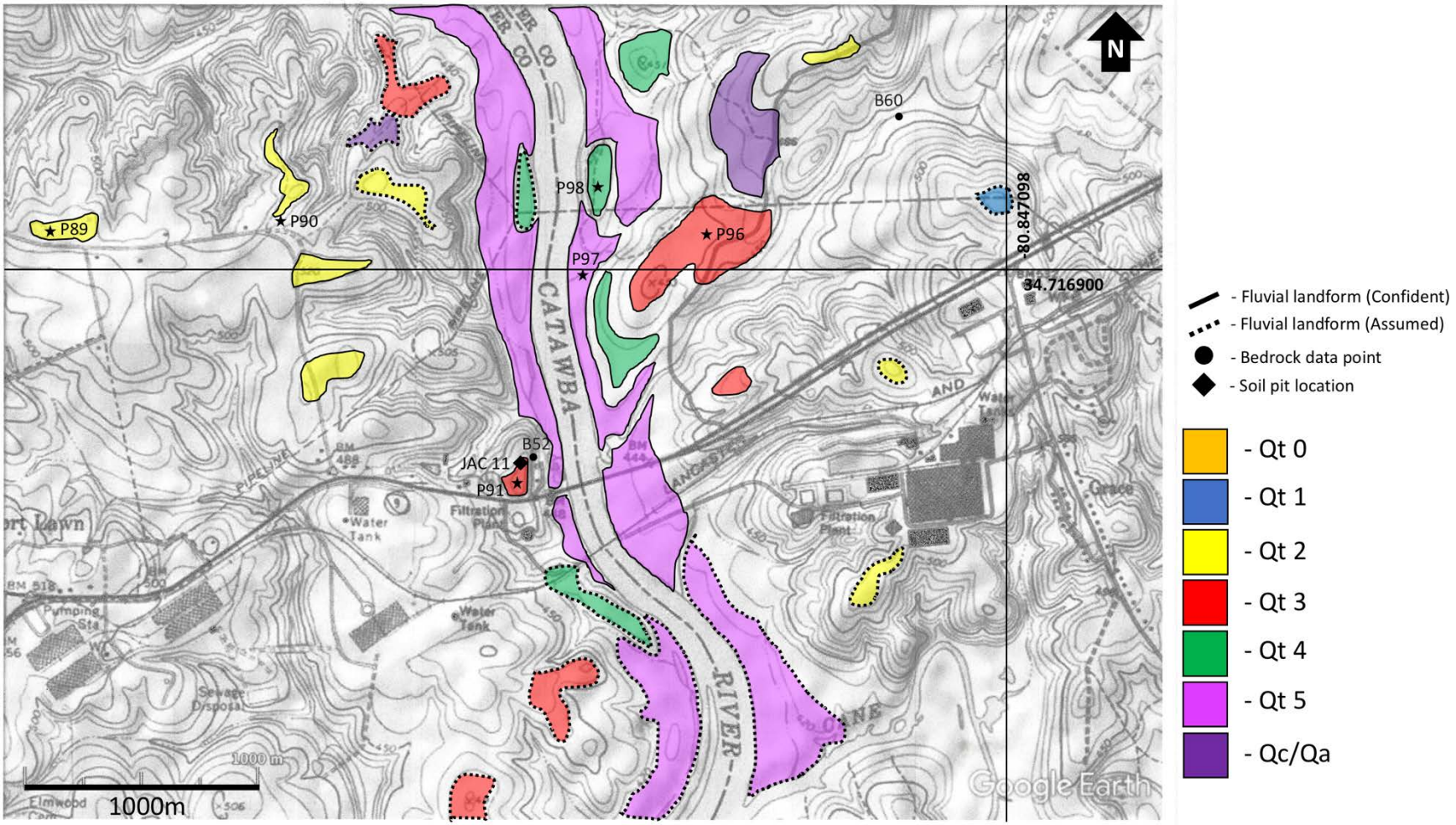

Figure A15: Detailed surficial geologic map of the Catawba River, at SC Highway 9 bridge in between Fort Lawn and Lancaster, SC (the end of the study area).

APPENDIX B: Annotated Soil Pit Photographs

Note: No annotated photograph for JAC 11 (Qt3) exposure.

Figure B1: JAC 1 (Qt4) Back property of North Rock Hill Church, Mt. Gallant Rd., Rock Hill, SC; 34.9935, -80.9981.

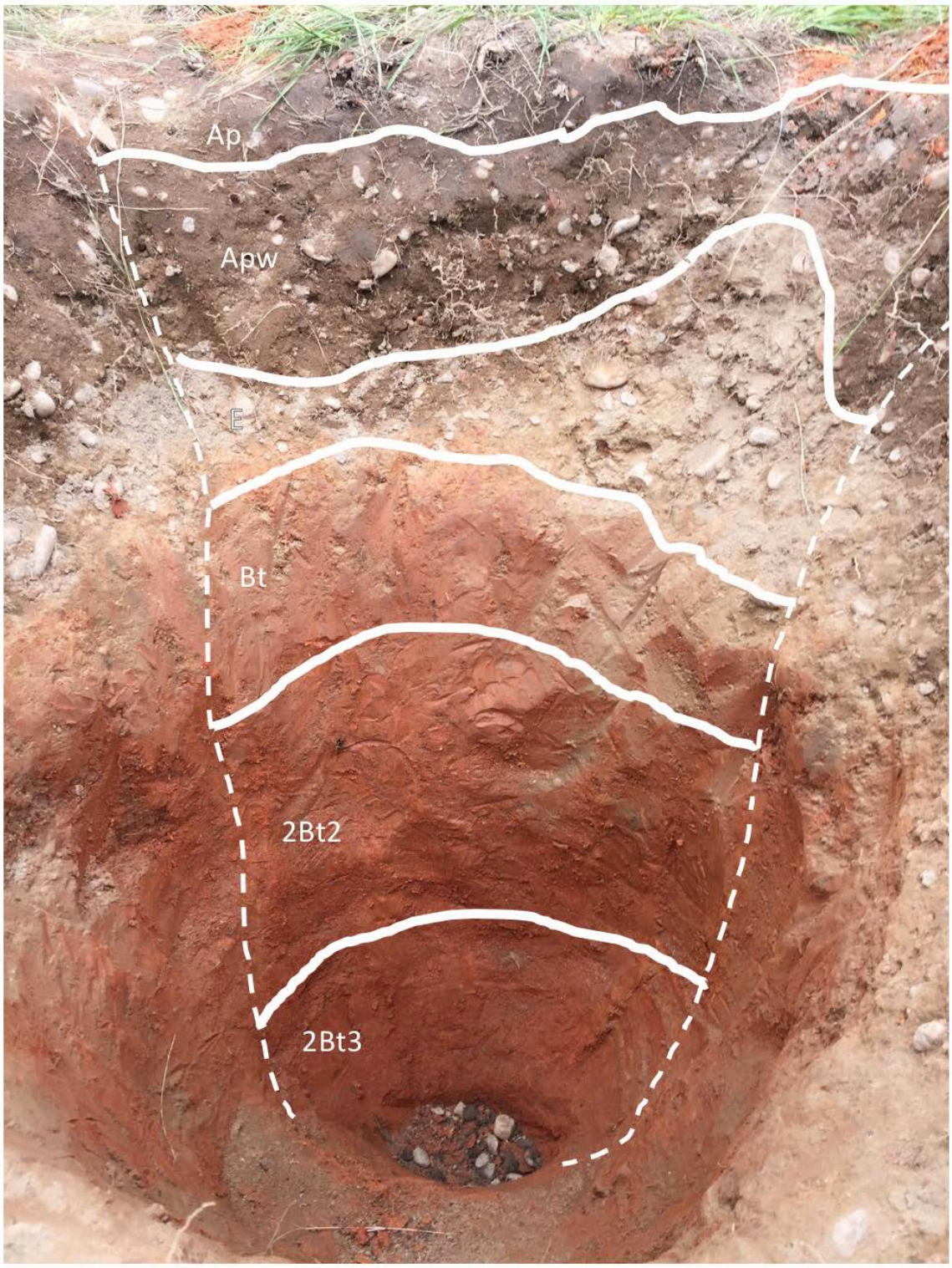

Figure B2: JAC 2 (Qt3) Adjacent property to North Rock Hill Church, Mt. Gallant Rd., Rock Hill, SC; 34.9953, -81.0025.

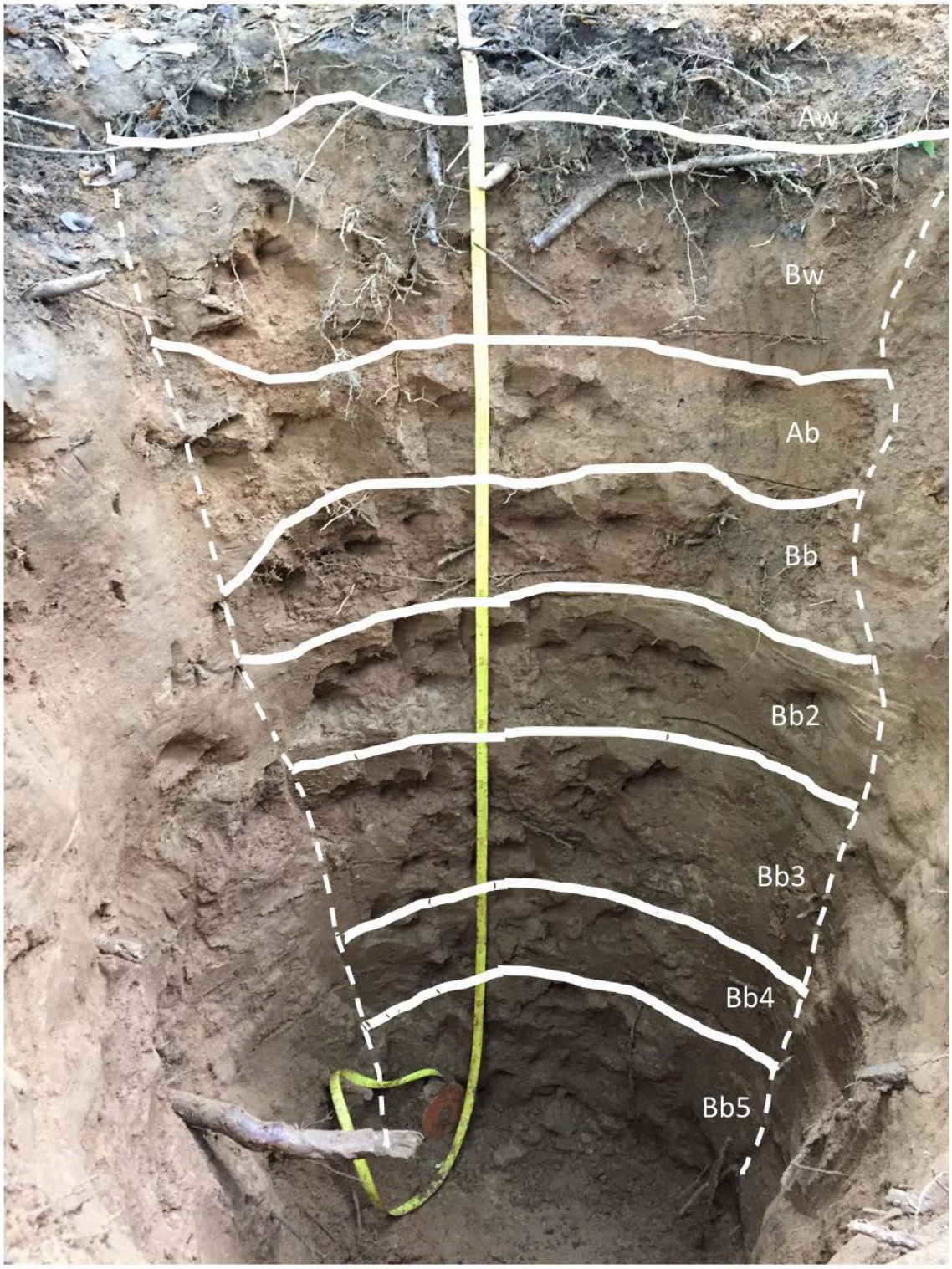

Figure B3: JAC 3 (Qt5) SE of Mason's Bend Neighborhood, near I-77 Bridge, Riverside, SC; 34.9888, -80.9844.

Figure B4: JAC 4 (Qt3) The Ivy Place event venue, Van Wyck, SC; 34.8885, -80.8696.

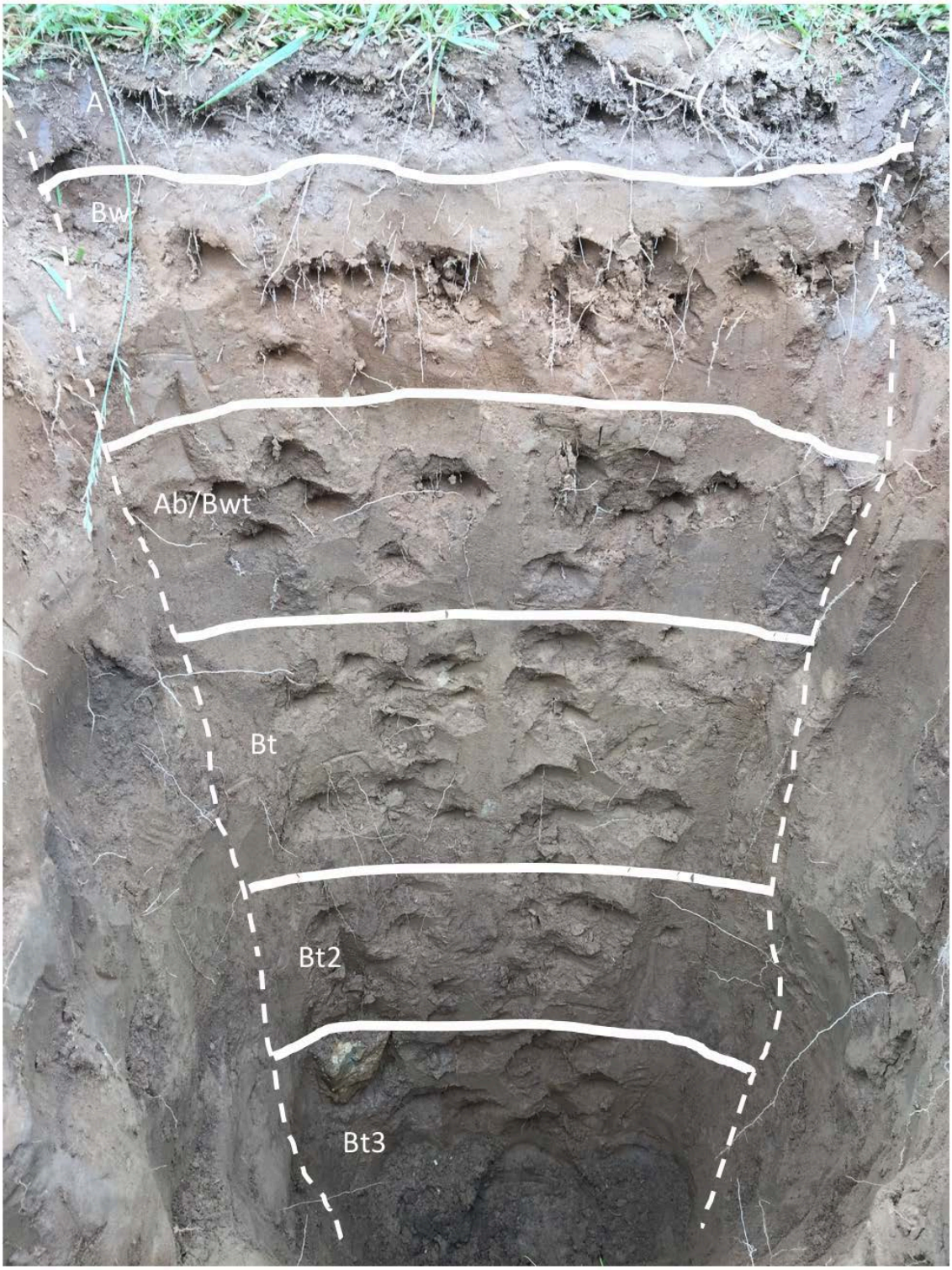

Figure B5: JAC 5 (Qt4) The Ivy Place event venue, Van Wyck, SC; 34.8913, -80.8769.

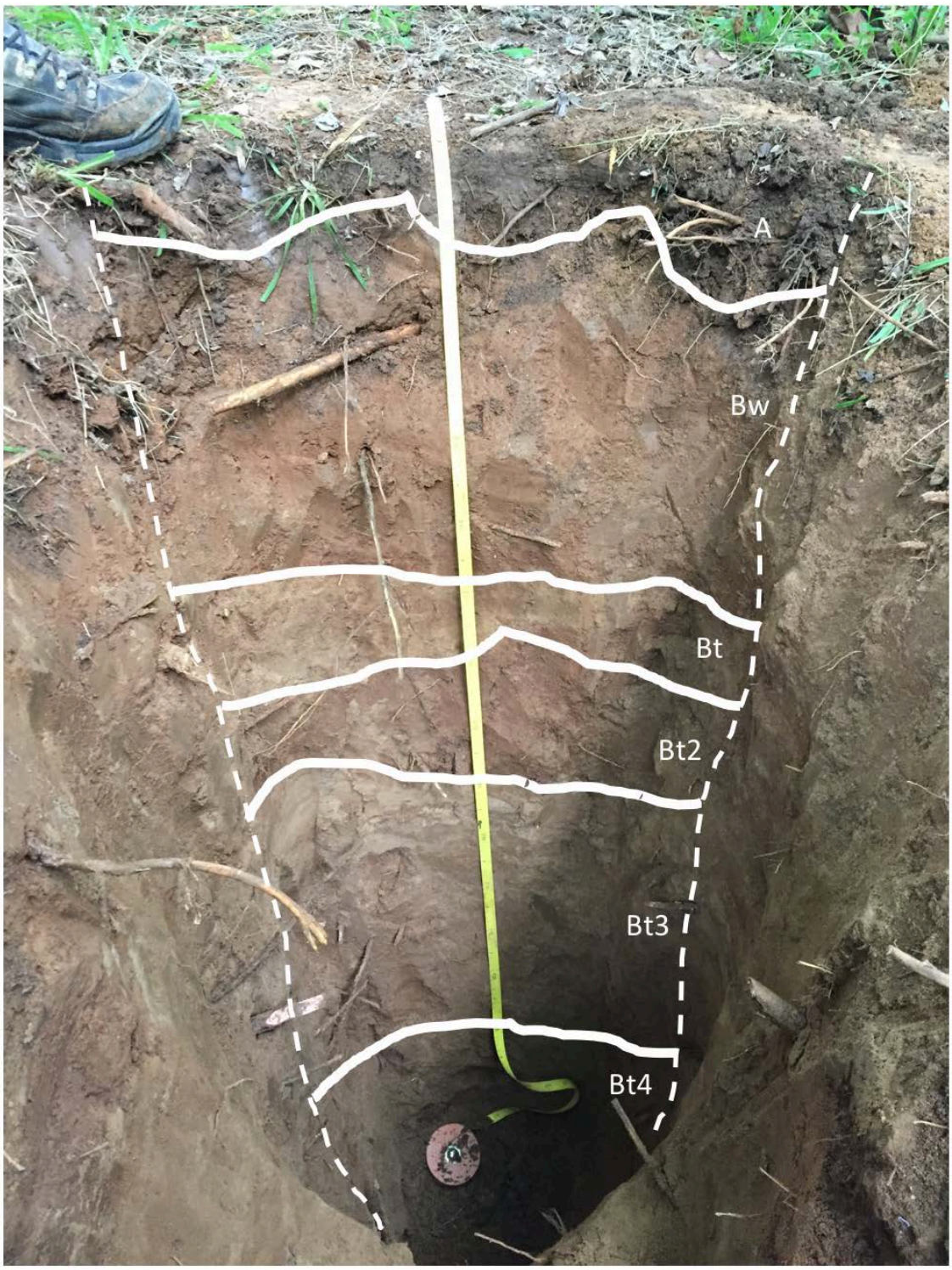

Figure B6: JAC 6 (Qt5) The Ivy Place event venue, Van Wyck, SC; 34.9037, -80.8771.

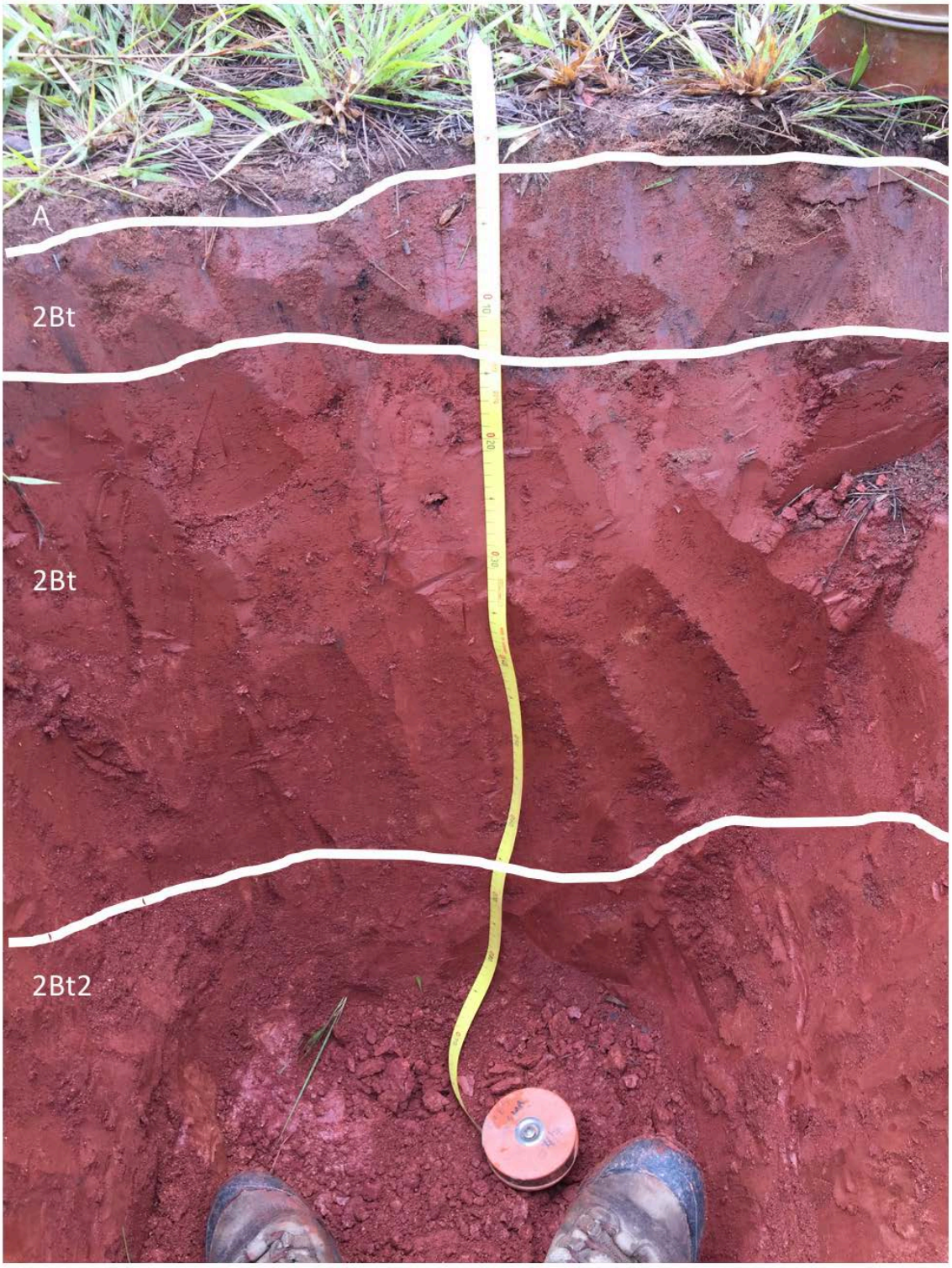

Figure B7: JAC 7 (Qt2) SCDNR Forest Legacy property at Landsford Canal State Park, Landsford, SC; 34.7770, -80.8891.

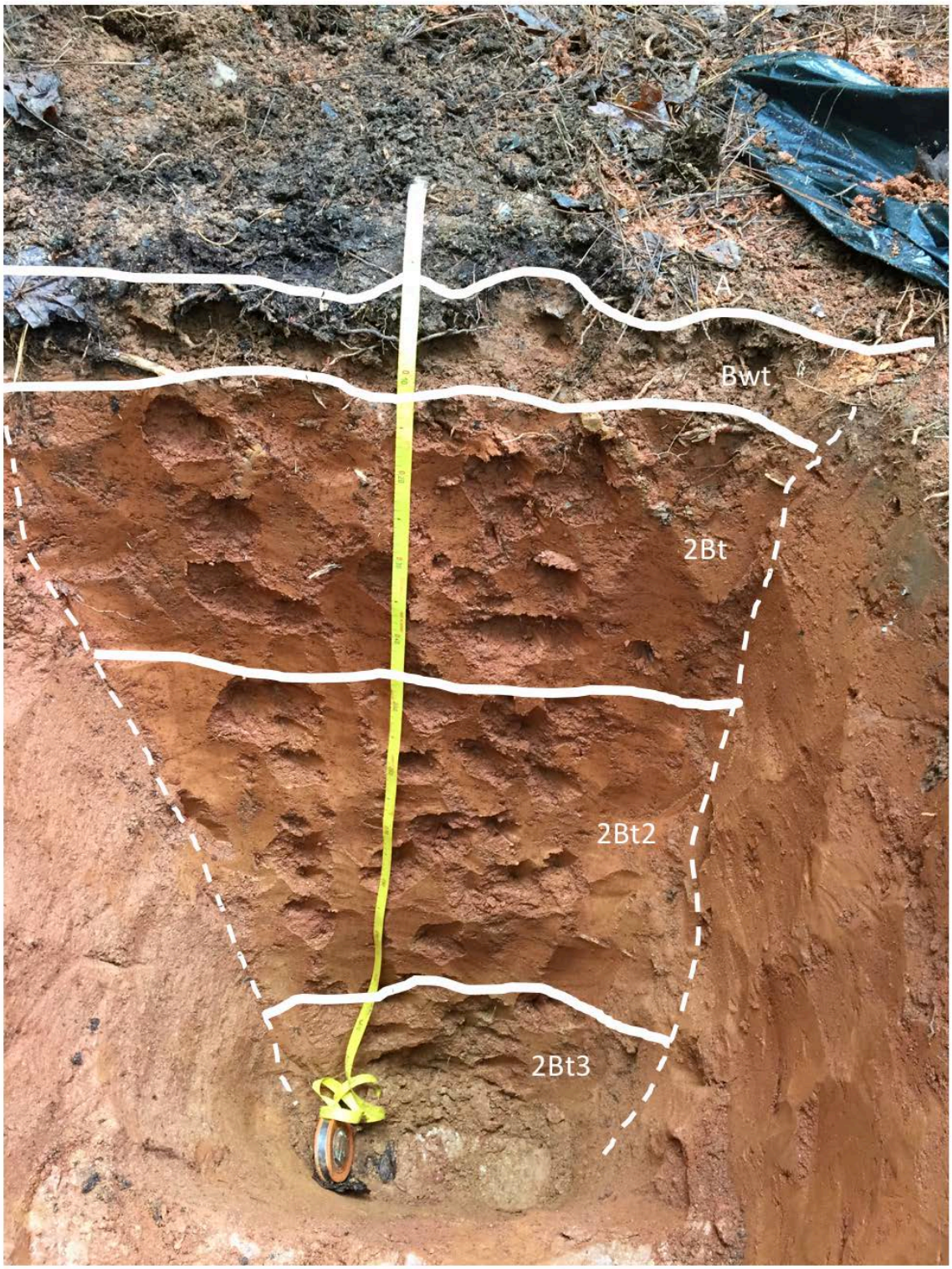

Figure B8: JAC 8 (Qt3) Landsford Canal State Park; Landsford, SC; 34.7909, -80.8871.

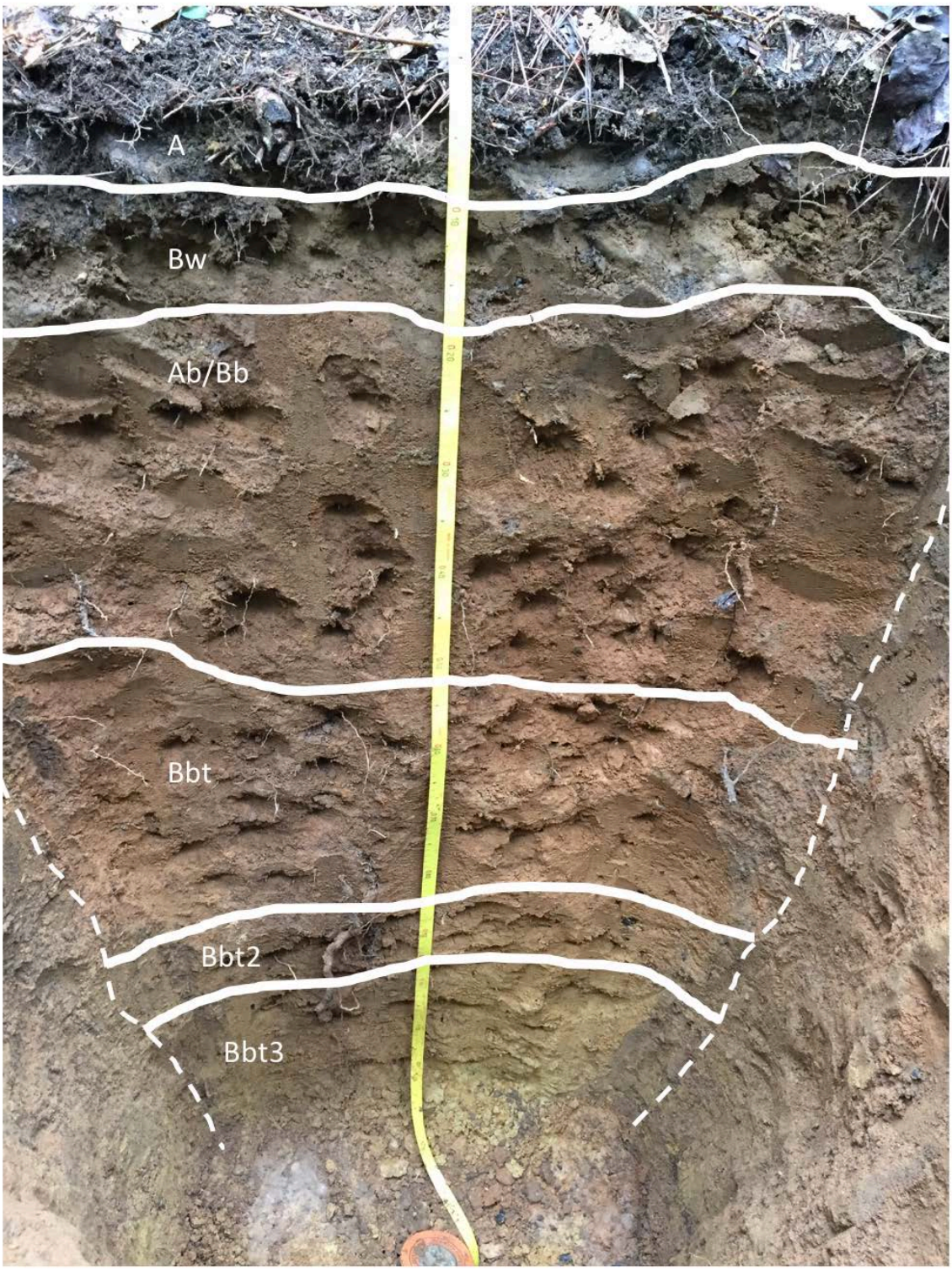

Figure B9: JAC 9 (Qt4) Landsford Canal State Park, Landsford, SC; 34.7865, -80.8801.

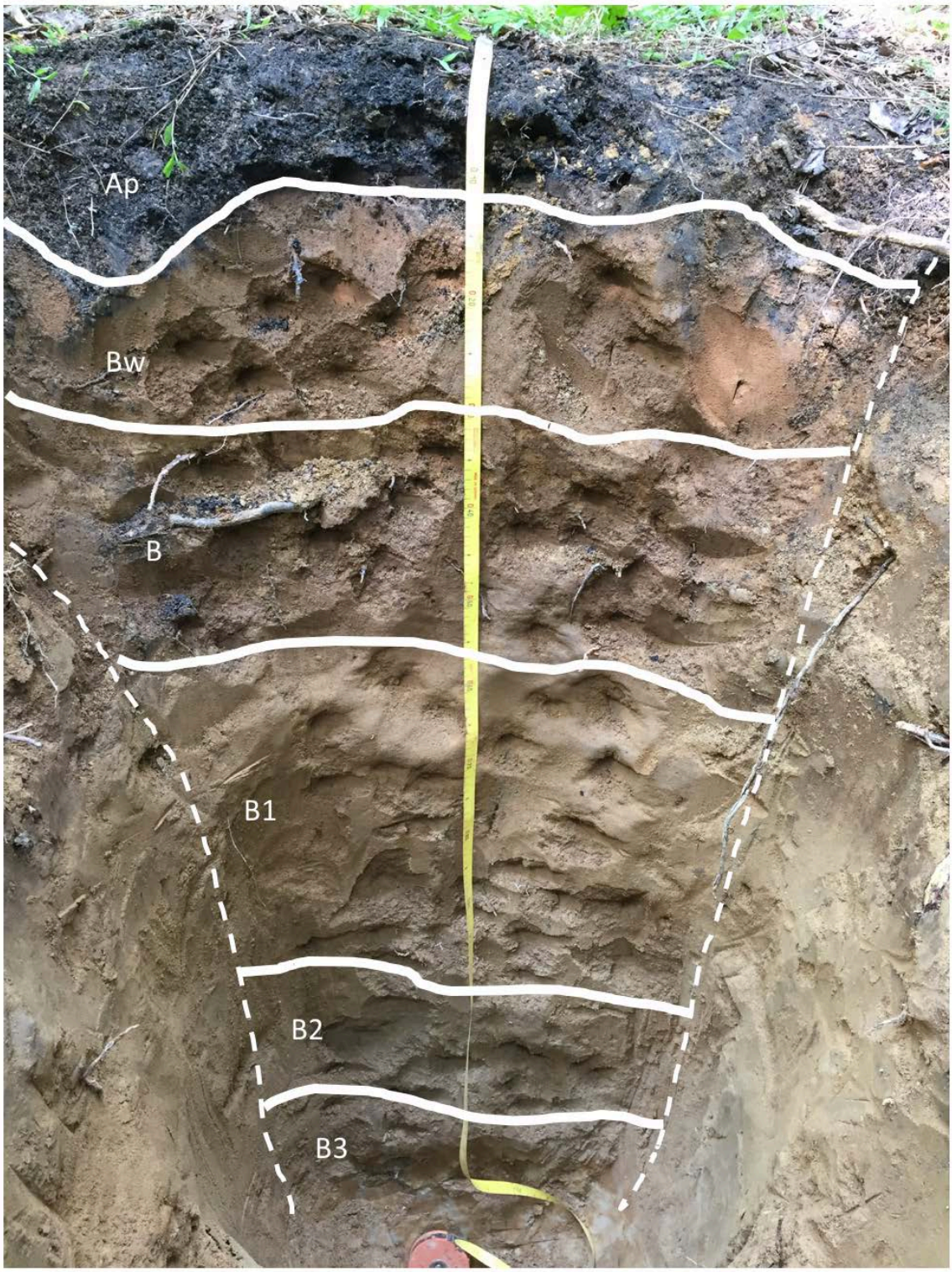

Figure B10: JAC 10 (Qt5) Landsford Canal State Park (east side of the river), Landsford, SC; 34.7777, -80.8714.

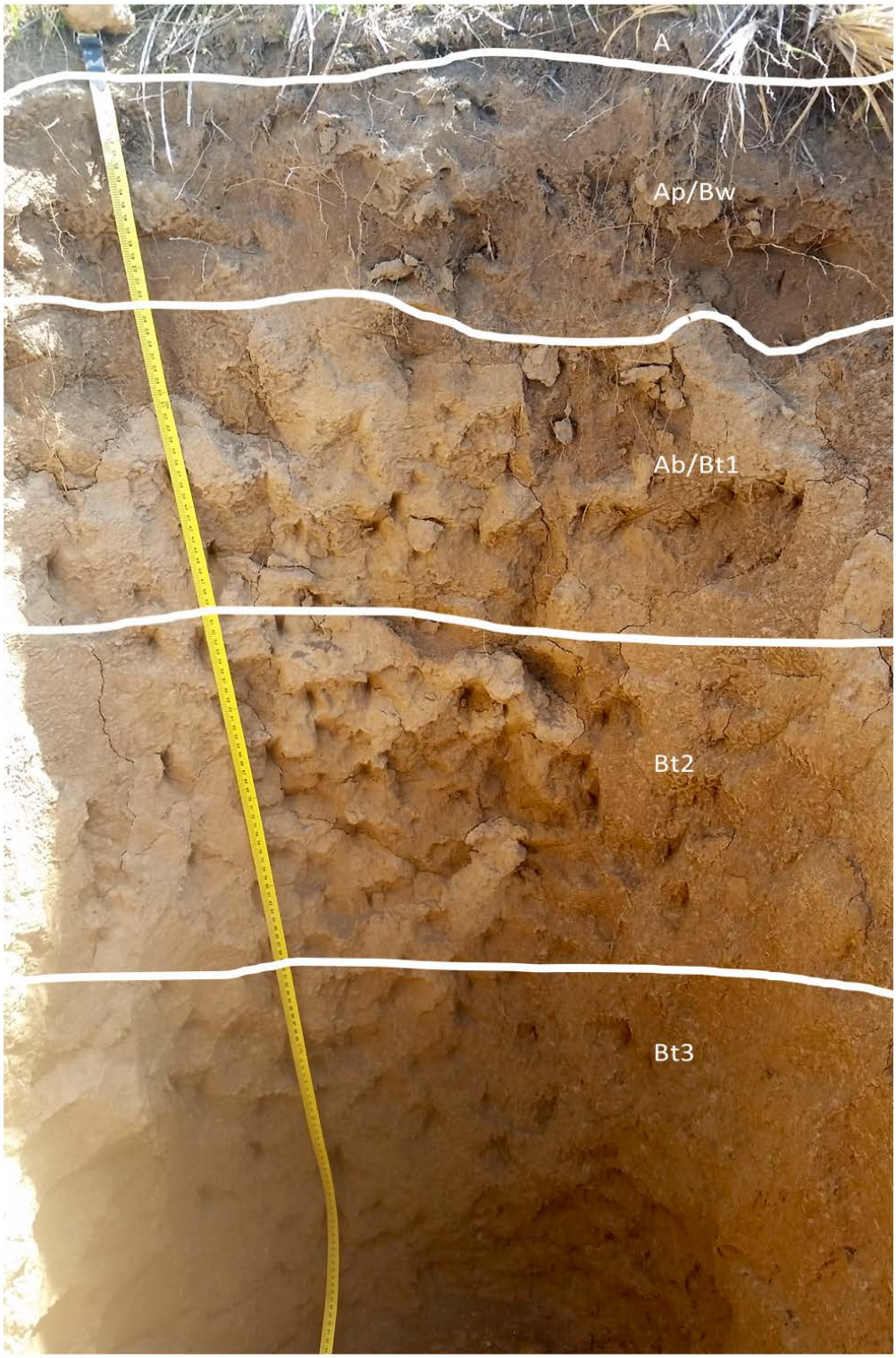

Figure B11: JAC 12 (Qt4) Back property of North Rock Hill Church, Mt. Gallant Rd., Rock Hill, SC; 34.9944, -80.9984.

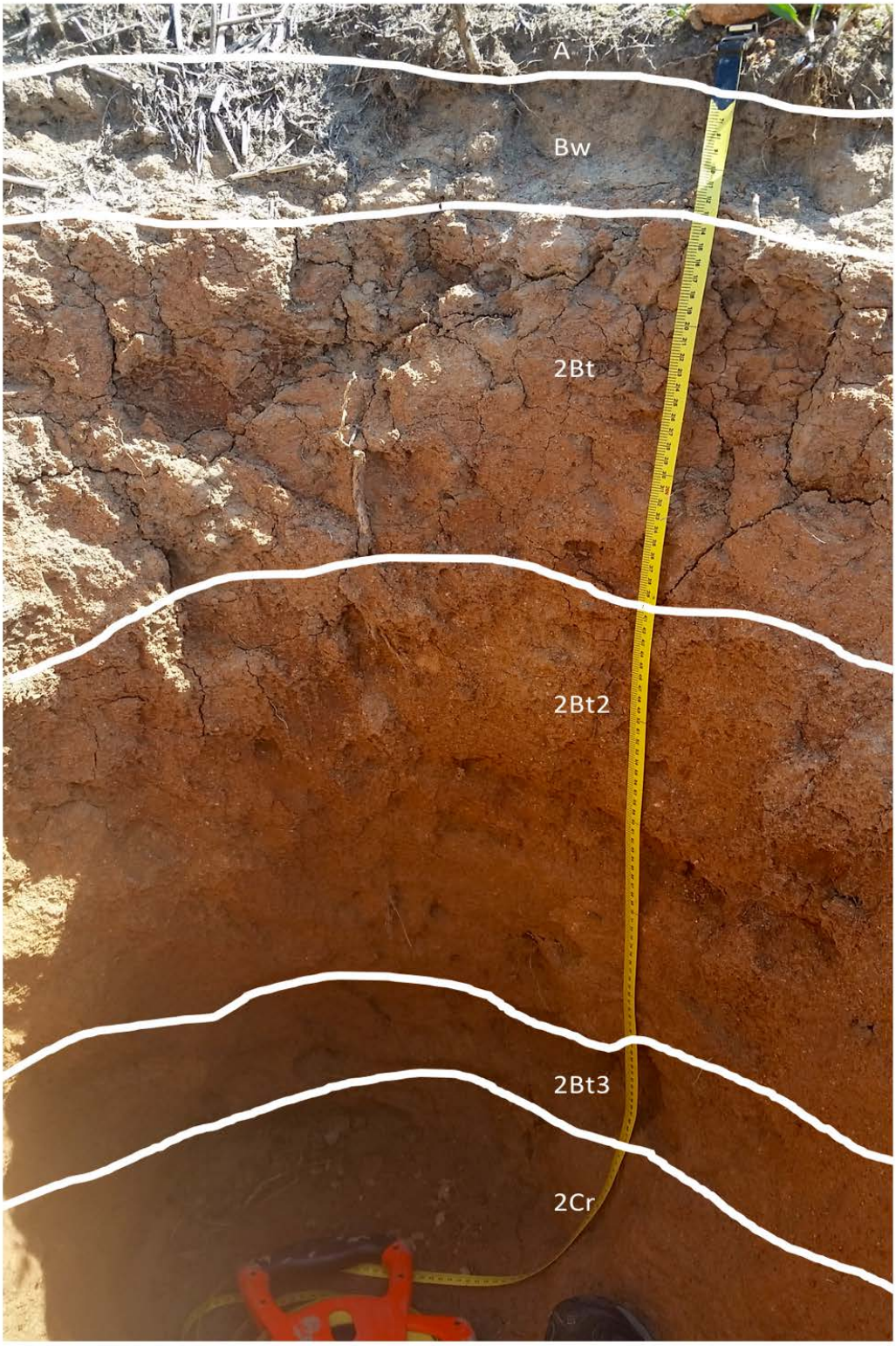

Figure B12: JAC 13 (Qt3) Across street from North Rock Hill Church, Mt. Gallant Rd., Rock Hill, SC ; 34.9947-80.0058.

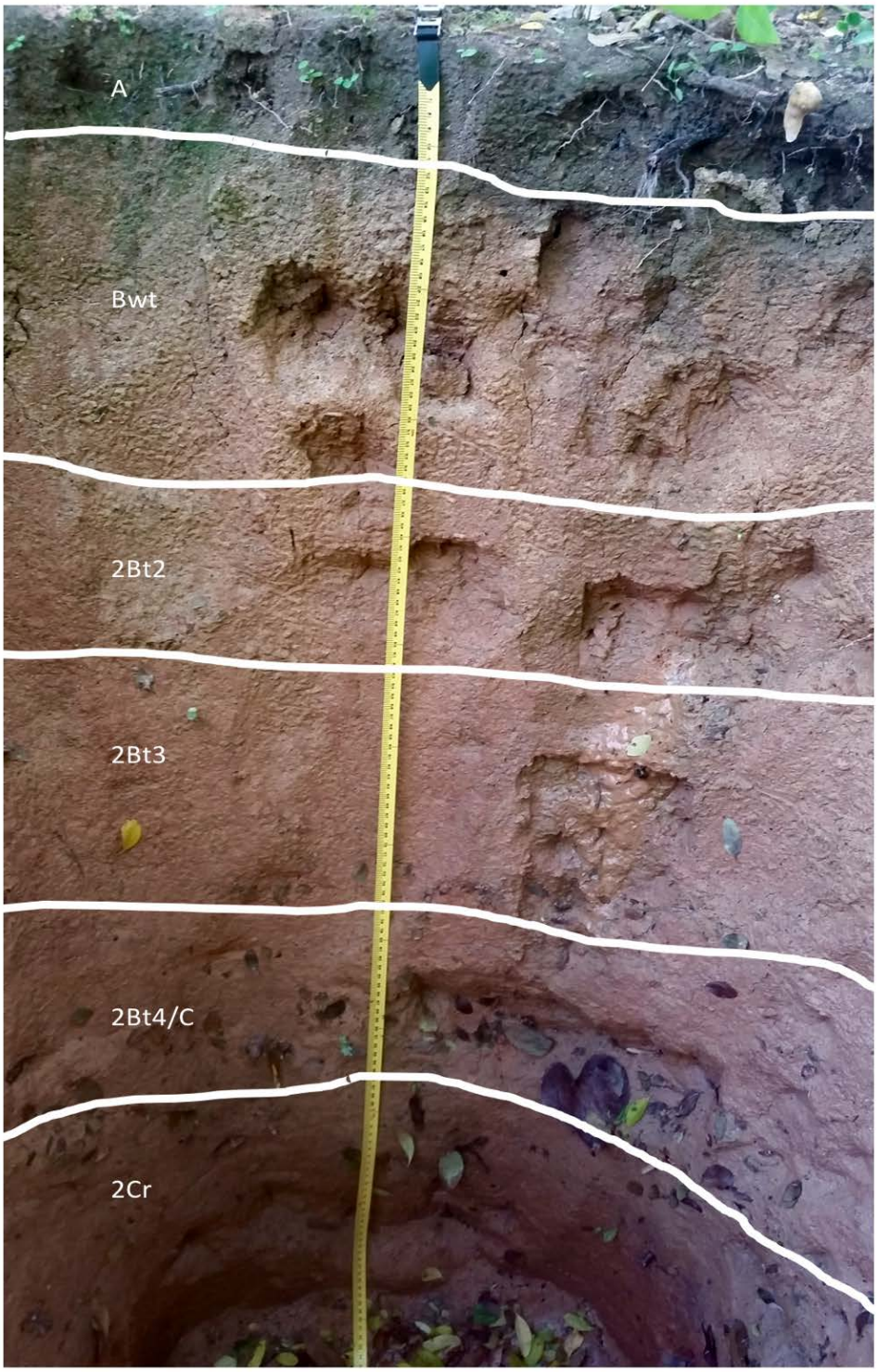

Figure B13: JAC 14 (Qt3) Back property of North Rock Hill Church, Mt. Gallant Rd., Rock Hill, SC; 34.9944, -80.0026.

Figure B14: JAC 15 (Qt3) Construction exposure at Mason's Bend neighborhood, Riverview, SC; 34.9921, -80.9874.

APPENDIX C: Supplementary Figures and Tables

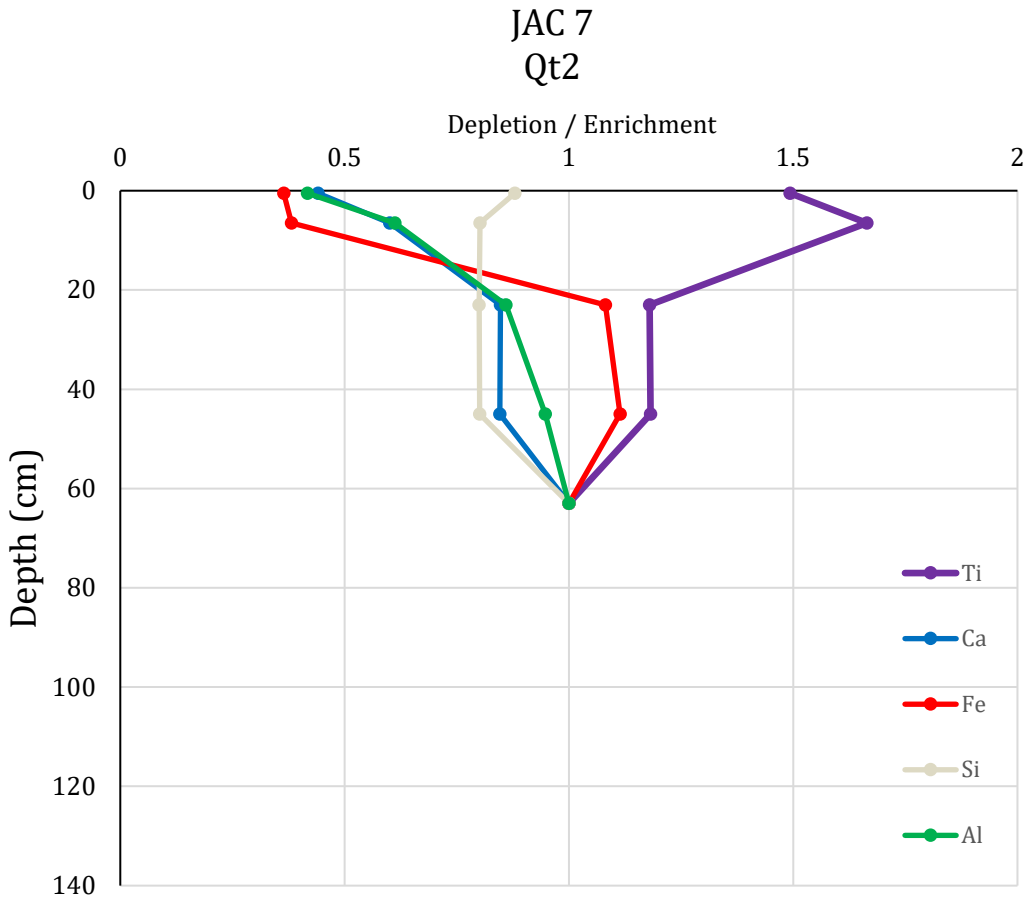

Figure C1: Depletion/Enrichment vs. depth plots for 5 base cations of JAC 7 (Qt2).

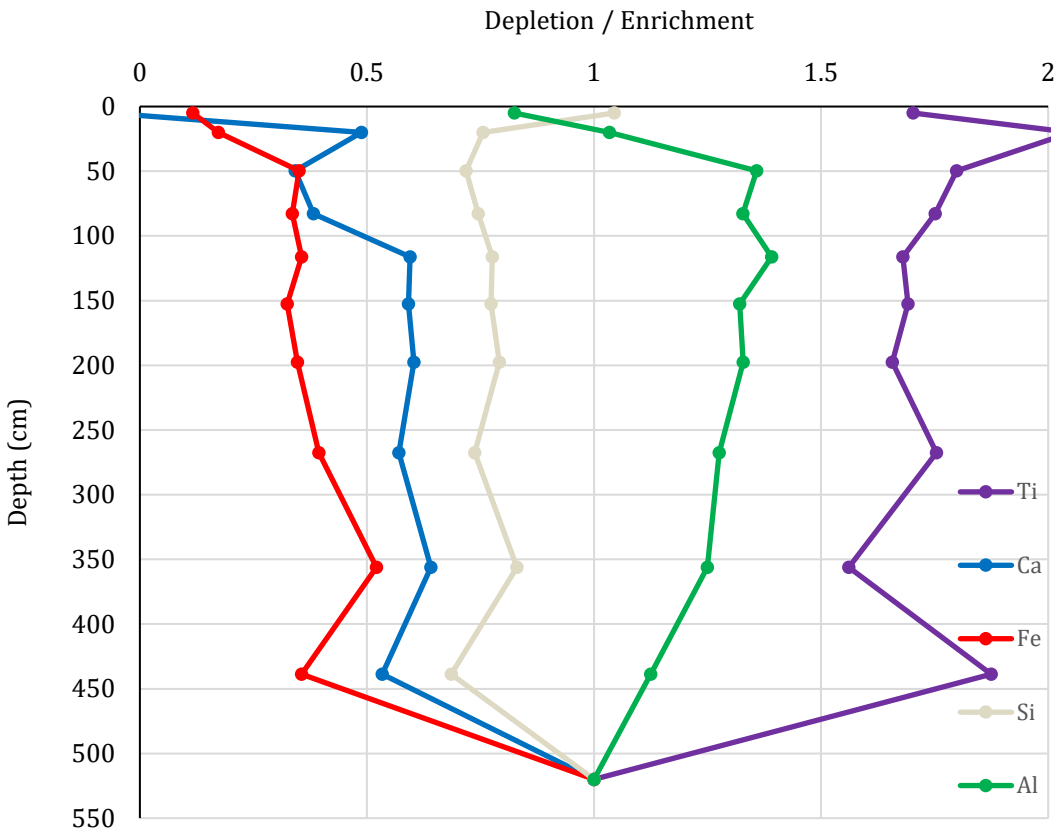

Figure C2: Depletion/Enrichment vs. depth plots for 5 base cations of JAC 15 (Qt3). Calcium registers at -0.07 at 5 cm depth. Titanium registers at 2.05 at 20 cm depth.

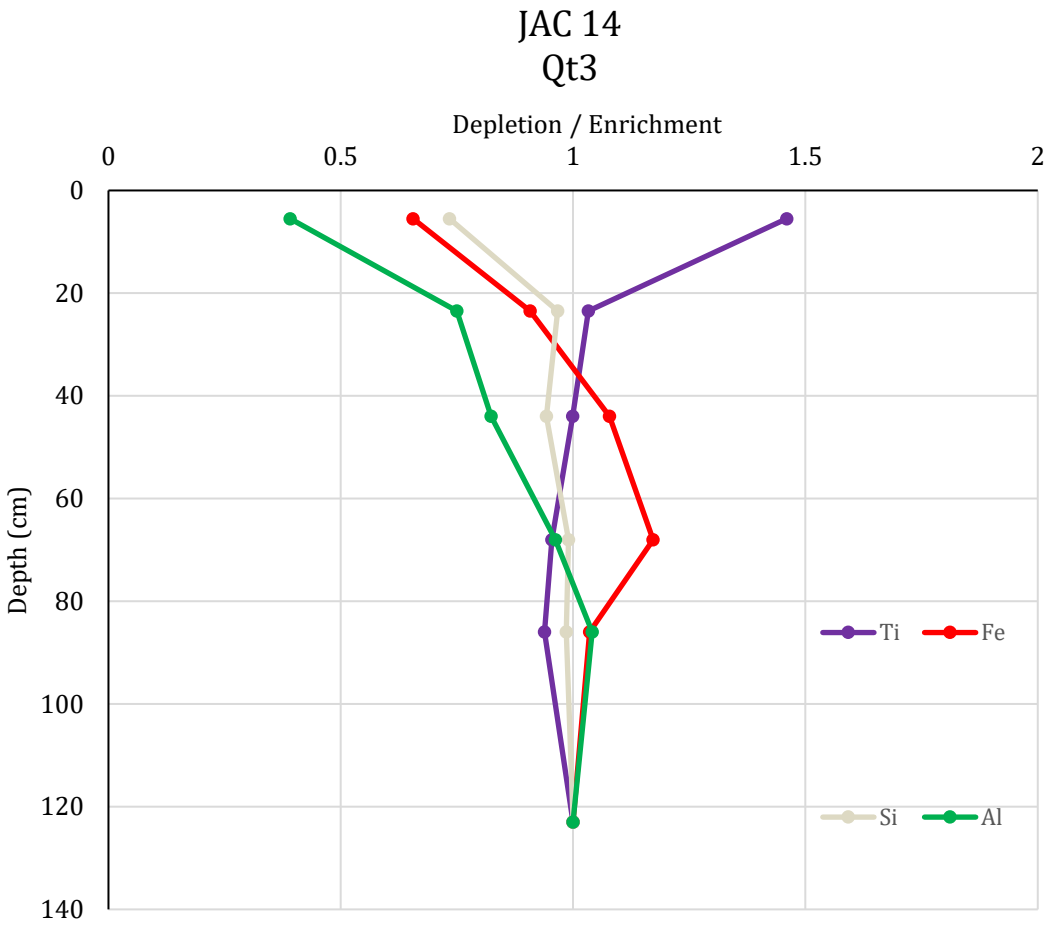

Figure C3: Depletion/Enrichment vs. depth plots for 4 base cations of JAC 14 (Qt3), Calcium was not measured during element analysis.

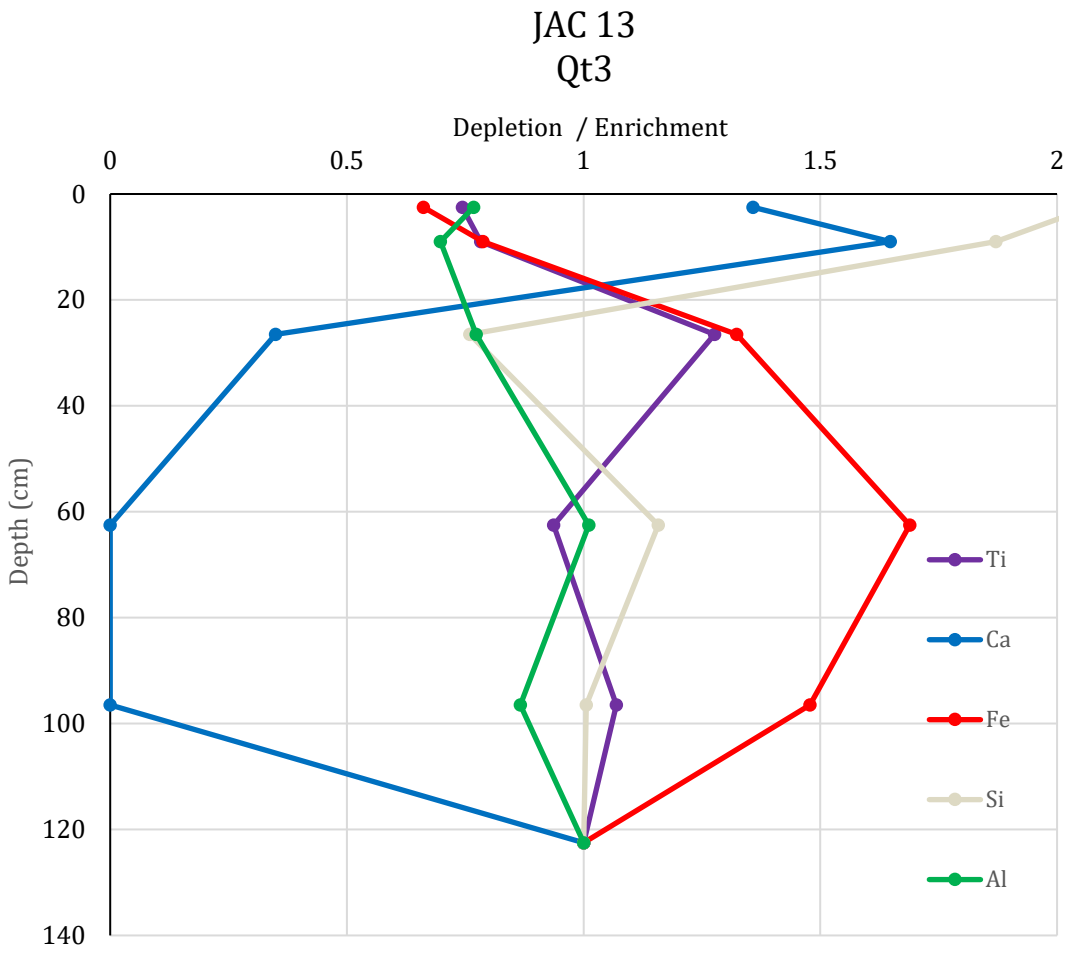

Figure C4: Depletion/Enrichment vs. depth plots for 5 base cations of JAC 13 (Qt3). Silicon registers at 2.06 at 2.5 cm depth.

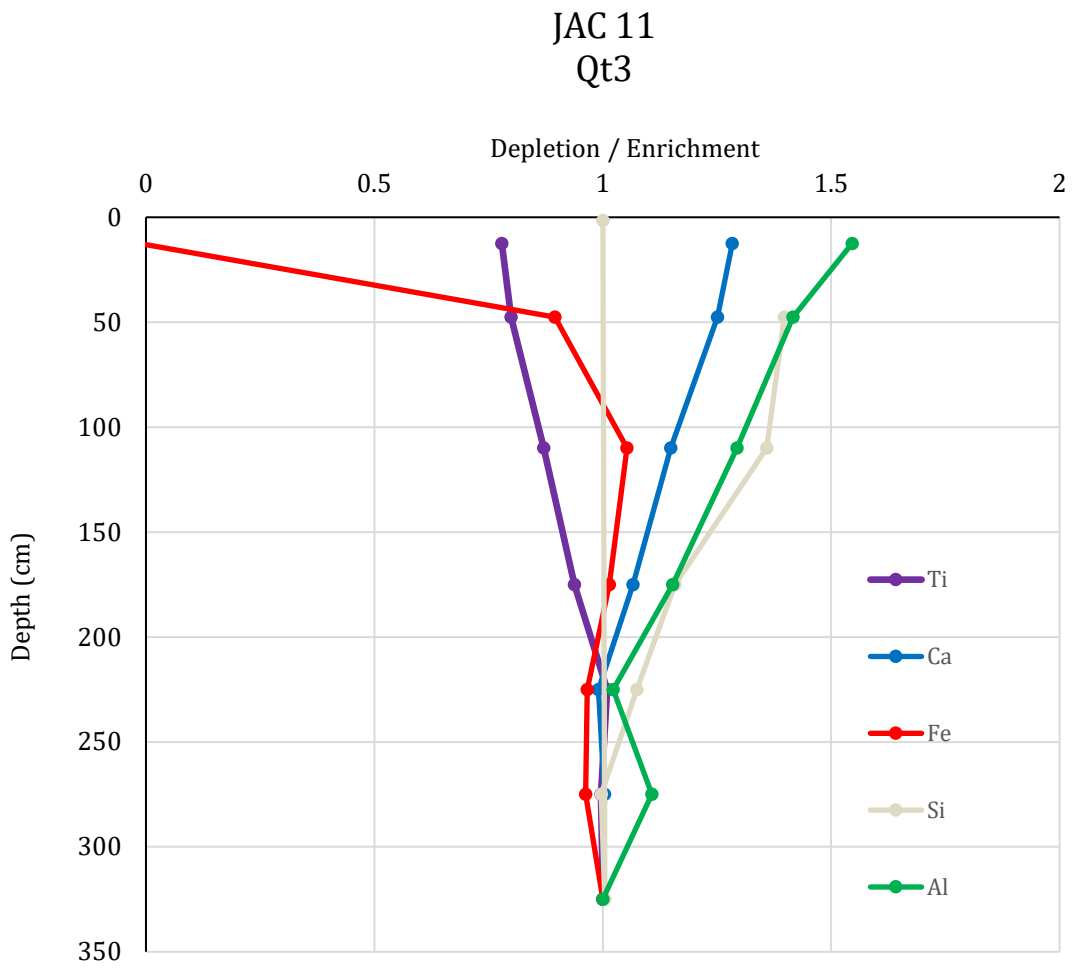

Figure C5: Depletion/Enrichment vs. depth plots for 5 base cations of JAC 11 (Qt3). Iron registers as -0.01 at 12.5 cm depth.

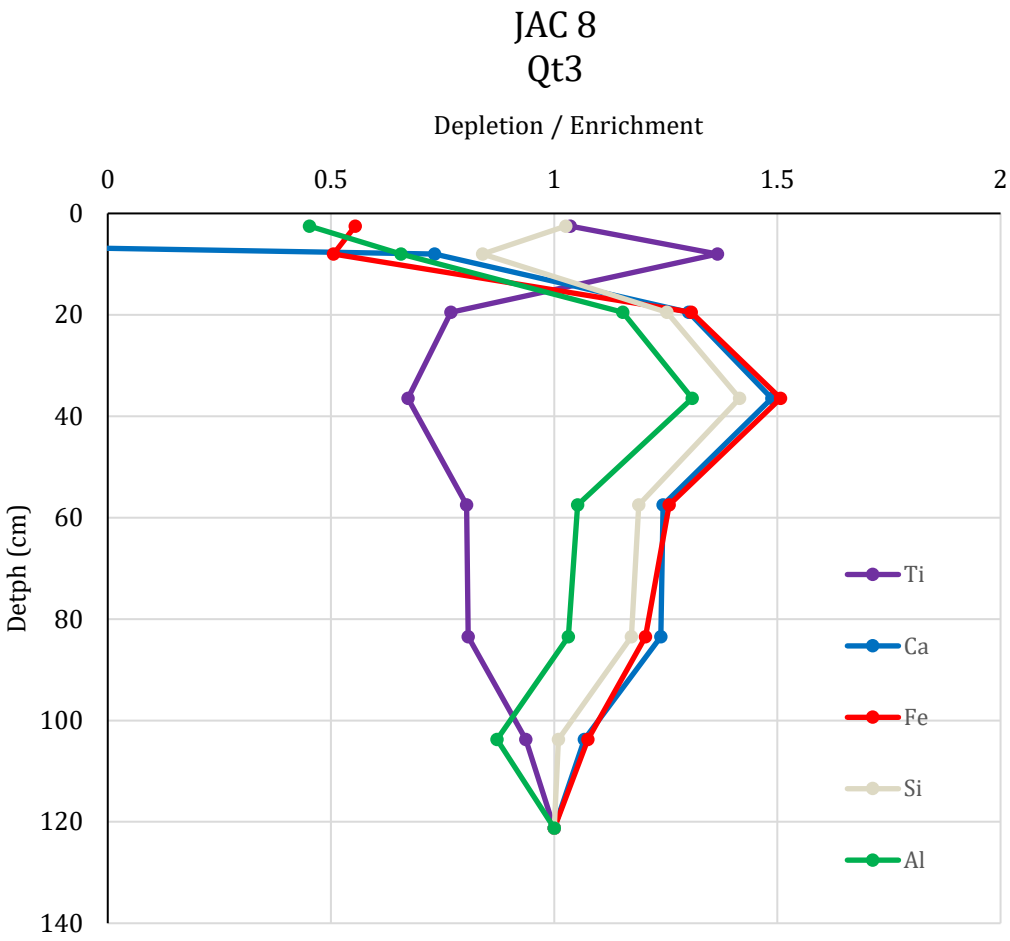

Figure C6: Depletion/Enrichment vs. depth plots for 5 base cations of JAC 8 (Qt3). Calcium registers as -2.8 at 2.5 cm depth.

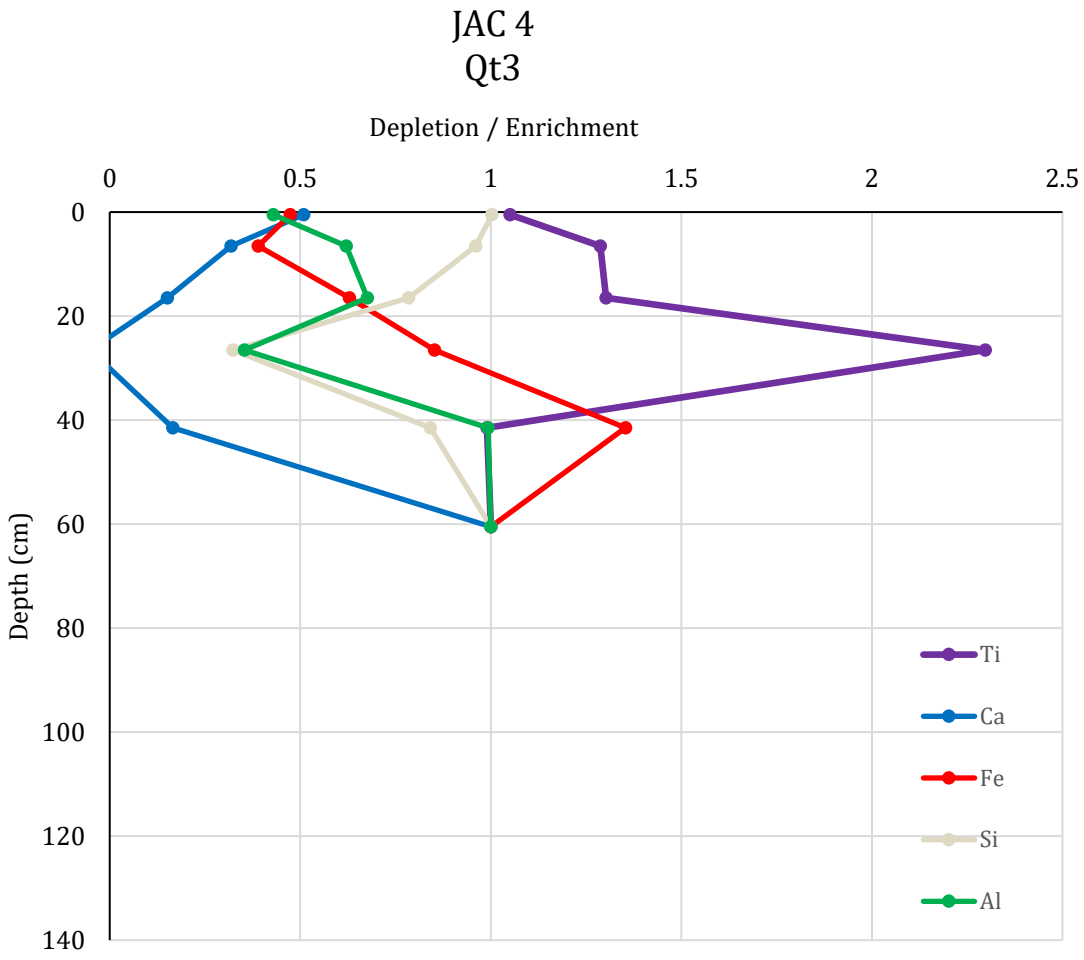

Figure C7: Depletion/Enrichment vs. depth plots for 5 base cations of JAC 4 (Qt3). Calcium registers as -0.05 at 26.5 cm depth.

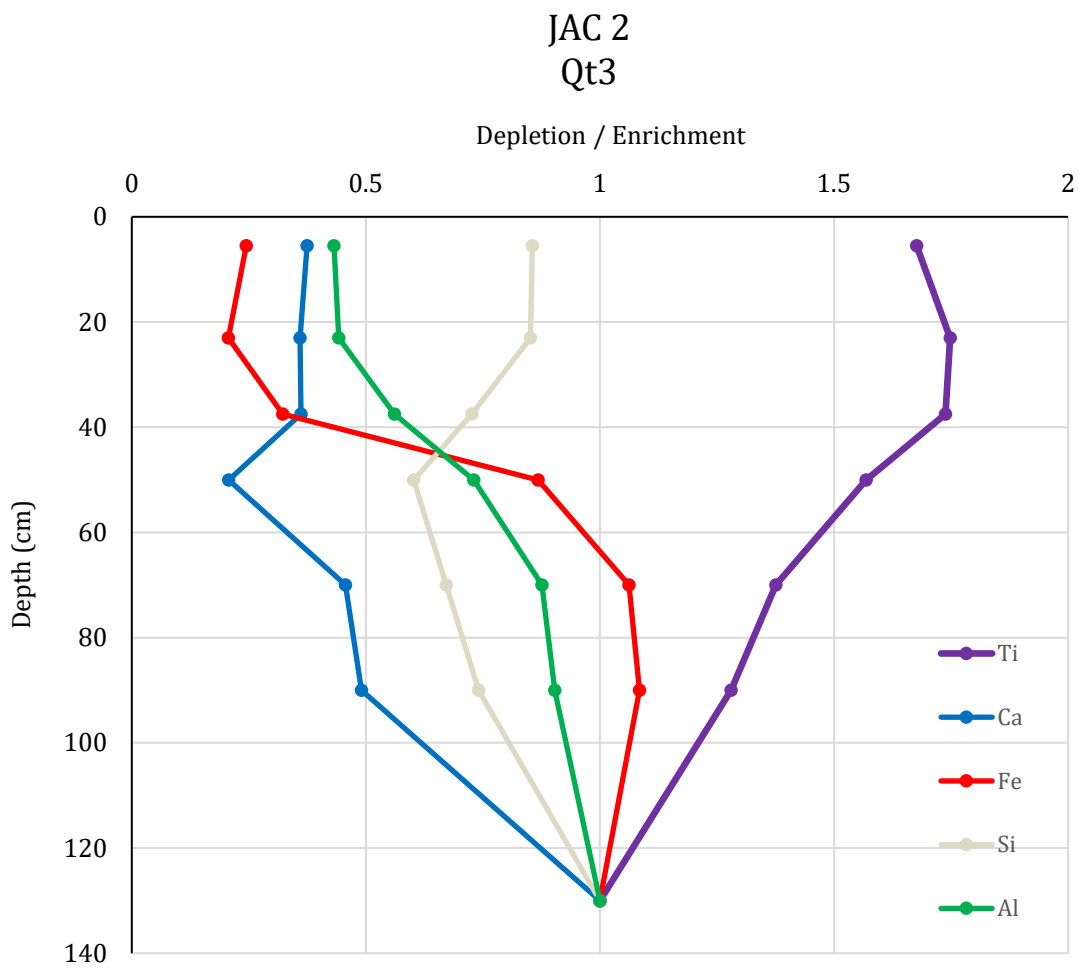

Figure C8: Depletion/Enrichment vs. depth plots for 5 base cations of JAC 2 (Qt3).

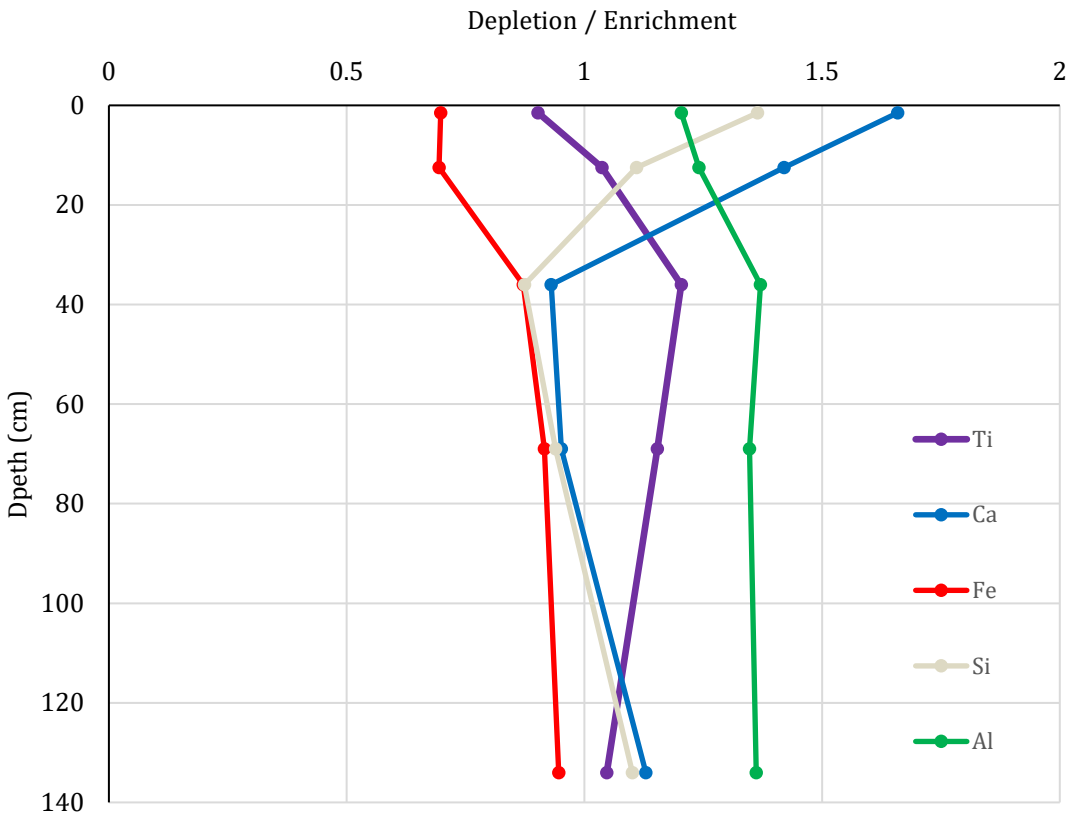

Figure C9: Depletion/Enrichment vs. depth plots for 5 base cations of JAC 12 (Qt4).

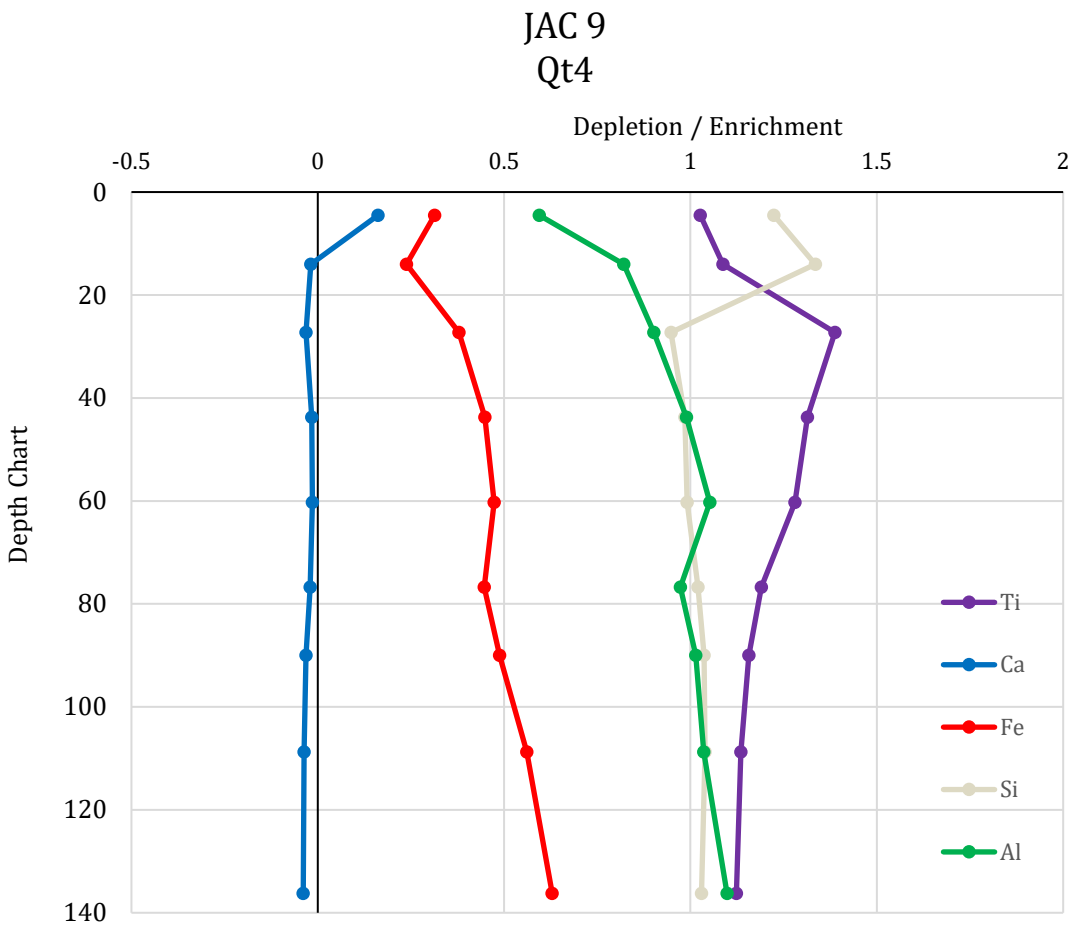

Figure C10: Depletion/Enrichment vs. depth plots for 5 base cations of JAC 9 (Qt4).

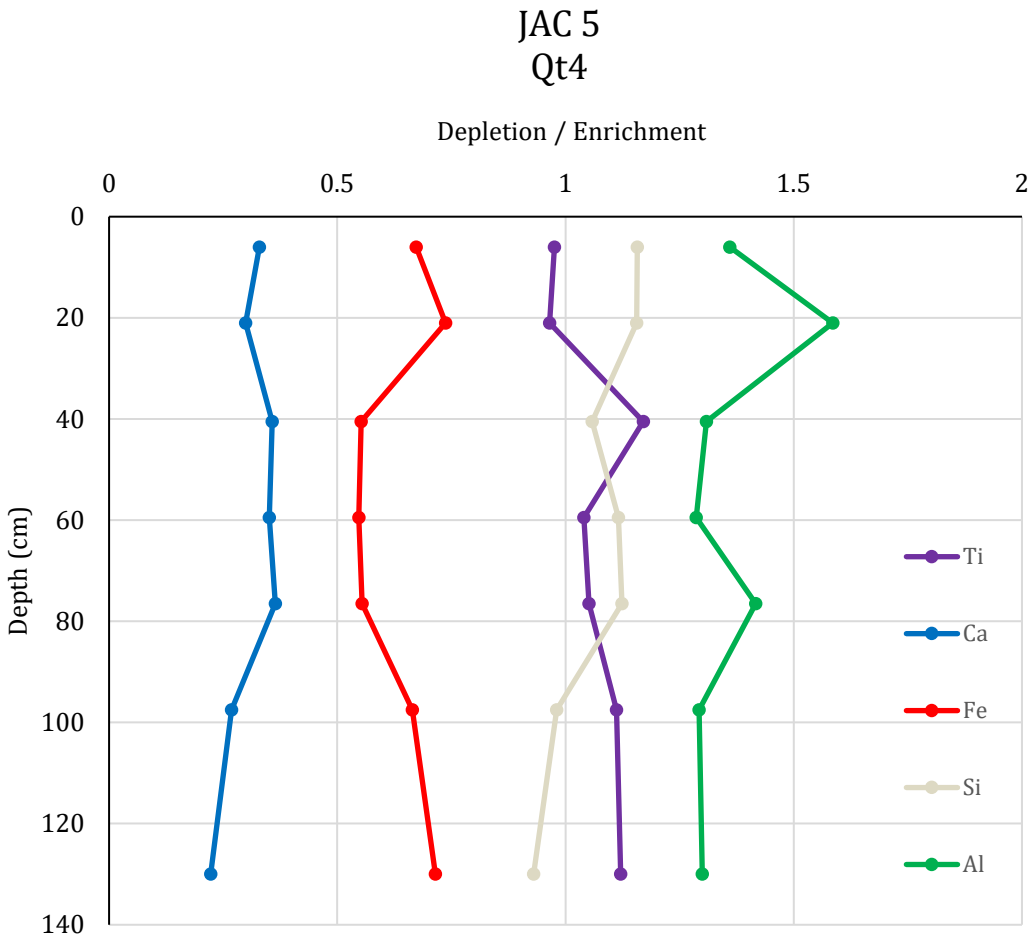

Figure C11: Depletion/Enrichment vs. depth plots for 5 base cations of JAC 5 (Qt4).

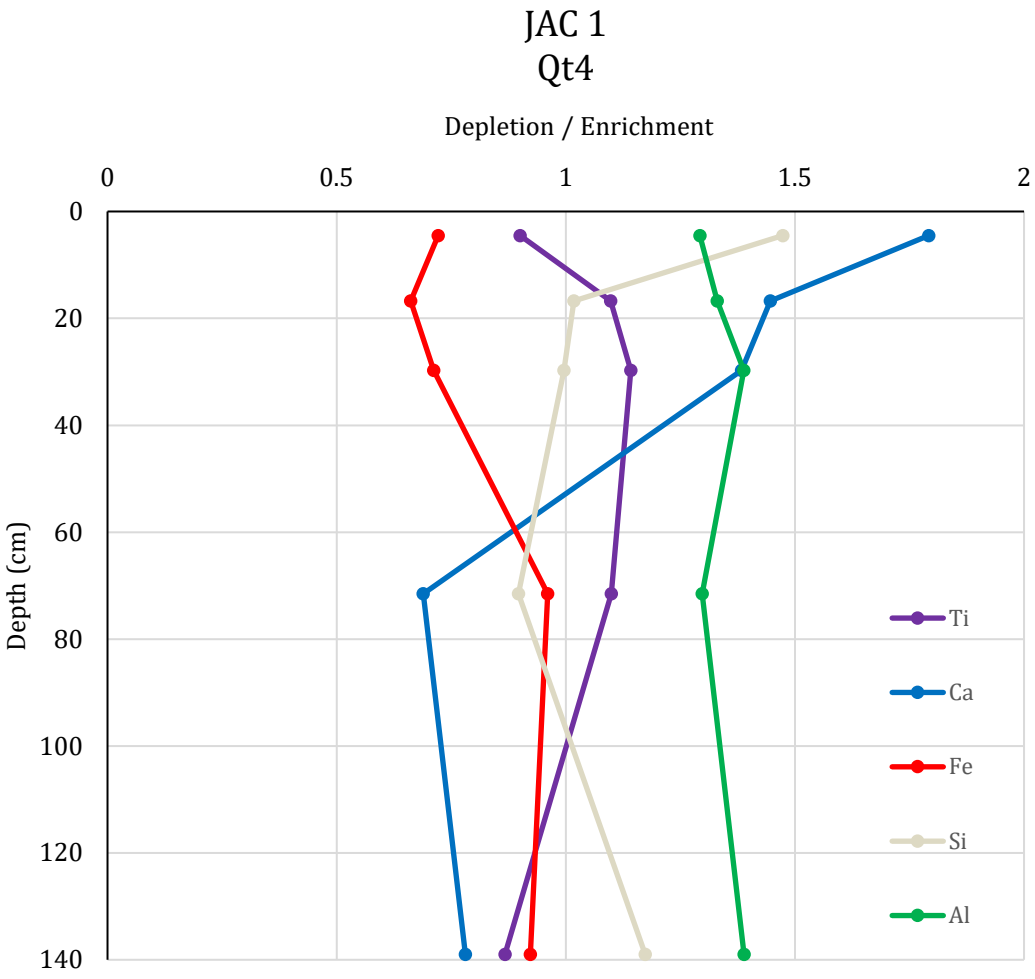

Figure C12: Depletion/Enrichment vs. depth plots for 5 base cations of JAC 1 (Qt4).

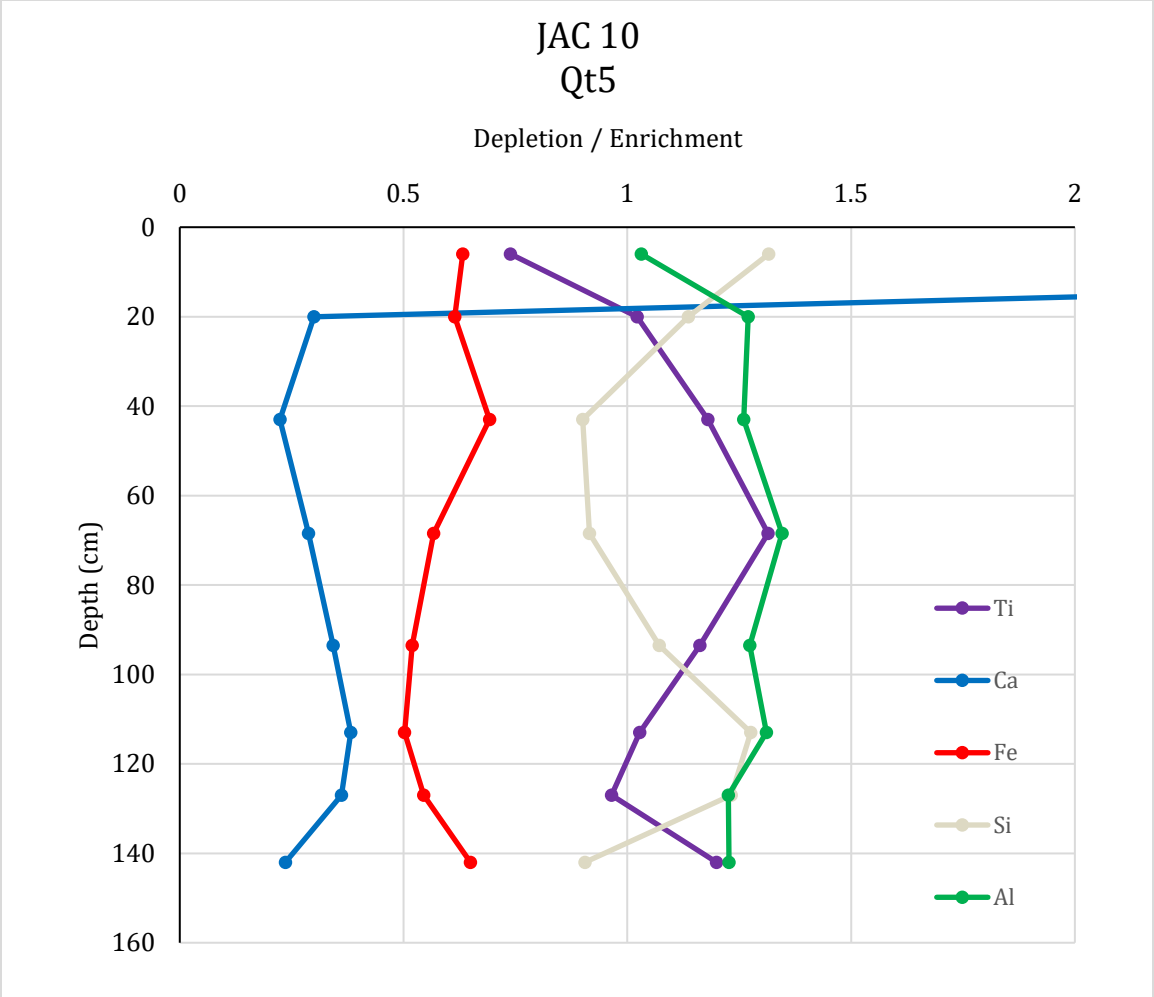

Figure C13: Depletion/Enrichment vs. depth plots for 5 base cations of JAC 10 (Qt5).

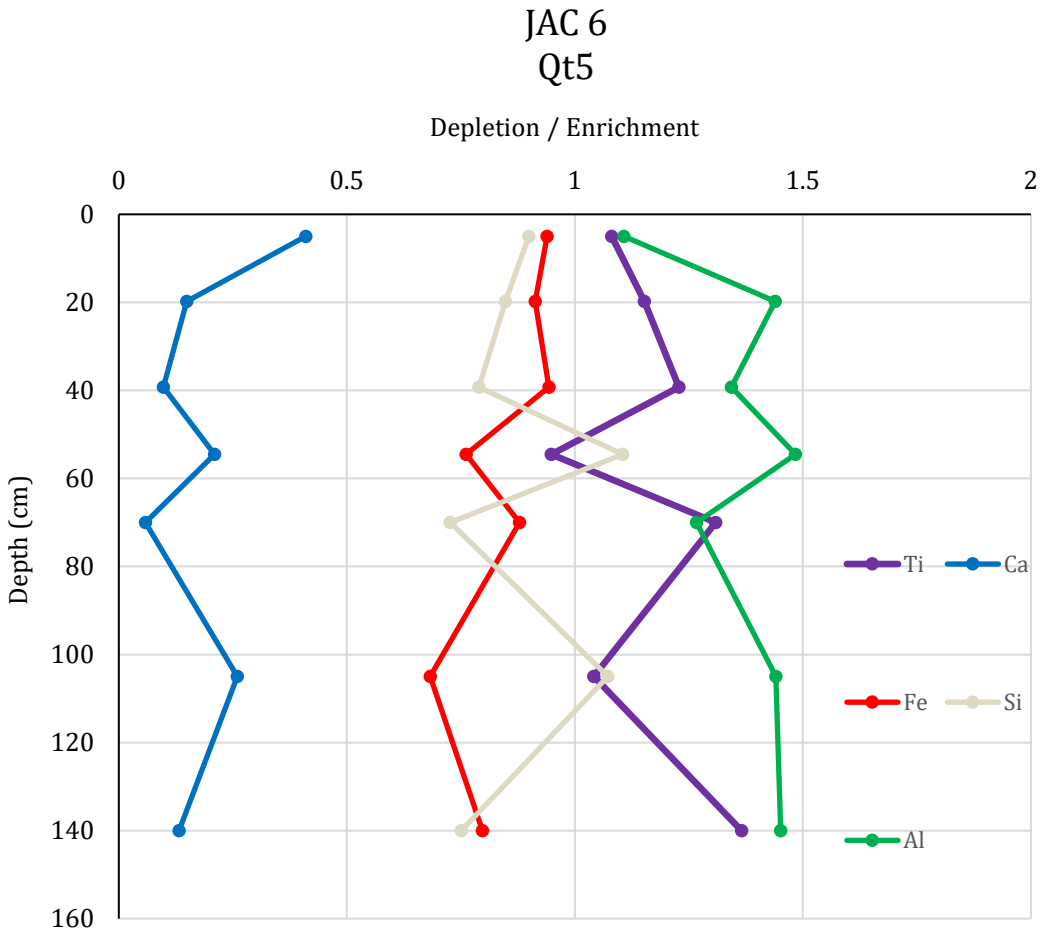

Figure C14: Depletion/Enrichment vs. depth plots for 5 base cations of JAC 6 (Qt5).

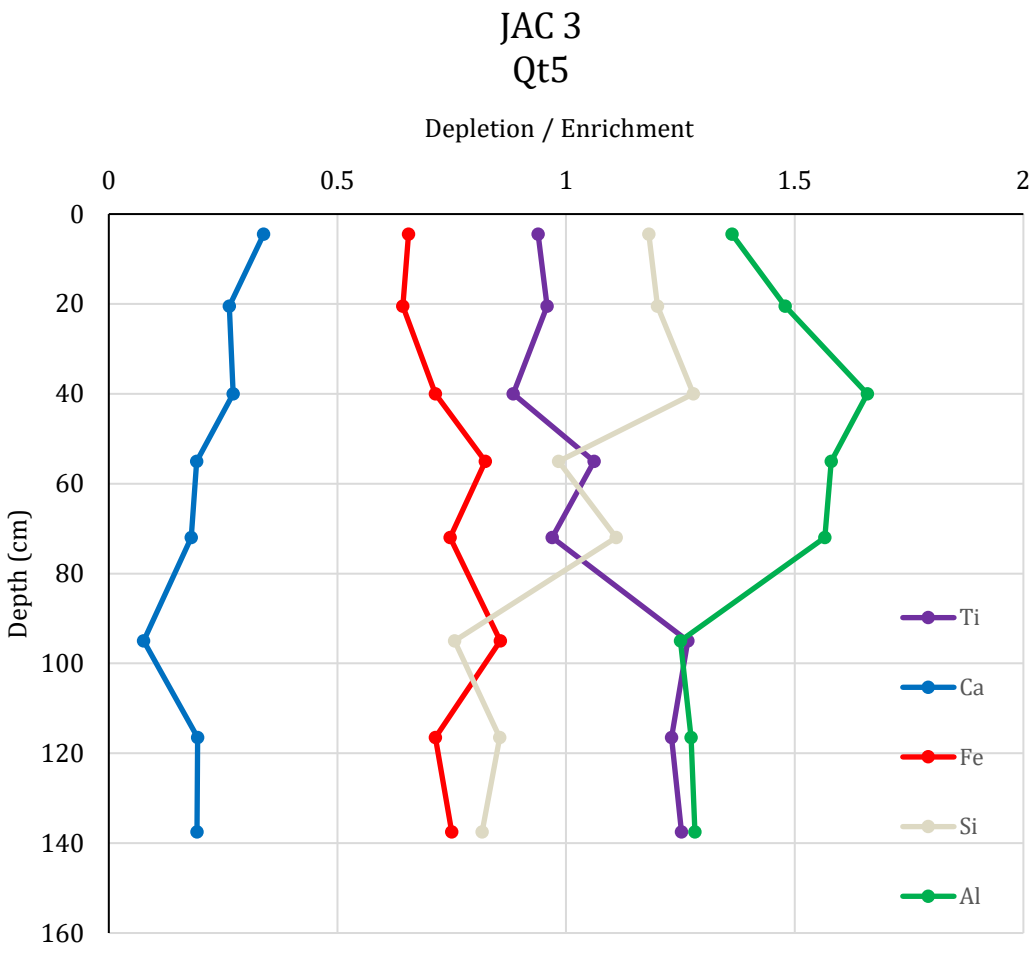

Figure C15: Depletion/Enrichment vs. depth plots for 5 base cations of JAC 3 (Qt5).

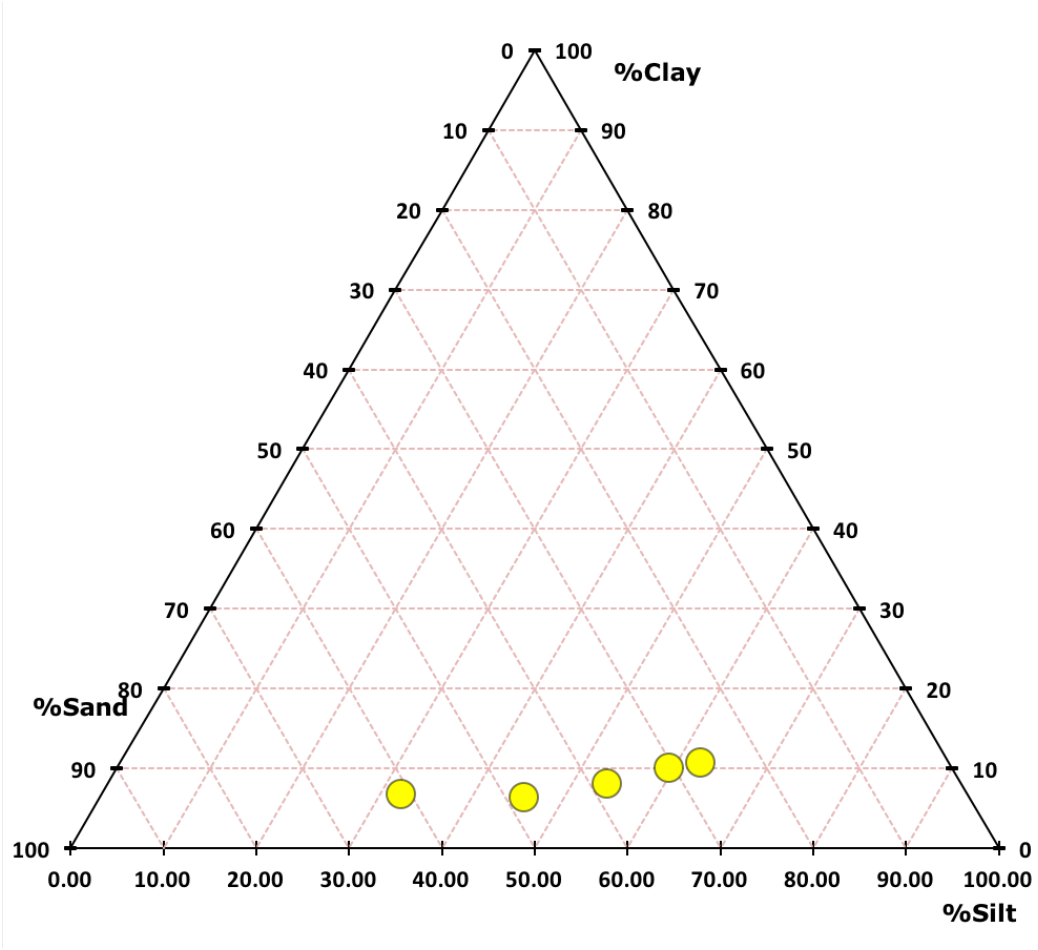

Figure C16: Ternary plot for all Qt2 horizons.

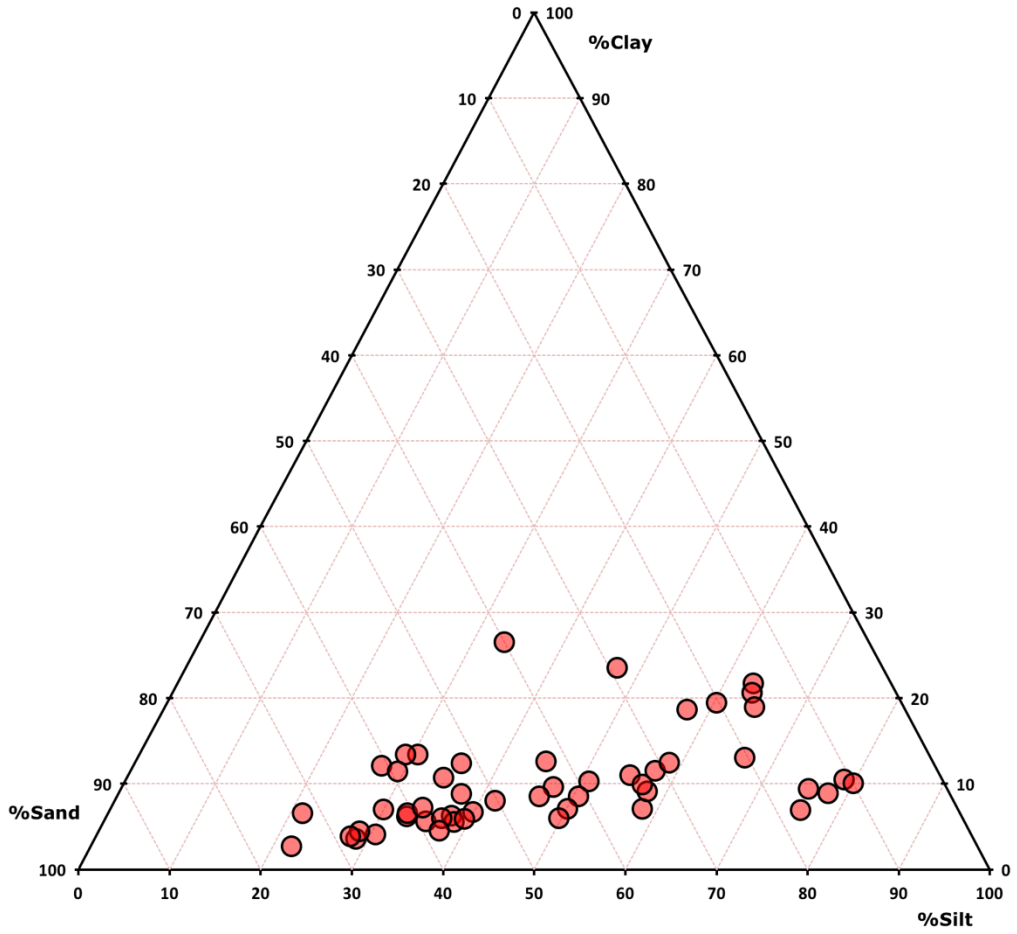

Figure C17: Ternary plot for all Qt3 horizons.

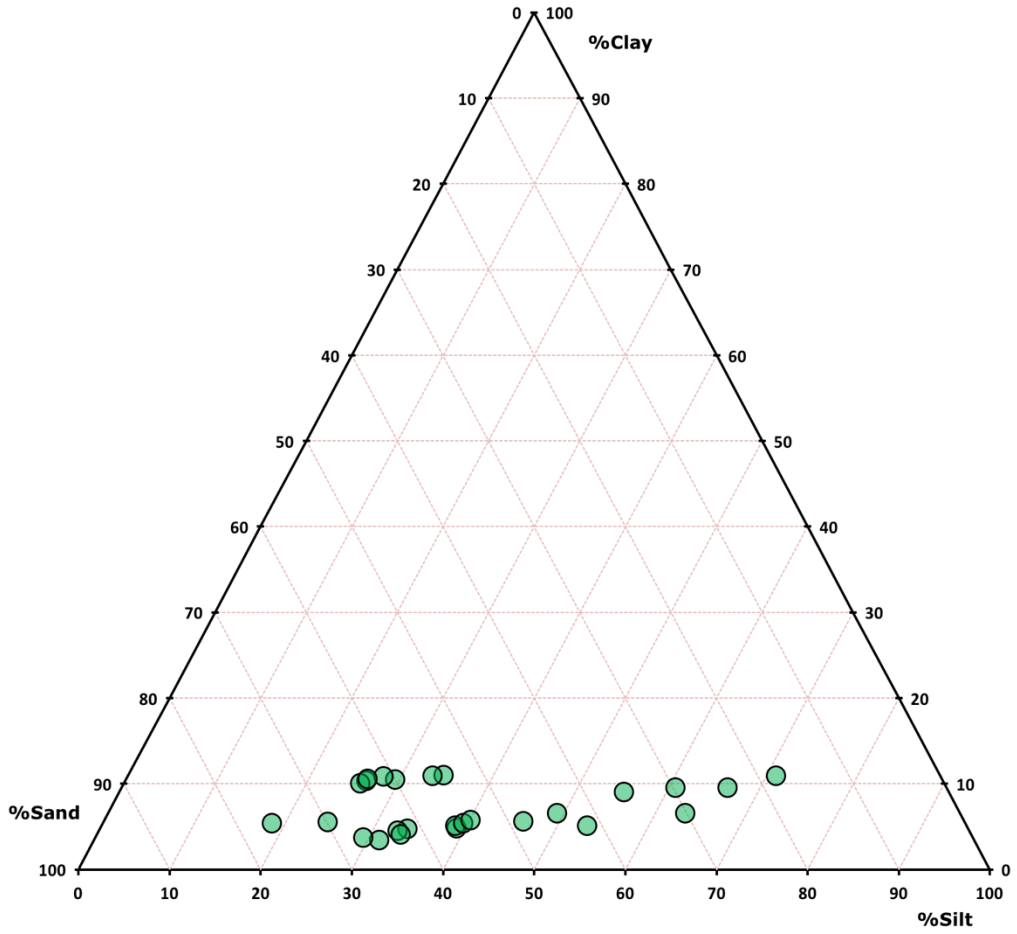

Figure C18: Ternary plot for all Qt4 horizons.

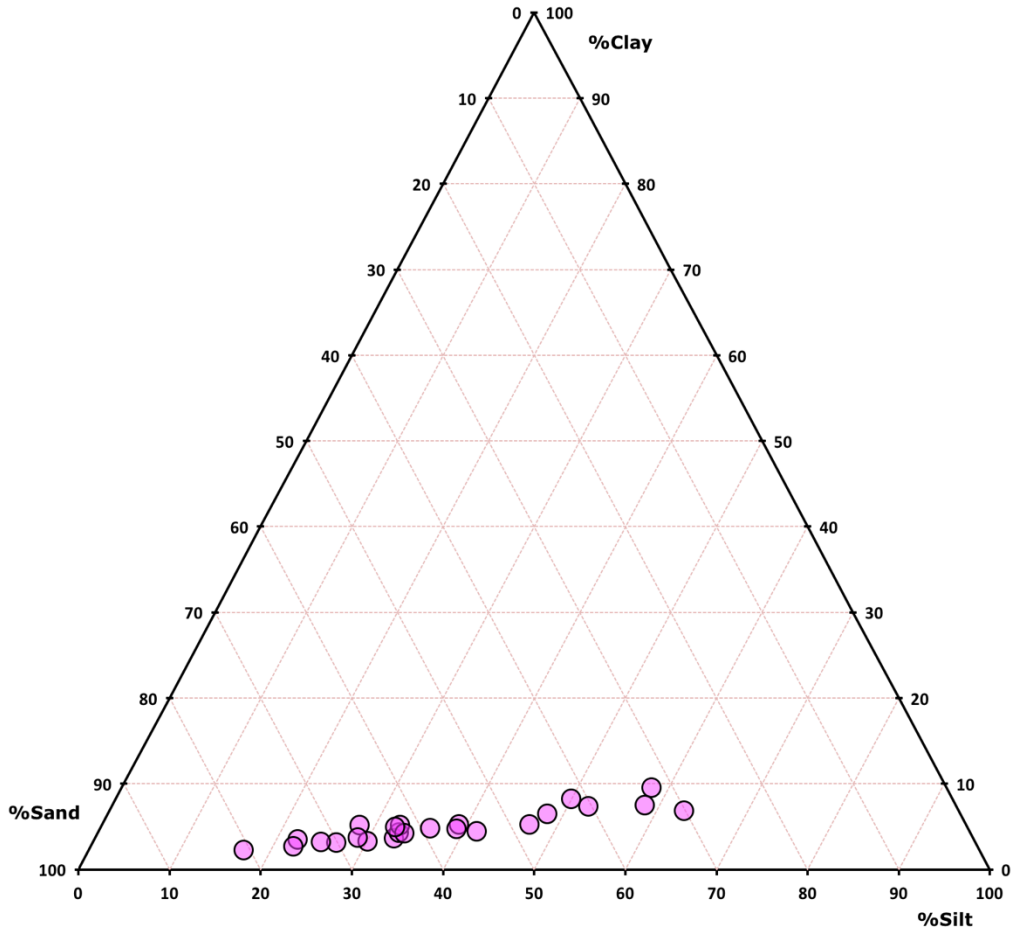

Figure C19: Ternary plot for all Qt5 horizons.

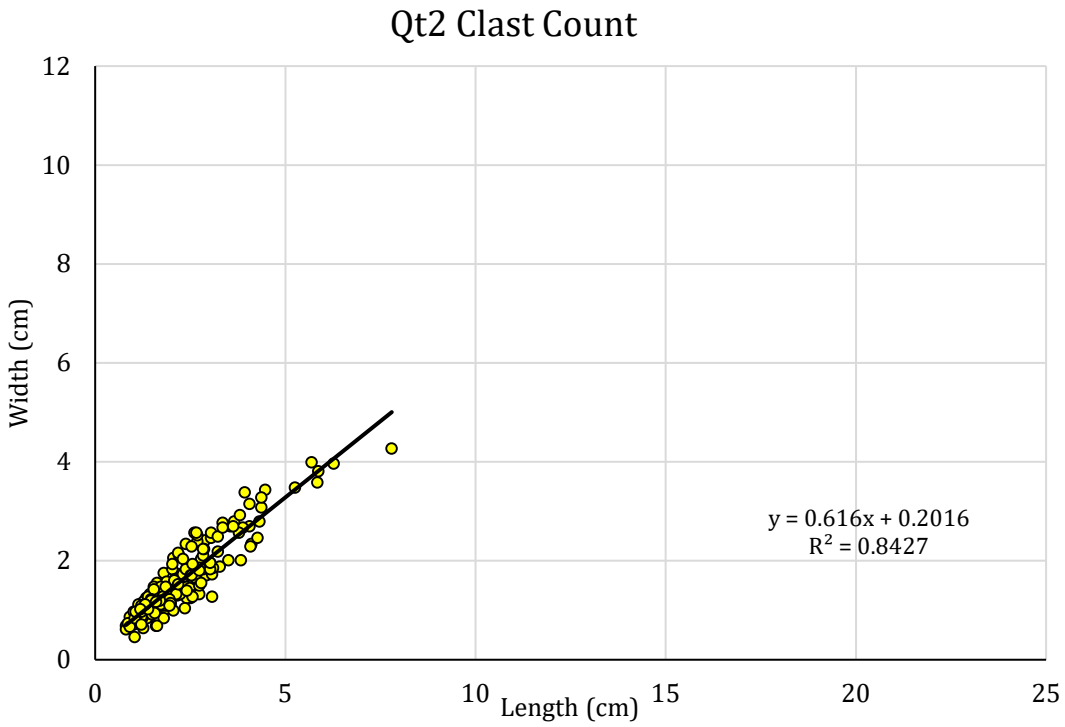

Figure C20: Clast count length vs. width for Qt2.

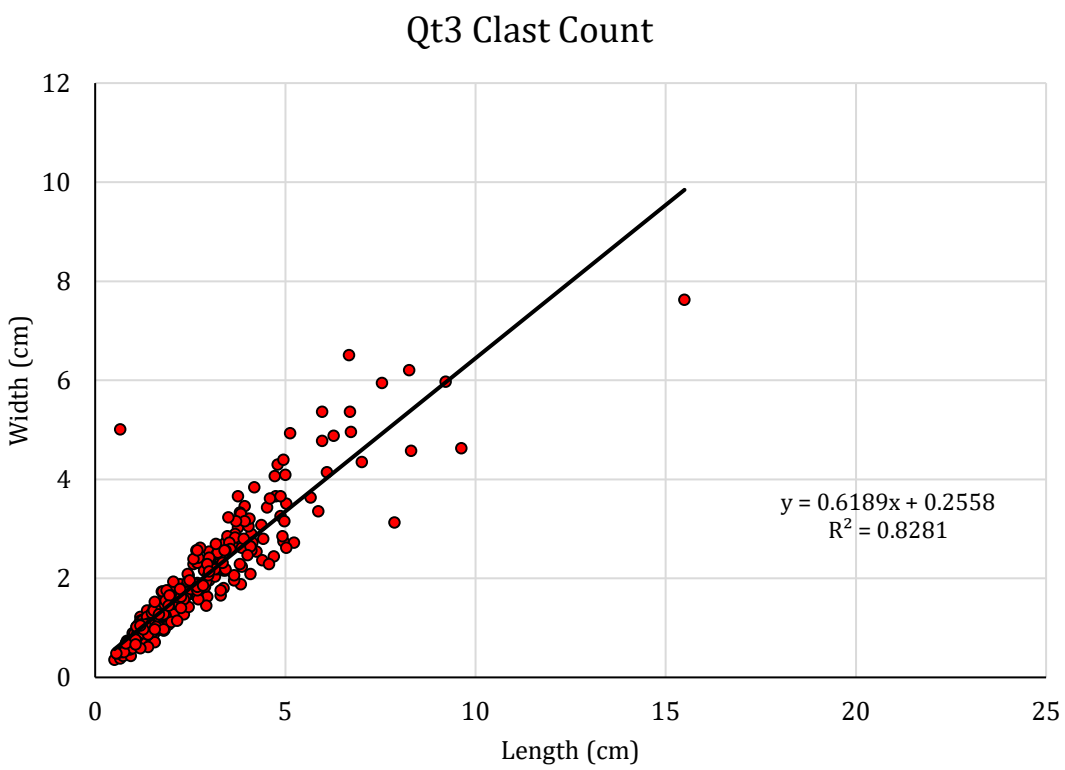

Figure C21: Clast count length vs. width for Qt5.

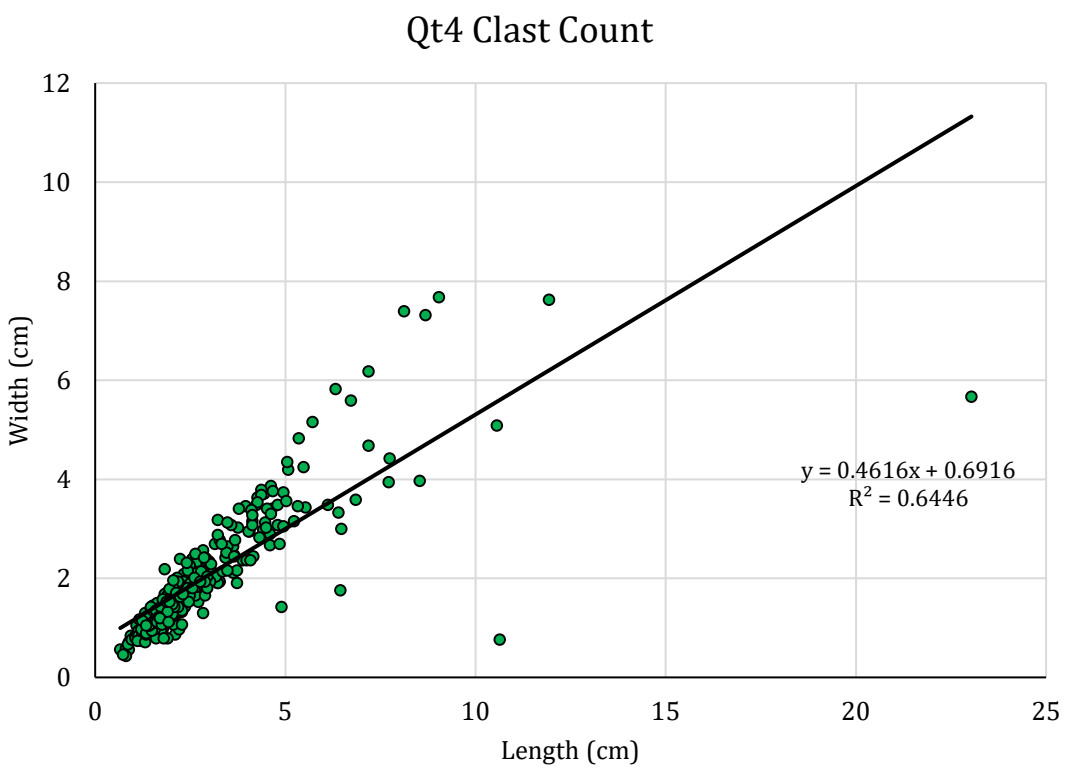

Figure C22: Clast count length vs. width for Qt4.

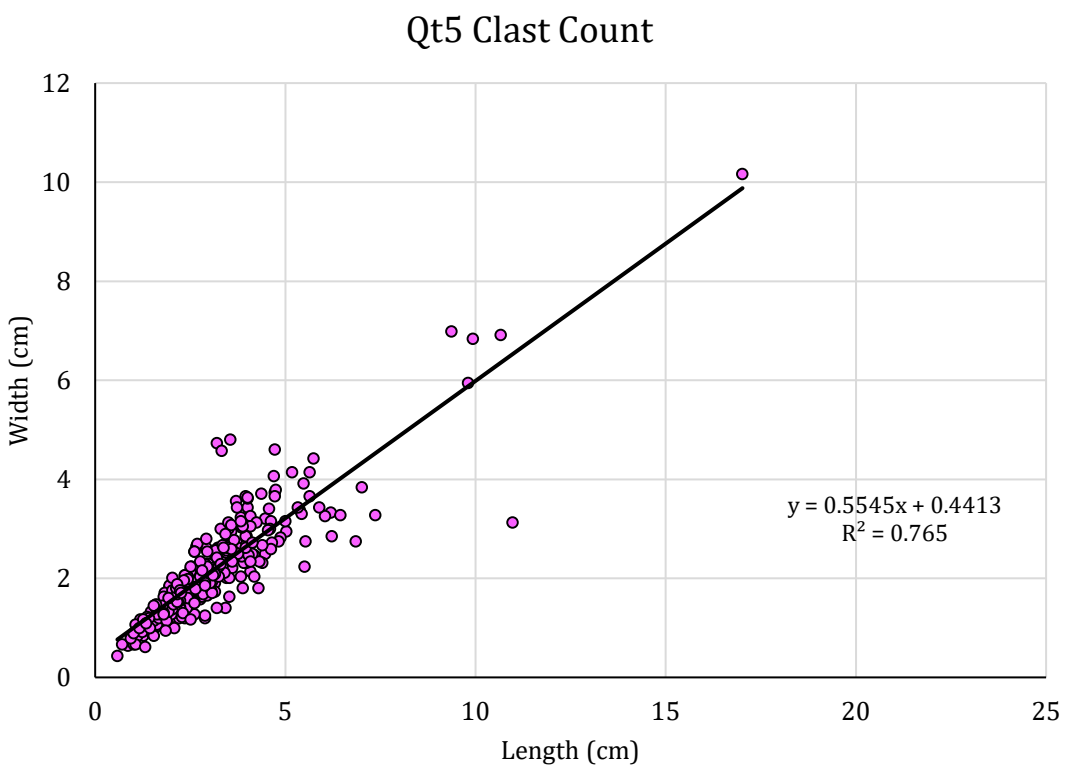

Figure C23: Clast count length vs. width for Qt5.

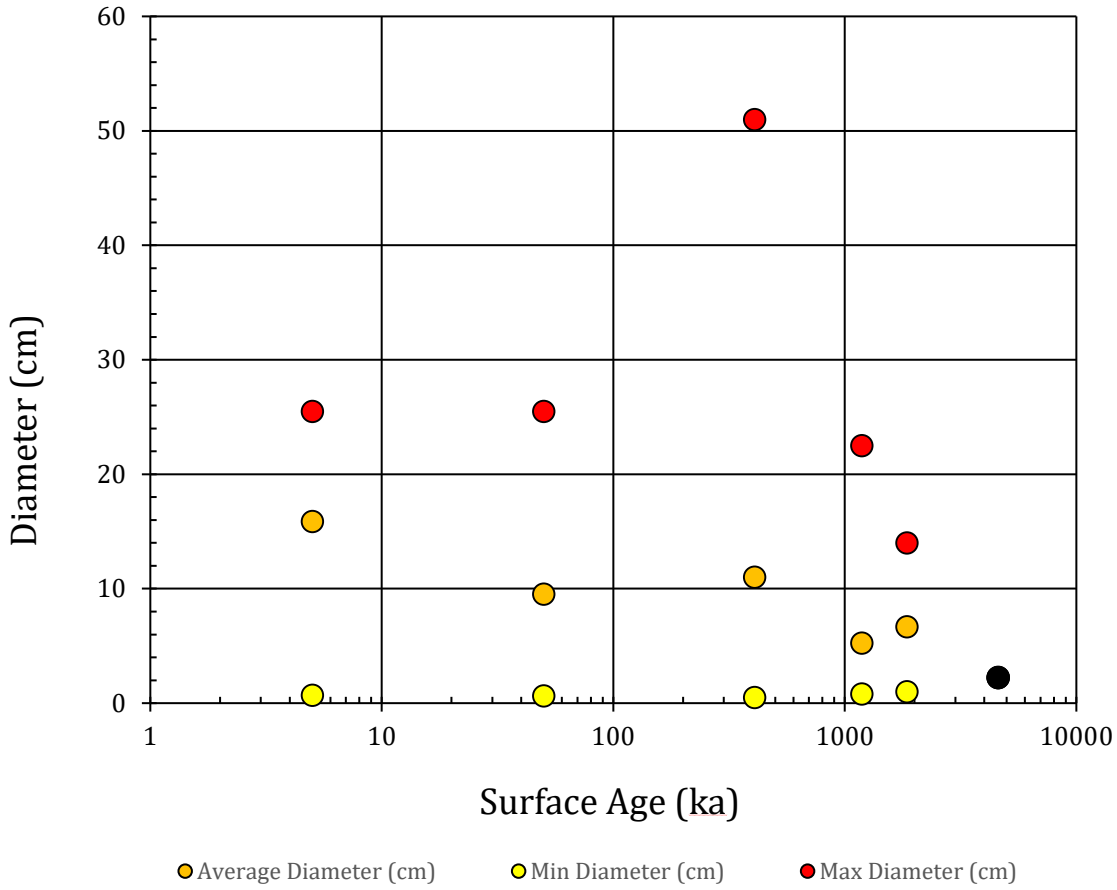

Figure C24: Average, Minimum and Maximum diameters (cm) for clasts of the Qt5 – Qt0 against Mills (2000) surface age (ka). Qt0 datum point marker is black because all three values are the same value at 2.25 (cm).

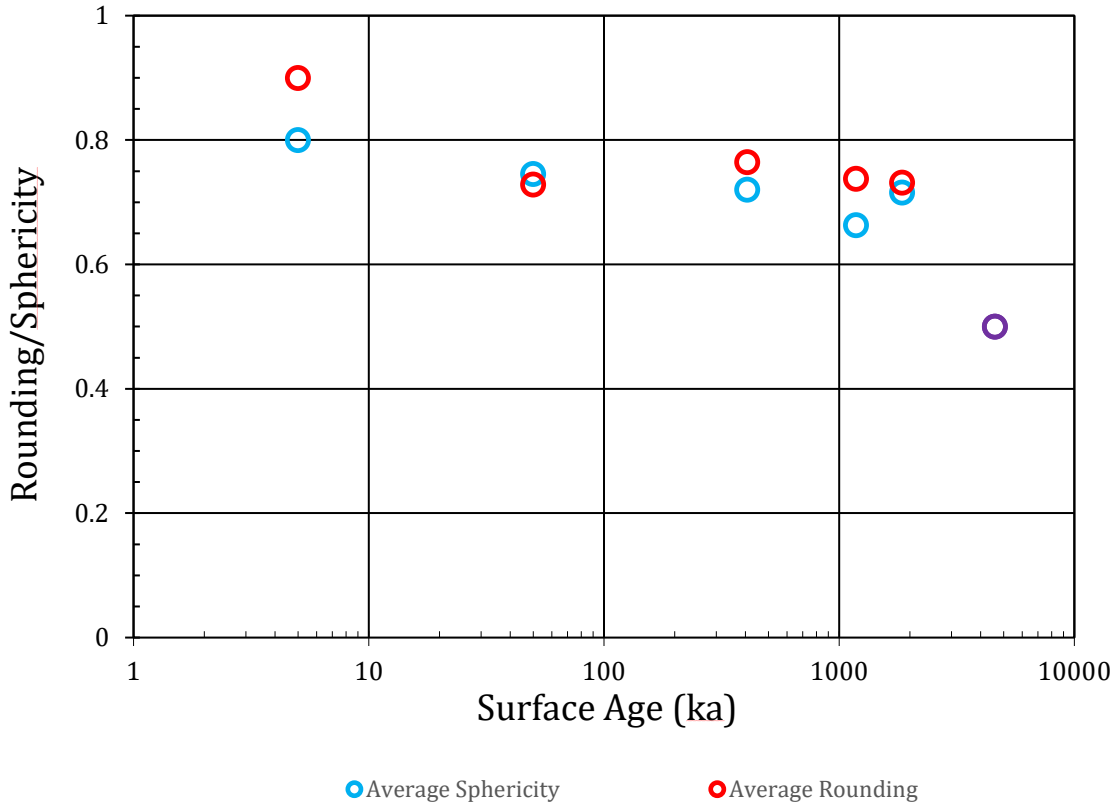

Figure C25: Average rounding and sphericity values for Qt5 – Qt0 against Mills (2000) surface age values (ka). Qt0 datum point marker is purple because rounding and sphericity share a value of 0.5.

Table C1: Averages of d10, 50 and 90 sizes for Qt5 – Qt2 terrace units. Sizes are reported in mm. For reference, clay ≤ 0.002 mm, silt = 0.002 – 0.063 mm, fine sand = 0.125 – 0.2 mm.

	d10 (mm)	d50 (mm)	d90 (mm)
Qt5	0.007	0.094	0.271
Qt4	0.004	0.085	0.280
Qt3	0.004	0.067	0.373
Qt2	0.003	0.052	0.298